Spinorbitronics

NICOLAS REYREN

http://www.cnrs-thales.fr

Acknowledgments

Unité Mixte de Physique CNRS/Thales, France

F. Ajejas, Q. Barbedienne, L. Baringthon, **K. Bouzehouane**, M. Cubukcu, **S. Collin**, J.-Y. Chauleau, **V. Cros**, T. H. Dang, **A. Fert**, K. Garcia, **J.-M. George**, **H. Jaffrès**, P. Laczkowski, W. Legrand, D. Maccariello, **N. Reyren**, J.-C. Rojas-Sánchez, J. Sampaio, A. Vecchiola

SOLEIL Synchrotron, France

J.-Y. Chauleau, **N. Jaouen**, H. Popescu → **XRMS @ SEXTANTS**

L. Baringthon, **F. Bertan**, **P. Lefèvre** → **MBE+ARPES @ CASSIOPEE**

CEA Grenoble / Spintec, France (SP-ISHE, TI, NLSV)

Y. Fu, S. Gambarelli, **M. Jamet**, P. Laczkowski, **A. Marty**, S. Oyarzún, C. Vergnaud, **L. Vila**

C2N, France

C. Gomez Carbonell, **A. Lemaître**

Samsung + CMMR (UCSD), USA (MRAM, DM anisotropy)

D. Apalkov, **A. V. Khvalkovskiy**, M. Kuteifan, **V. Lomakin**

University of Glasgow, UK (L-TEM)

S. Hughes, K. Fallon, S. McFadzean, **S. McVitie**

ANRs
TOPSKY
TOP-RISE

Samsung Global MRAM Innovation Program

SKYTOP – Skyrmion-Topological insulator and Weyl semimetal technology

Overview

Short Introduction: from Spintronics to Spinorbitronics

Electronic and Spin Transport

- Spin dependent scattering in bulk materials

  QUESTIONS

- 2D surface states and spin-charge conversion

  QUESTIONS

Magnetization texture

- Dzyaloshinskii-Moriya interaction (DMI)
- Measuring the chirality and the DMI by XRMS, L-TEM, BLS, domain extension, …

  QUESTIONS

- Examples: DM-MRAM and DM-anisotropy

  QUESTIONS

Magnetization Control using SOT and DMI

- Spin-orbit torques (SOT)

  QUESTIONS

Ferromagnetic material

Ferromagnetic metal : Co

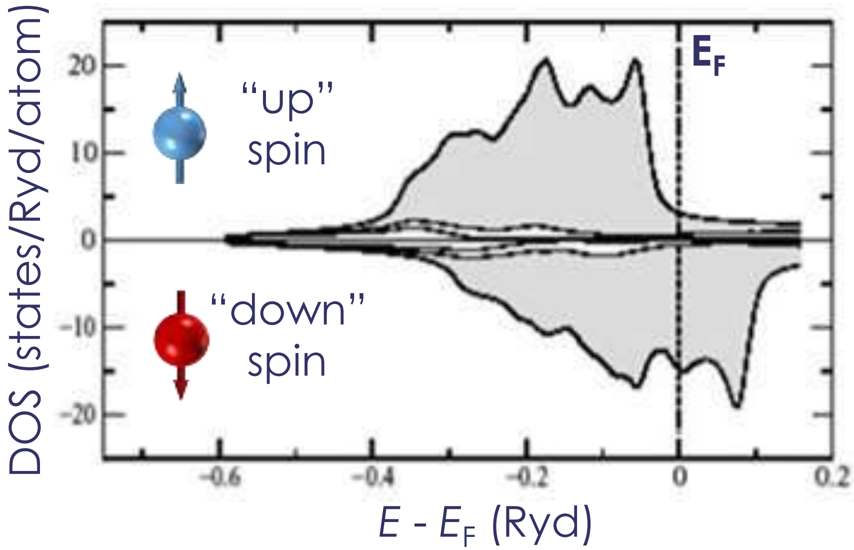

Normal metal : Cu

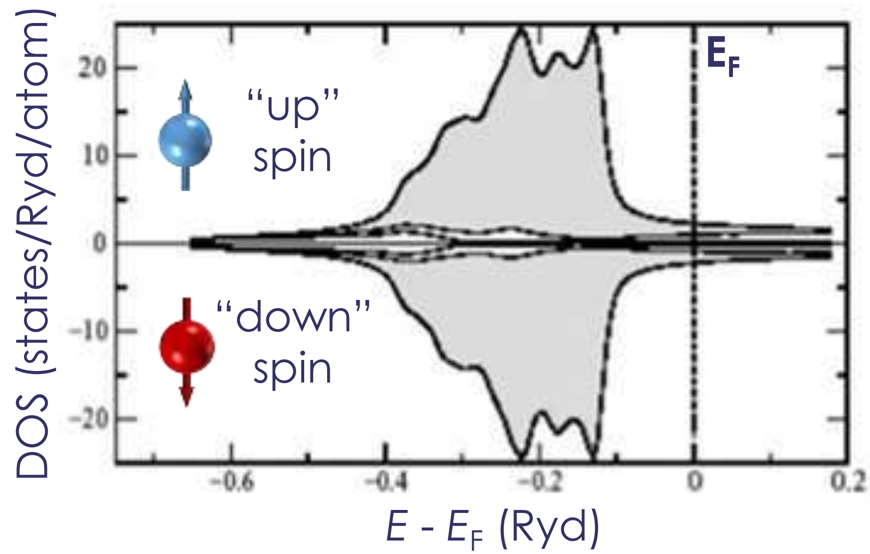

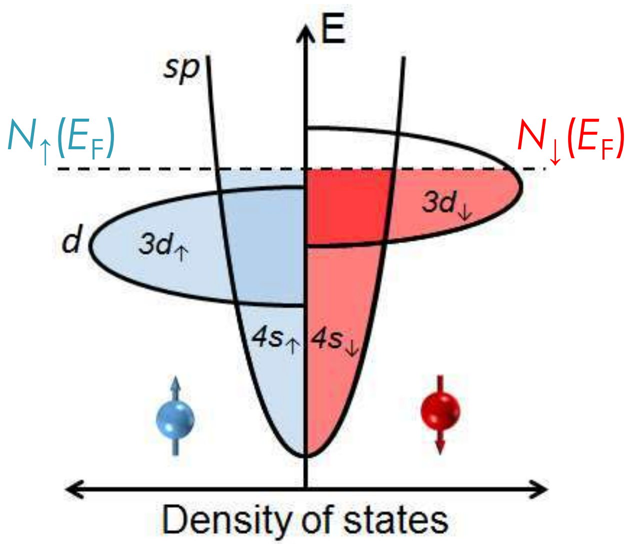

Exchange

$\sigma_\uparrow \neq \sigma_\downarrow$

Two channels conduction

From J.-M. George ISOE2017 lecture

Conduction in ferromagnetic metal

❖ **Two currents model : Mott's model**

- Conduction due to *s* electrons.
- Magnetism due to *d* electrons and bands are shifted.
- Resistivity arises from $s \rightarrow d$ transitions.

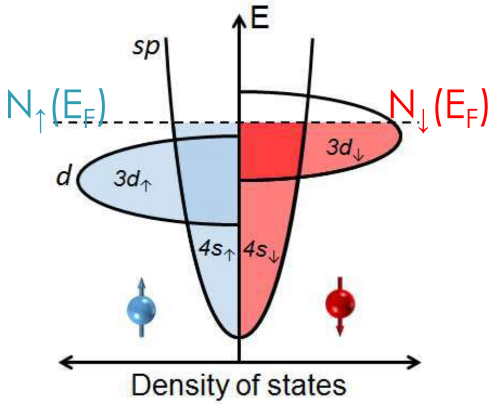

➔ The current flows through two largely independent conducting channels corresponding to the spin ↑ and spin ↓ electrons.

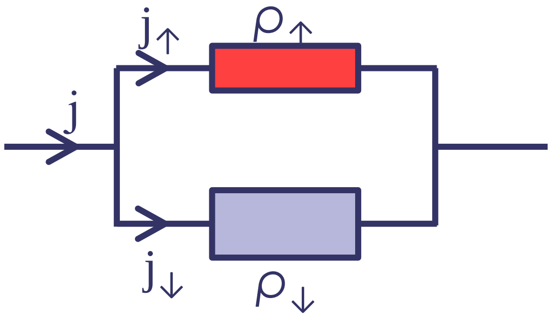

$$\frac{1}{\rho} = \frac{1}{\rho_\uparrow} + \frac{1}{\rho_\downarrow}$$

$$\rho = \frac{\rho_\uparrow \rho_\downarrow}{\rho_\uparrow + \rho_\downarrow}$$

From J.-M. George ISOE2017 lecture

Variation of Magnetization induced change of resistivity via spin current

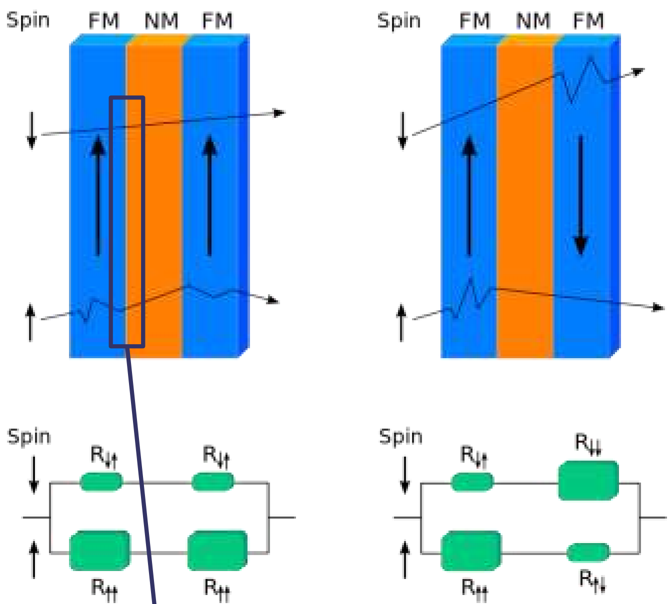

https://fr.wikipedia.org/wiki/Magn%C3%A9tor%C3%A9sistance_g%C3%A9ante#/media/Fichier:Spin-valve_GMR.svg

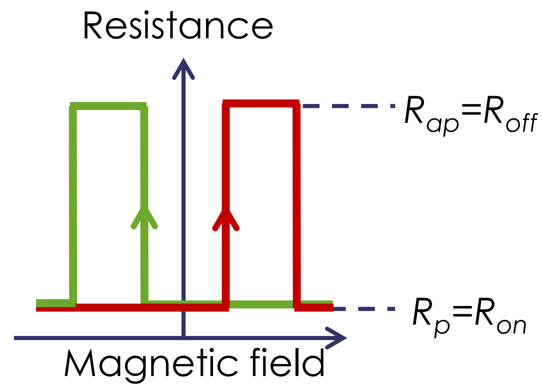

Spin signal

$$\Delta R = R_{ap} - R_p$$

Magneto-Resistance

$$MR = \Delta R / R_p$$

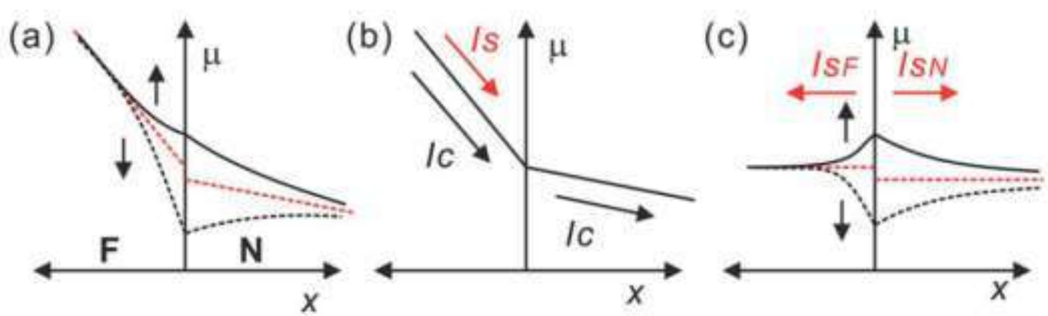

Two channels conduction

Polarization of normal metal

T. Kimura *et al*, *Phys. Rev. B* **72**, 014461 (2005)

« Classical » Spintronics: the Giant MagnetoResistance (GMR)

Variation of Magnetization induced change of resistivity via spin current

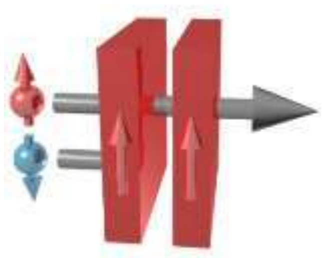

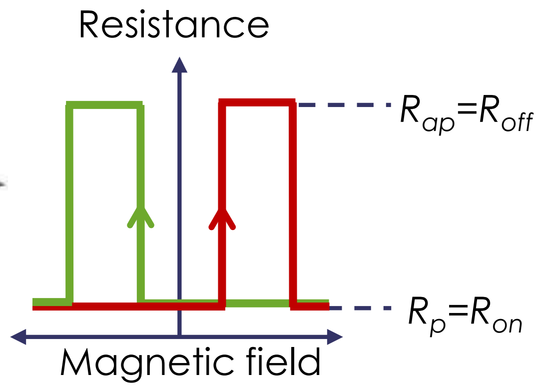

Spin signal

$$\Delta R = R_{ap} - R_p$$

Magneto-Resistance

$$MR = \Delta R / R_p$$

GMR

TMR

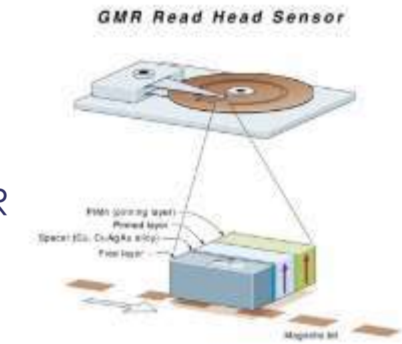

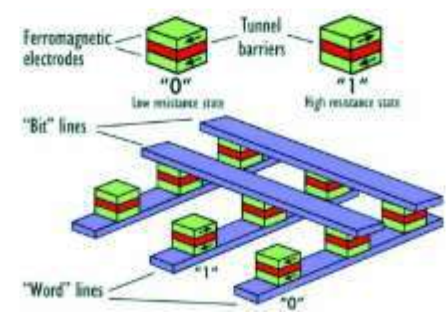

Spin current can act on the magnetization

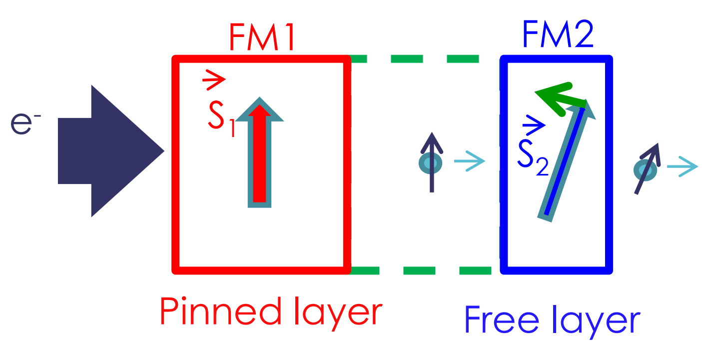

STT

STO

From J.-M. George ISOE2017 lecture

Spinorbitronics

Spin-Orbit Coupling

Transport in bulk

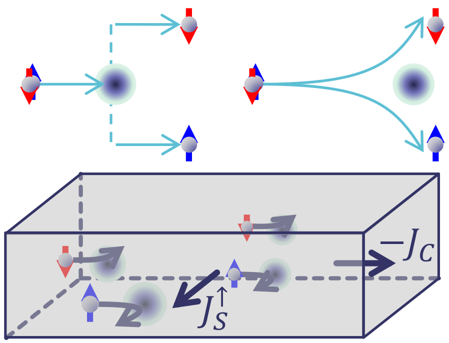

$\vec{J}_C \propto \theta_{SHE} \vec{S} \times \vec{J}_s$

Spin-Charge conversion

Magnetic configuration

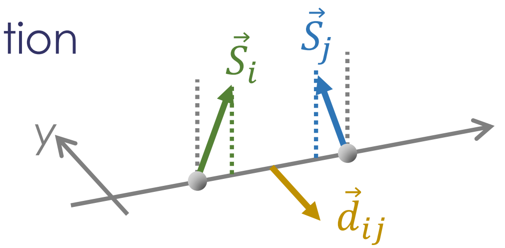

$H_{H+DM} = -J\sum(\vec{S}_i \cdot \vec{S}_j) - \sum \vec{d}_{ij} \cdot (\vec{S}_i \times \vec{S}_j)$

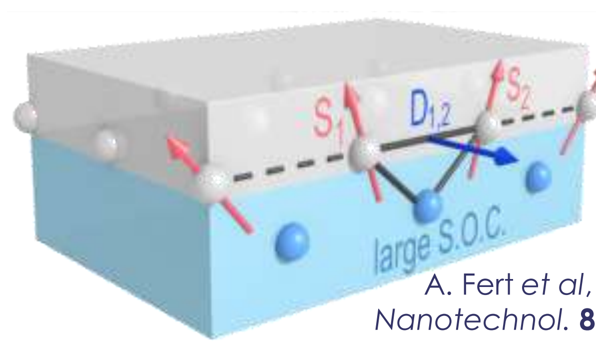

A. Fert *et al*, *Nat. Nanotechnol.* **8**, 152 (2013)

Chiral interaction:

→ Chiral domain walls,
→ Skymions (*Friday lecture*),
→ etc.

Transport at interfaces

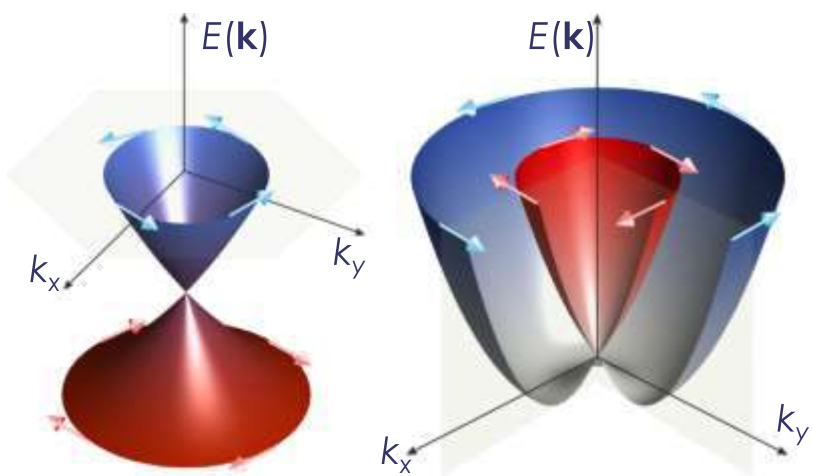

$H \propto (\vec{k} \times \hat{z}) \cdot \vec{\sigma}$

A. Soumyanarayanan *et al*, *Nature* **539**, 509 (2016)

Transverse resistivity (or conductivity?)

Resistivity and conductivity matrices for an isotropic thin film (xy-plane):

$$\vec{E} = \boldsymbol{\rho}\,\vec{J} \quad \text{and} \quad \boldsymbol{\sigma}\vec{E} = \vec{J}$$

Hence $\boldsymbol{\rho} = \boldsymbol{\sigma}^{-1}$, i.e. $\begin{pmatrix} \rho_{xx} & \rho_{xy} \\ \rho_{yx} & \rho_{yy} \end{pmatrix} = \frac{1}{\sigma_{xx}\sigma_{yy} - \sigma_{xy}\sigma_{yx}} \begin{pmatrix} \sigma_{xx} & \sigma_{xy} \\ \sigma_{yx} & \sigma_{yy} \end{pmatrix}$.

Then, using $\rho_{xx} = \rho_{yy}$ and $\rho_{yx} = -\rho_{xy}$:

$$\sigma_{xx} = \frac{\rho_{xx}}{\rho_{xx}^2 + \rho_{xy}^2} \quad \text{and} \quad \sigma_{xy} = \frac{\rho_{xy}}{\rho_{xx}^2 + \rho_{xy}^2}$$

Electrical transport measurement: What are you measuring?

- What are your boundary conditions? Do you fix the voltage or the current?

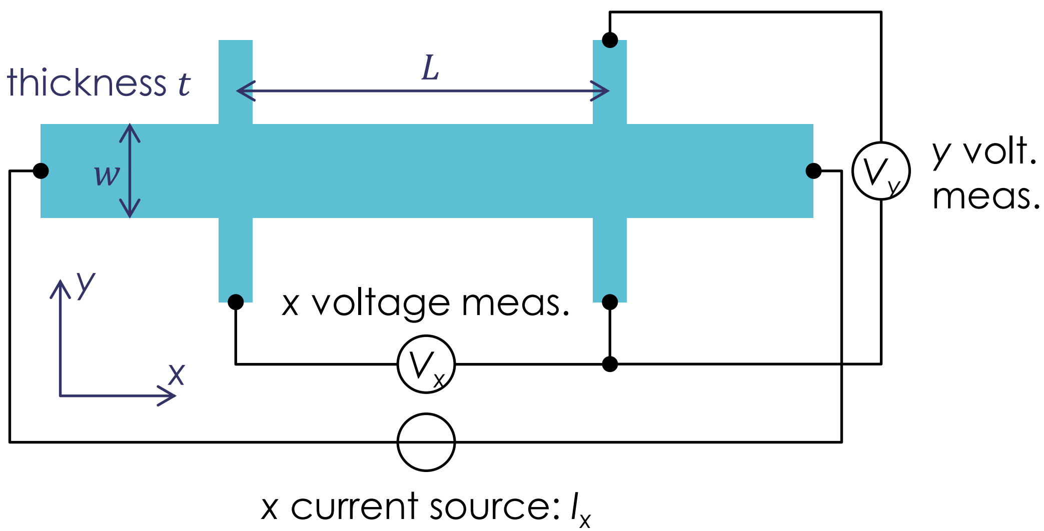

In this case, assuming ideal voltmeters (infinite impedances):

$$\vec{J} = \begin{pmatrix} J_x \\ 0 \end{pmatrix},\ \vec{E} = \begin{pmatrix} E_x \\ E_y \end{pmatrix},$$

hence:

$$\rho_{xx} = \frac{E_x}{J_x} = \frac{V_x}{I_x}\frac{L}{w\,t}.$$

However, in general, $\sigma_{xy}E_y \neq 0$, so:

$$\sigma_{xx} \neq \frac{J_x}{E_x}\ !$$

$$\sigma_{xx}E_x = J_x + \sigma_{xy}E_y$$

Ordinary Hall Effect

Ordinary Hall effect (OHE):

Applying magnetic field B along $\hat{z}$:

$$\boldsymbol{\rho} = \begin{pmatrix} \rho & R_0 B \\ -R_0 B & \rho \end{pmatrix}$$

for simple metals with
$\rho_{xy}(H = 0) = 0.$

R_0 in units of 10^{-10} Ω m/T (= m^3/C) for a few metals:

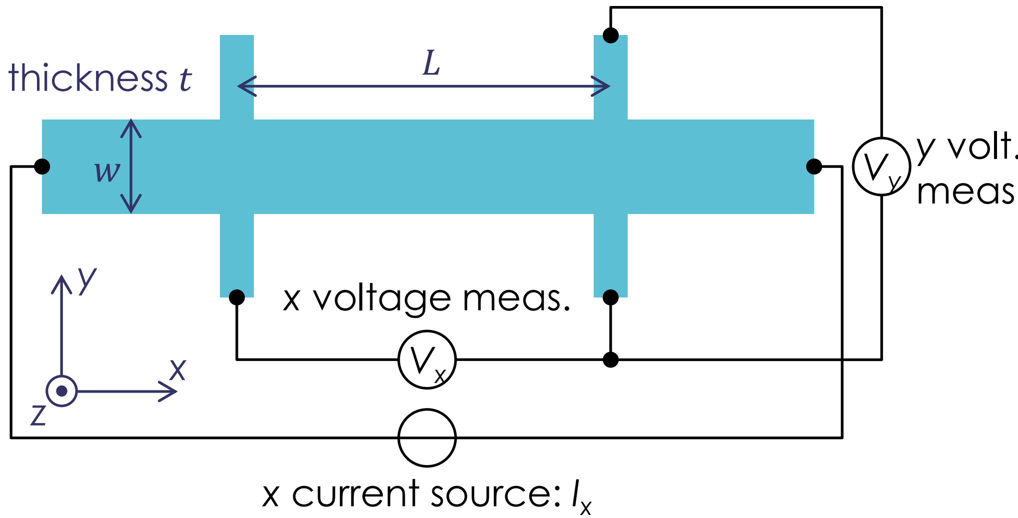

Al	Fe	Co	Cu	Ta	Pt	Au	Pb
-0.3	0.245	-1.33	-0.55	1.01	-0.24	-0.72	0.09

AIP handbook, 3rd Ed. D.E. Gray, 1972, New York

What happens in magnetic materials?

- Is the magnetic field from magnetization responsible for an OHE-type of Hall effect? e.g. Co: $\mu_0 M_s$ = 1.4 T

  → "R_0"($\mu_0 M_s$) = 1.9 10^{-10} Ωm/T

- No! Then what's appening?

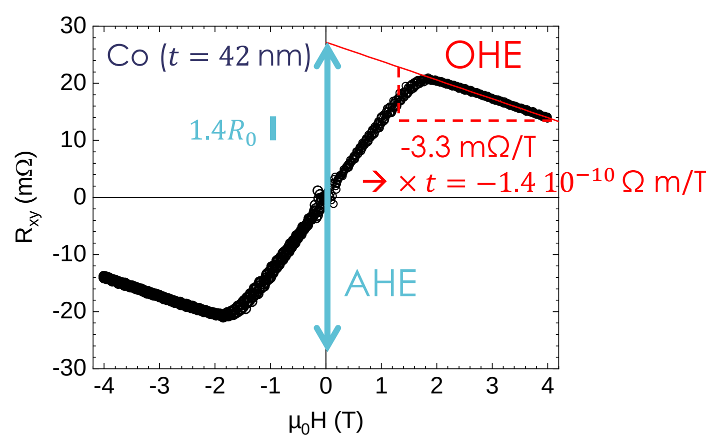

Anomalous Hall Effect

What happens in magnetic materials?

- Is the magnetic field from magnetization responsible for an OHE-type of Hall effect? e.g. Co: $\mu_0 M_s = 1.4$ T

  → "R_0"($M_z=M_s$) = 1.9 10^{-10} Ωm/T

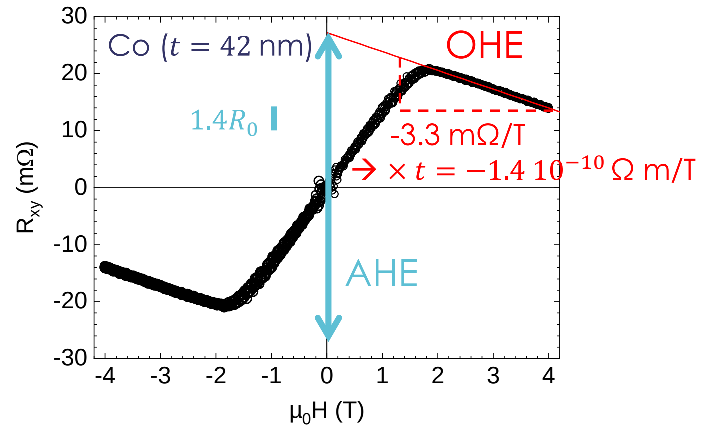

- Anomalous Hall Effect (AHE):

$$\rho_{xy}(H) = R_0\mu_0 H + R_{\mathrm{AHE}}(\vec{m}\cdot\hat{z})$$

Ferromagnetic metal : Co

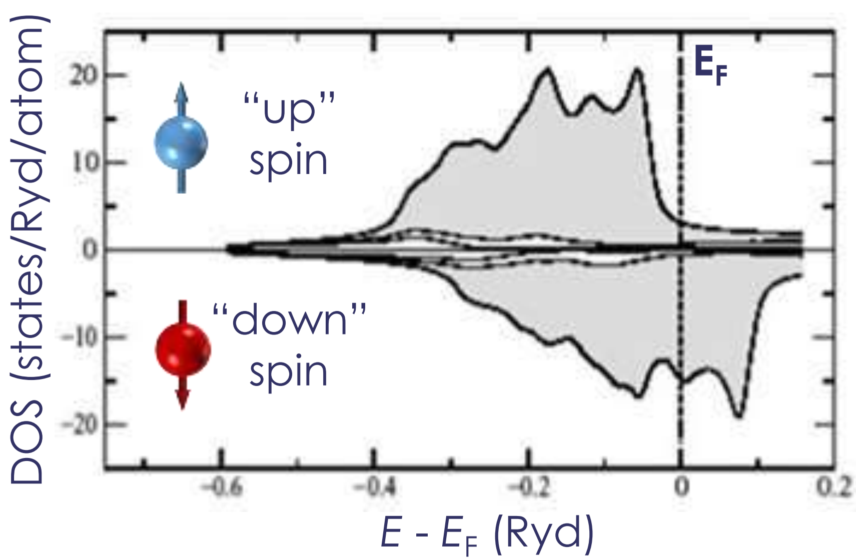

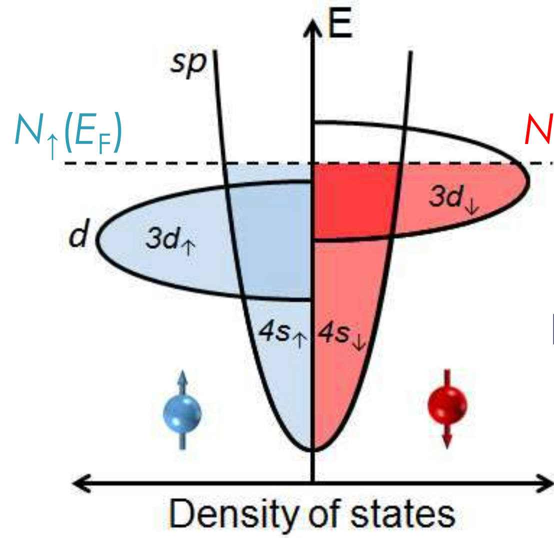

Exchange

$\sigma_\uparrow \neq \sigma_\downarrow$

Similar Effect for Non-Magnetic Materials? Spin Hall Effect

Anomalous Hall effect in magnetic materials (a.k.a. Extraordinary Hall effect)

$$\rho_{xy}(H) = R_0\mu_0 H + R_{\mathrm{AHE}}(\vec{m}\cdot\hat{z})$$

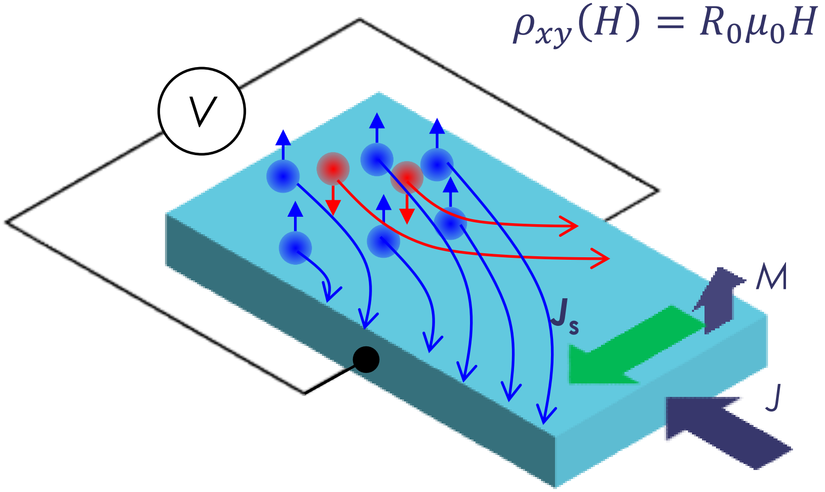

$$M \neq 0 \Rightarrow P = \frac{N_\uparrow - N_\downarrow}{N_\uparrow + N_\downarrow} \neq 0$$

Spin dependent scattering with:

$$\sigma_{xy}^{\uparrow} = -\sigma_{xy}^{\downarrow}$$

Spin dependent scattering with:

$$V_{xy} \propto P$$

What Happens for $P = 0$?

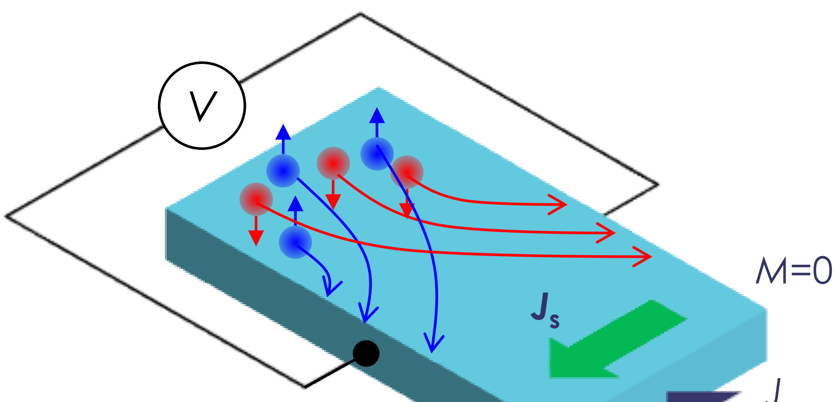

$$M = 0\,,, N_\uparrow = N_\downarrow \Rightarrow P = 0$$

Spin dependent scattering with:

$$\sigma_{xy}^{\uparrow} = -\sigma_{xy}^{\downarrow}$$

Spin dependent scattering with:

$$V_{xy} = 0$$

No external field!

spin accumulation
SPIN HALL EFFECT

Observation of the Spin Hall Effect

Can we observe such effect?

Direct observation of the spin accumulation using magneto-optic Kerr effect.

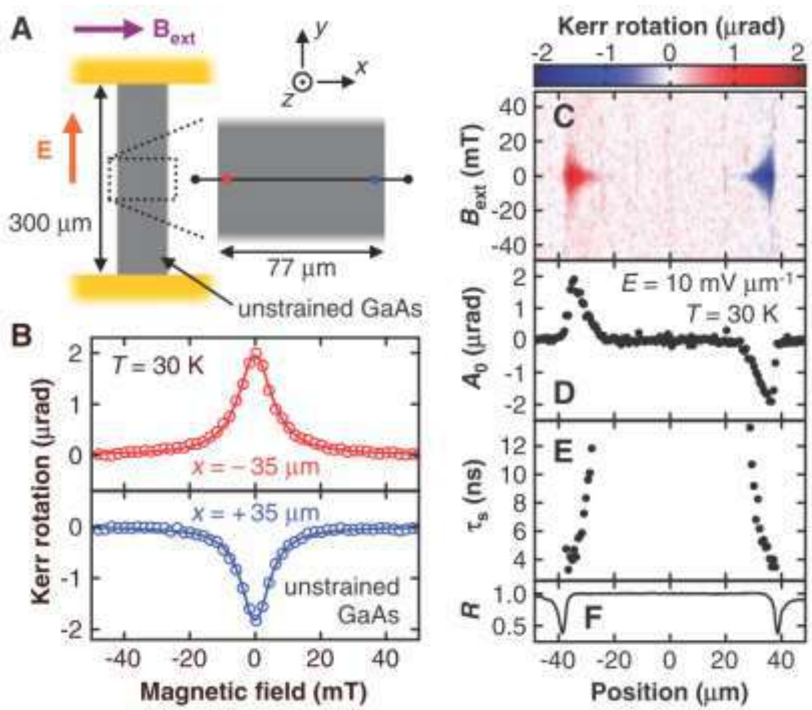

Y. K. Kato *et al*, *Science* **306**, 1910 (2004)

Electrical measurement of the SHE.

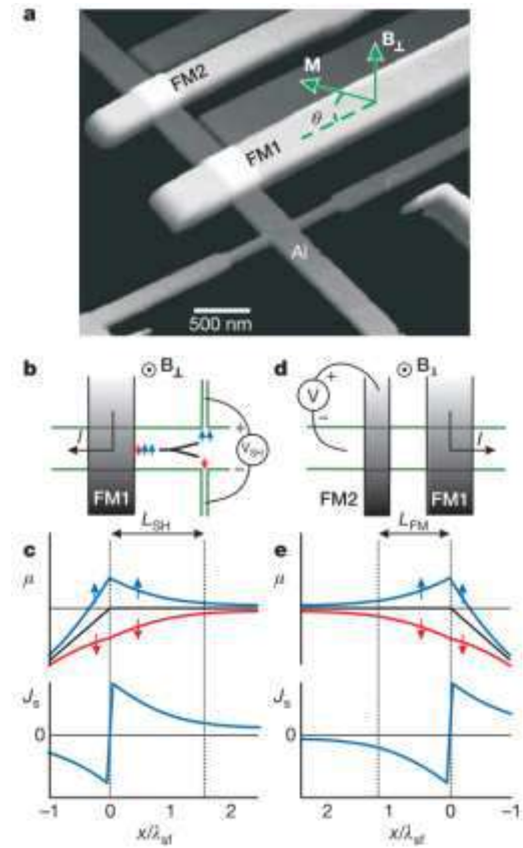

S. O. Valenzuela & M. Tinkham, *Nature* **442**, 176 (2006)

Spin Hall Effect - Mechanisms

J. Sinova *et al*, *Rev. Mod. Phys.* **87**, 1213 (2015)

Spin-dependent diffusion on impurities (extrinsic SHE)

- Scattering on impurities

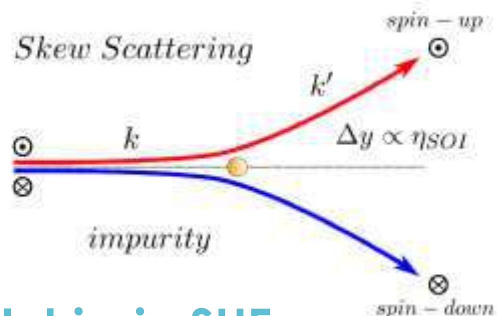

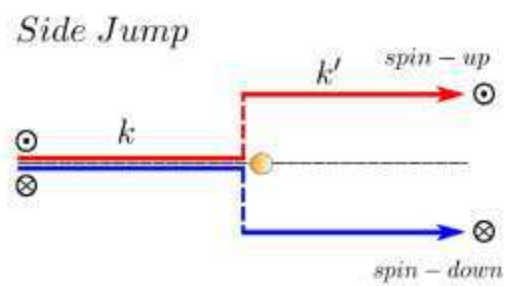

Intrinsic SHE

$$\rho_{xy} = a\rho_{xx} + b\rho_{xx}^2$$

- Origin in the band structure (Berry phase)

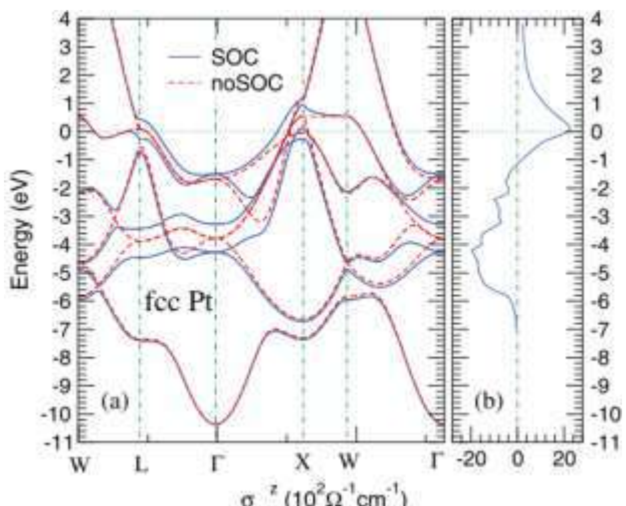

G. S. Guo *et al*, *Phys. Rev. Lett.* **100**, 096401(2008)

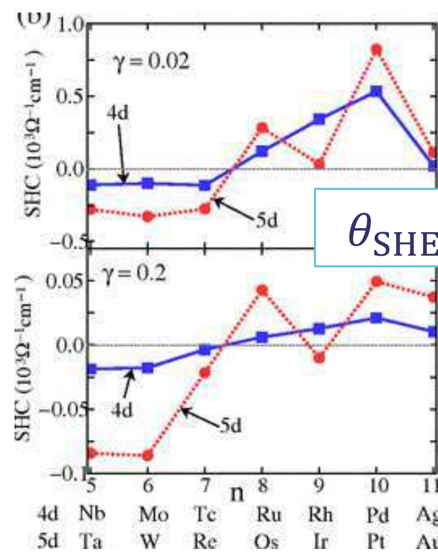

$$\theta_{\text{SHE}} = a + b\rho_{xx}$$

T. Tanaka *et al*, *Phys. Rev. B* **77**, 165117 (2008)

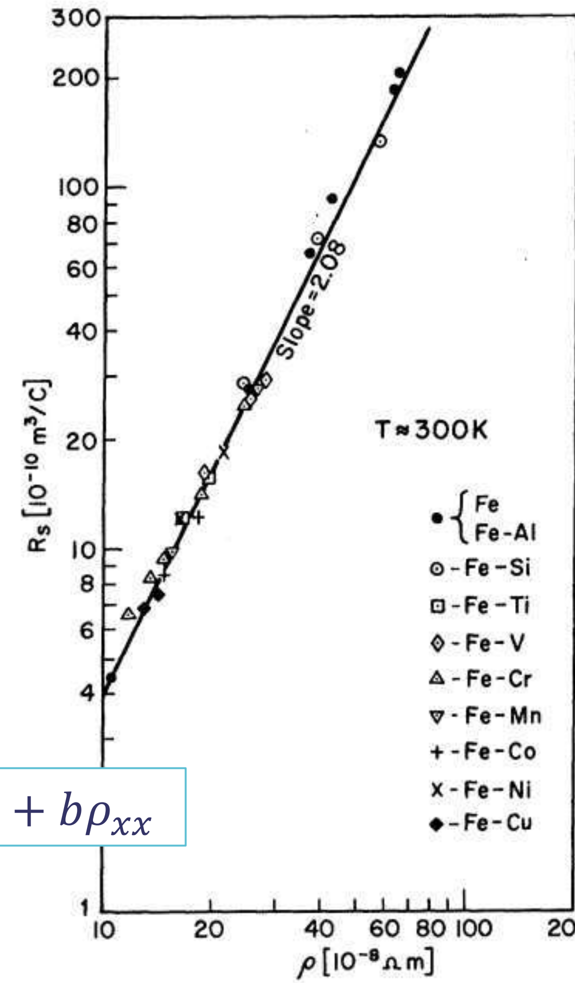

L. Berger, *Phys. Rev. B* **2**, 4559 (1970)

Spin Hall Effect and Inverse Spin Hall Effect

Reciprocal: A spin current can generate a charge accumulation (open circuit) or a charge current (closed circuit)

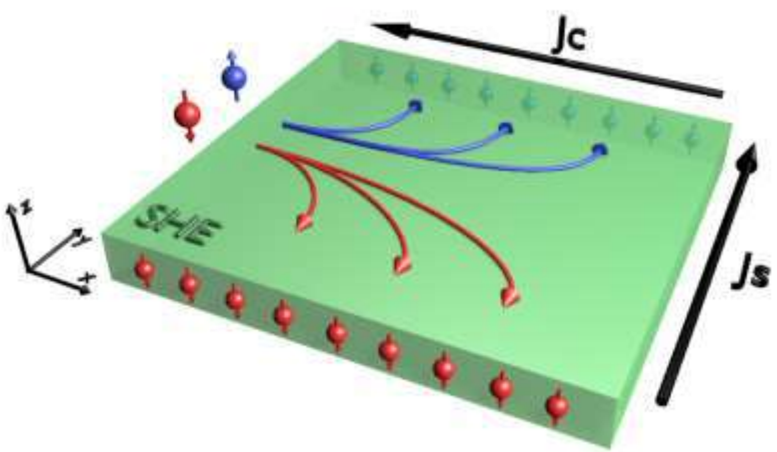

Direct spin Hall effect (SHE)

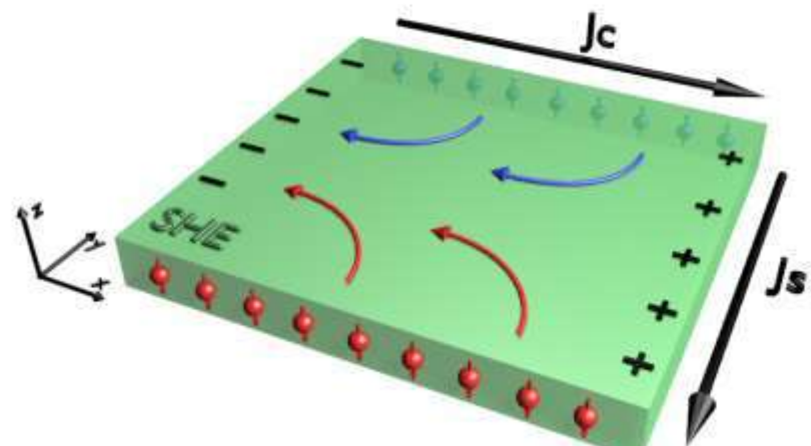

Inverse spin Hall effect (ISHE)

$$\vec{J}_c \overset{?}{\leftrightarrow} \vec{J}_s$$

direction of spin polarization

$$\vec{J}_s = \theta_{\text{SHE}}^{\text{eff}} \vec{J}_c \times \vec{S}$$

$$\vec{J}_c = \theta_{\text{SHE}}^{\text{eff}} \vec{J}_s \times \vec{S}$$

Inverse Spin Hall Effect – Measuring the Bulk Spin Hall Angle

Reciprocal: A spin current can generate a charge accumulation (open circuit) or a charge current (closed circuit)

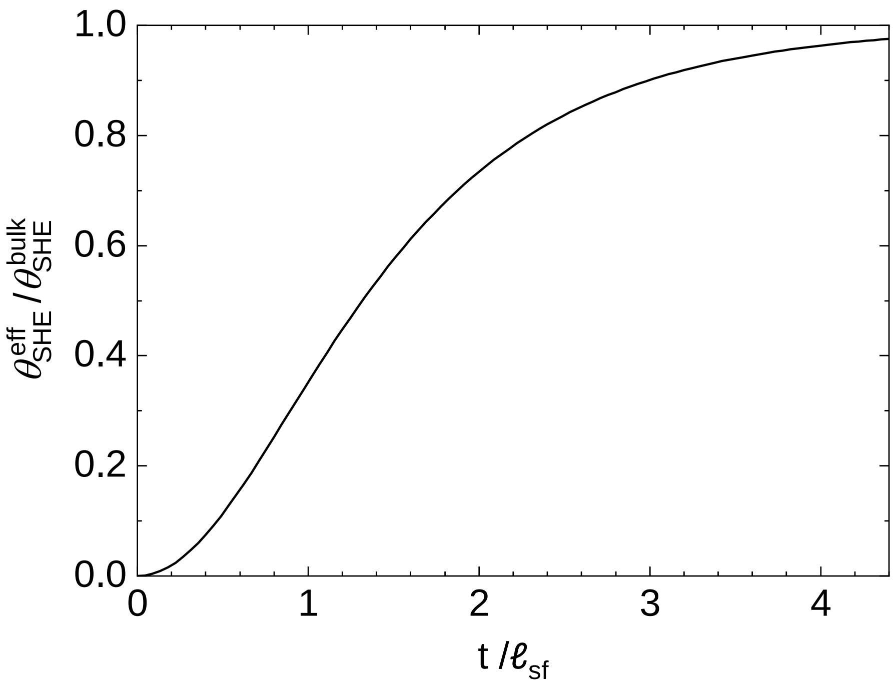

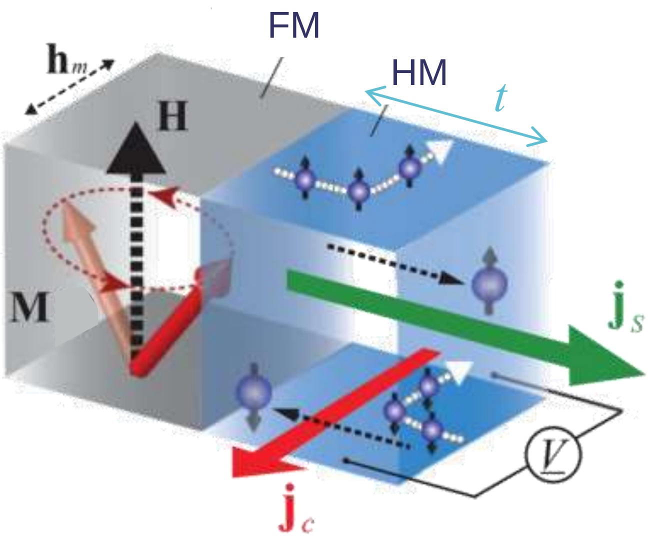

H. Nakayama *et al*, *Phys. Rev. B* **85**, 144408 (2012)

$$\vec{J}_c = \theta_{SHE}^{eff} \vec{J}_s \times \vec{S}$$

Including the SML…

Considering a more realistic interface, including the *Spin Memory Loss or spin current discontinuities…*

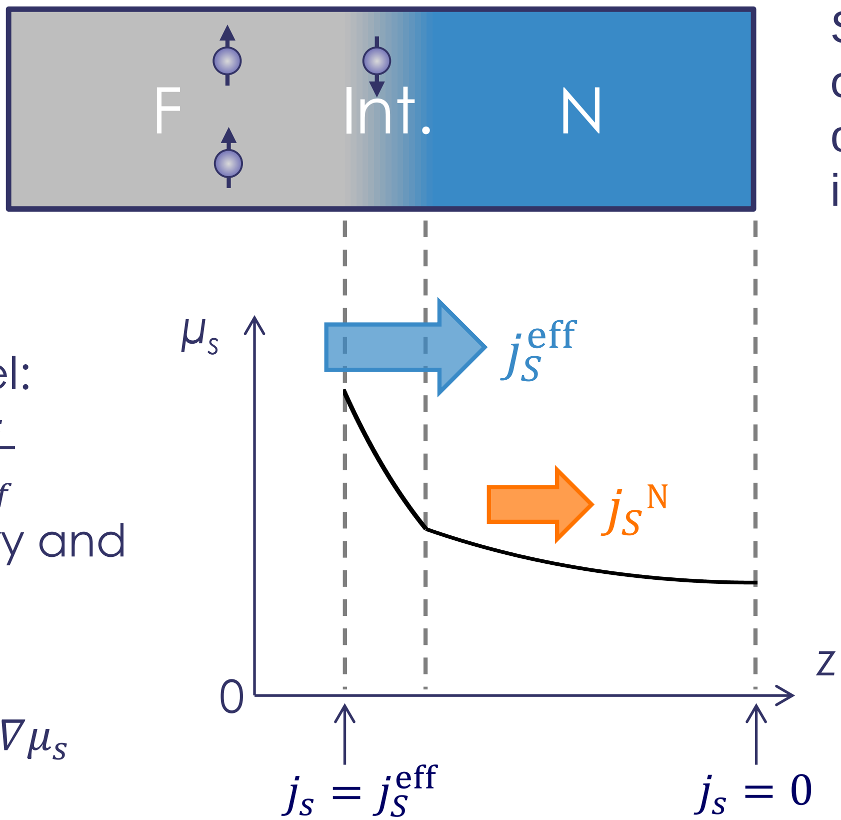

Some spin relaxation called "*spin memory loss*" occurs at metallic interfaces (→ GMR).

H.Y.T. Nguyen, W.P. Pratt and J. Bass, *JMMM* **361**, 30 (2014)

Diffusion model:

$$\nabla^2 \mu_s = \frac{\mu_s}{\ell_{sf}^2}$$

Using boundary and continuity conditions…

$$j_s = -\frac{\hbar}{2e}\frac{1}{e\rho}\nabla \mu_s$$

T. Valet and A. Fert, *Phys. Rev. B* **48**, 7099 (1993)

Our Model Including the SML

Considering a more realistic interface, including the *Spin Memory Loss or spin current discontinuities…*

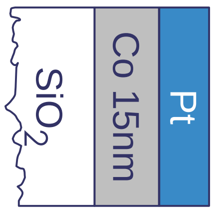

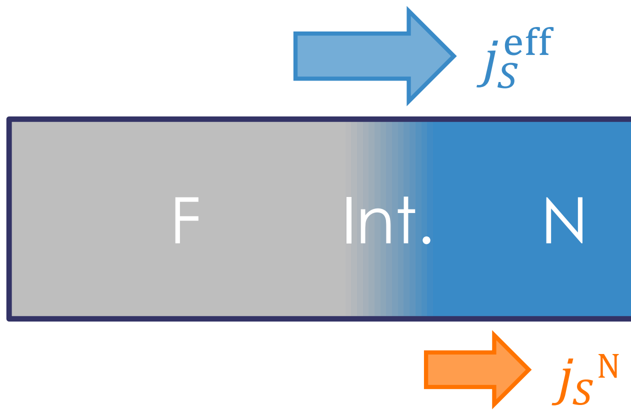

Some spin relaxation called “*spin memory loss*” occurs at metallic interfaces.

$$I_C = -\theta_{\mathrm{SH}}\ell_{\mathrm{sf}} w \tanh\left(\frac{t_{\mathrm{N}}}{2\ell_{\mathrm{sf}}}\right) j_S{}^{\mathrm{N}} = -\theta_{\mathrm{SH}}\ell_{\mathrm{sf}} w \tanh\left(\frac{t_{\mathrm{N}}}{2\ell_{\mathrm{sf}}}\right) R_{\mathrm{SML}}\, j_S^{\mathrm{eff}}$$

$$R_{\mathrm{SML}} = \frac{j_S^{N}}{j_S^{\mathrm{eff}}} = \frac{r_{\mathrm{sI}}}{r_{\mathrm{sI}}\cosh(\delta) + r_{\mathrm{sN}}\coth\left(\frac{t_{\mathrm{N}}}{\ell_{\mathrm{sf}}}\right)\sinh(\delta)}$$

J.-C. Rojas-Sánchez *et al*, *Phys. Rev. Lett.* **112**, 106602 (2014)

For example, in the Co|Pt, one has:

$\delta = 0.9$ $(P = 1 - \exp(-\delta) = 60\%)$
$r_{\mathrm{sI}} = 0.83$ fΩm^2

} $R_{\mathrm{SML}} \approx 0.5$ for $t_{\mathrm{N}} \geq \ell_{\mathrm{sf}}$

H.Y.T. Nguyen *et al*, *JMMM* **361**, 30 (2014)

Spin Hall Angle

K. Fujiwara *et al*, *Nat.Commun.* **4**, 2893 (2013)

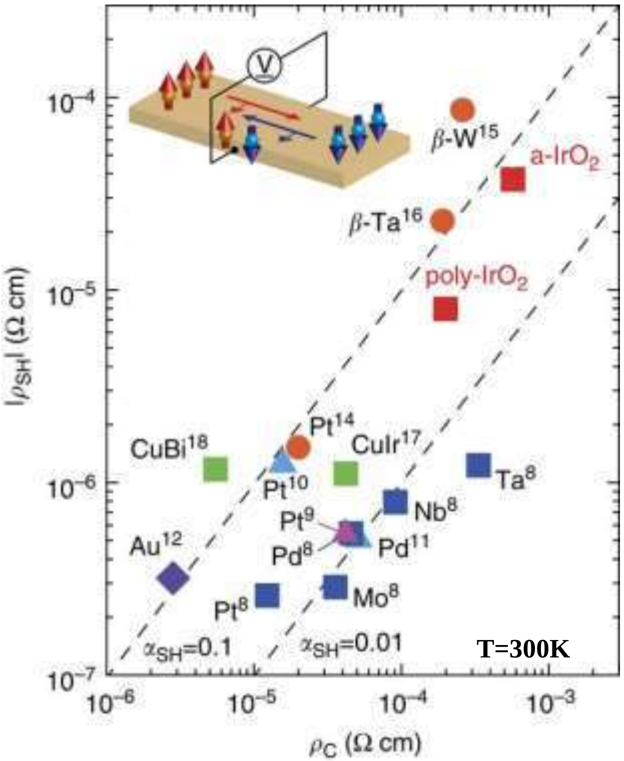

8. Morota, M. et al. PRB 83, 174405 (2011).
9. Mosendz, O. et al. PRB 82, 214403 (2010).
10. Ando, K. et al. PRL, 101, 036601 (2008).
11. Ando, K. & Saitoh, E. JAP, 108, 113925 (2010).
12. Seki, T. et al. Nat. Mater. 7, 125–129 (2008).
14. Liu, L., et al. PRL, 106, 036601 (2011).
15. Pai, C.-F. et al., APL, 101, 122404 (2012).
16. Liu, L. et al., Science 336, 555–558 (2012).
17. Niimi, Y. et al. PRL, 106, 126601 (2011).
18. Niimi, Y. et al. PRL, 109, 156602 (2012).

Spin Hall Angles at low T:

$material$	l_{sf} $[nm]$	α_{SHE} $[\%]$
Pd, Mo, Ta, Nb		1
Pt	$3-12$	$2/12$
$CuIr$	10	2.1
$CuBi$	40	-25
$CuPb$		10
$\beta-Ta$	<20	$-2/-15$
$\beta-W$		-30
IrO_2	8.5	6.5

- No magnetic materials nor magnetic fields

- Short SDL → thinner layers

- Precise control of SHA through mag. impurities

- Conversion rate comparable with F/N

J.-C. Rojas-Sánchez at al, PRL. 112, 106602 (2014)

From J.-M. George ISOE2017 lecture

Spin Hall Effect

Materials:

semiconductors — *metals*: Pt, Nb, Pd — *Alloys,oxides*: CuIr, CuBi, Ta, W, **AuW** IrO

spin Hall angle:

<0.001 — 0.01-0.02(Pt) — 0.021(CuIr), -0.25(CuBi) — 0.3(β-Ta)

1971 — **Prediction**
[M.I. D'yakonov, V. I. Perel, Phys. Lett. A. 35, 459 (1971)]

1984 — **First ISHE Optical detection**
[A. A. Bakun *et al.*, Sov. Phys. JETP Lett. 40: 1293 (1984)]

1999 — **Introduction of a term "SHE" in a paramagneticc metals**
[J. E. Hirsh, PRL. 83, 1834–1837 (1999)]

2004 — **3D layers**
[Y. K. Kato *et al.*, Science 306, 1910 (2004)]

2005 — **2D hole gas**
[J. Wunderlich *et al.*, PRL. 94, 047204 (2005)]

2006 — **Spin Sumping**
[E. Saitoh et al., APL, 88, 182509 (2006)]

LSVs
[S.O. Valenzuela et al. Nature 442, 176-179 (2006)]

2011 — **Shunting effect**
[Niimi *et al.*, PRL, 106, 126601 (2011)]

1D and 3D corrections
[Y. Niimi *et al.*, arXiv:1208.6208]

2012 — **ST Experimets**
M. Miron *et al.*, Nature 476, 189 (2012)

ST-FMR

From J.-M. George ISOE2017 lecture

Experiments to probe SHE

Non local measurement

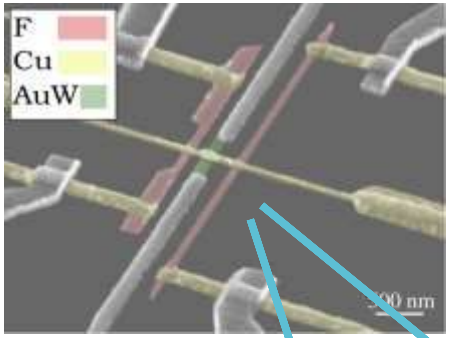

P. Laczkowski et al., APL. 104, 142403 (2014)

FMR-Spin pumping

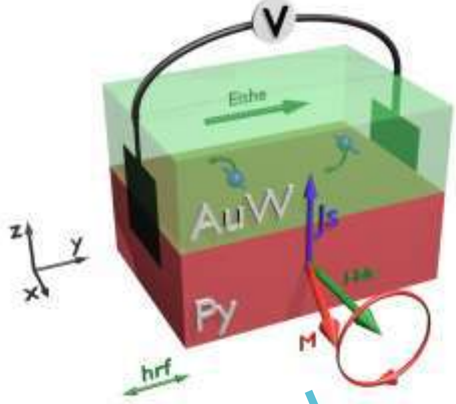

Spin transfert torque

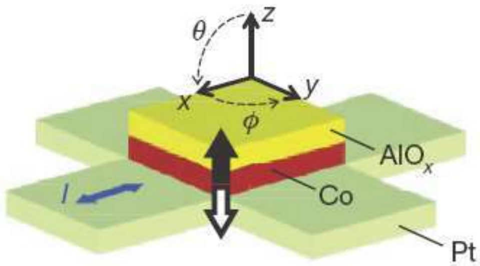

I. M. Miron *et al.*, Nature 476, 789 (2011)

L. Yu et al. Science 333, 555 (2012)

Direct SHE

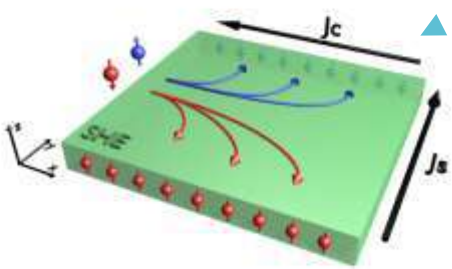

Inverse SHE

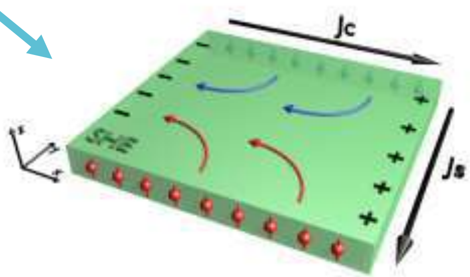

Reversal of the magnetization

From J.-M. George ISOE2017 lecture

Spin signal in metallic devices

Van Wees *et al.*

F. J. Jedema *et al.*, PRB, 67 085319 (2003)

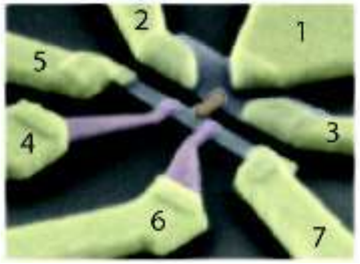

Ni, Py, Co, Al, Cu

Otani *et al.*

T. Kimura, *et al.*, PRB 72, 014461 (2005)
L. Vila *et al.*, PRL 99, 226604 (2007)

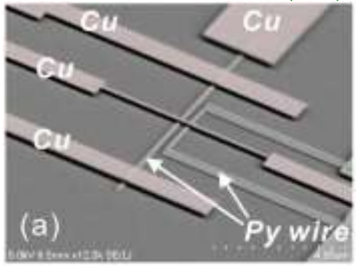

Py, Co, Cu, Ag, Mn, MgO

Valenzuela *et al.*

S. O. Valenzuela *et al.*, Nature 442, 176 (2006)

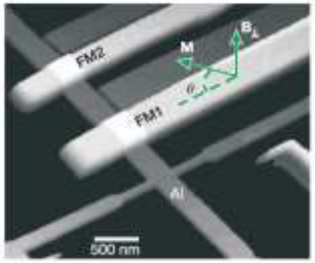

Co, CoFe, Al, AlO

Hoffmann *et al.*

G. Mihajlović *et al.*, PRL 103, 166601 (2009)

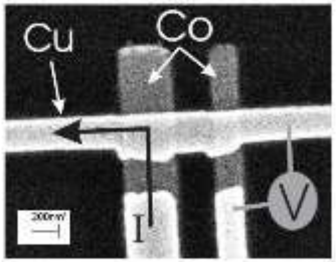

Py, Co, Ag, Cu, Au

Studied effects:

Non-local, Seebeck, Hanle, SHE effects ...

Usually:

Geometries: w ≈ 100nm

Spin signal ≈ mΩ

From J.-M. George ISOE2017 lecture

Question session

?

Spin-Orbit at Surfaces and Interfaces – the Rashba Effect

Interface electric field

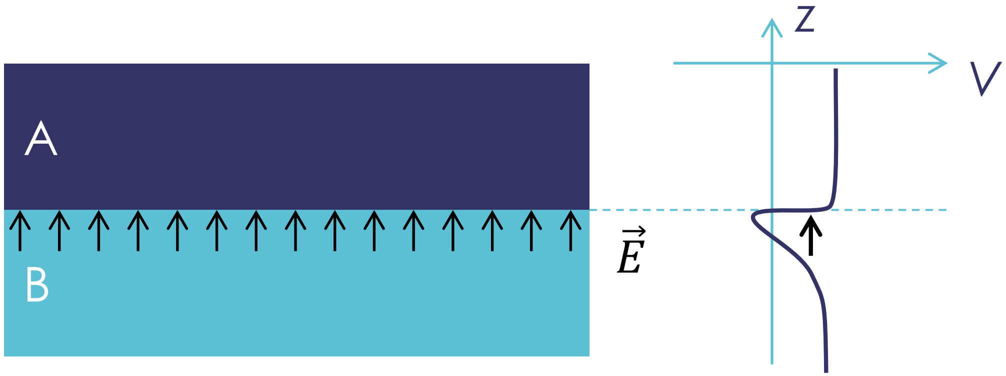

Valid for 2DEG, also for metals, but…

Relativistic correction: spin-orbit coupling

Rashba Hamiltonian: $H_R \propto (\hat{z} \wedge \vec{k}) \cdot \vec{S}$

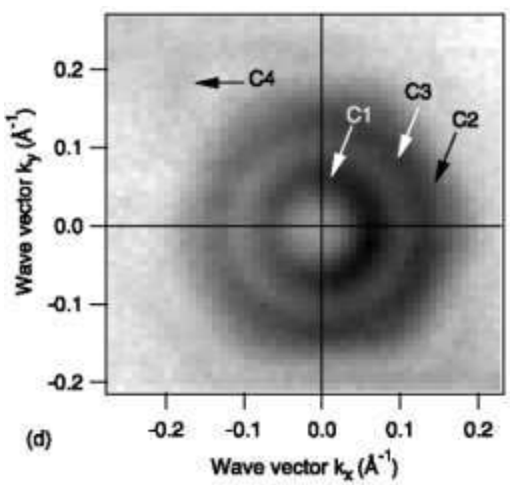

Bi|Ag (1 1 1)

Constant energy map at -0.17 eV

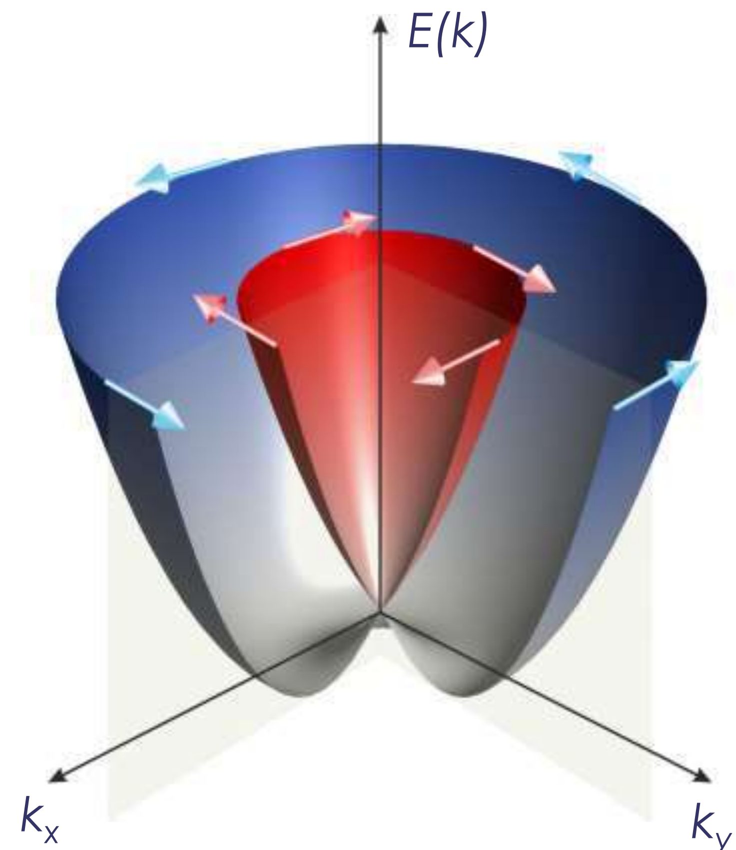

Ch. R. Ast *et al*, *Phys. Rev. Lett.* **98**, 186807 (2007)

A. Soumyanarayanan *et al*, *Nature* **539**, 509 (2016)

Spin-Orbit at Surfaces and Interfaces – Topological Insulator

Bulk energy gap, "inverted" band structure

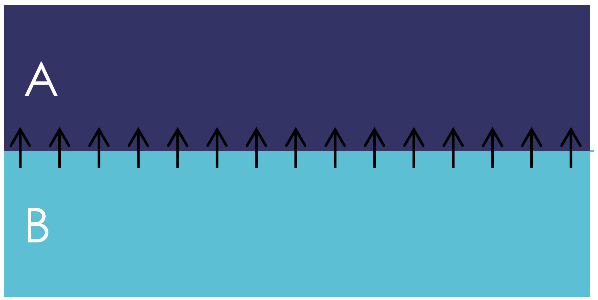

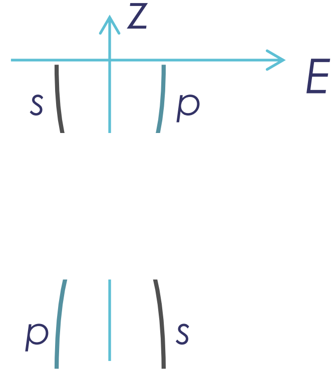

"inverted band"

Dirac cone surface state

- Dirac cone linear dispersion

- Topological insulator Hamiltonian:

$$H_{TI} = \hbar v_F (\hat{z} \wedge \vec{k}) \cdot \vec{\sigma}$$

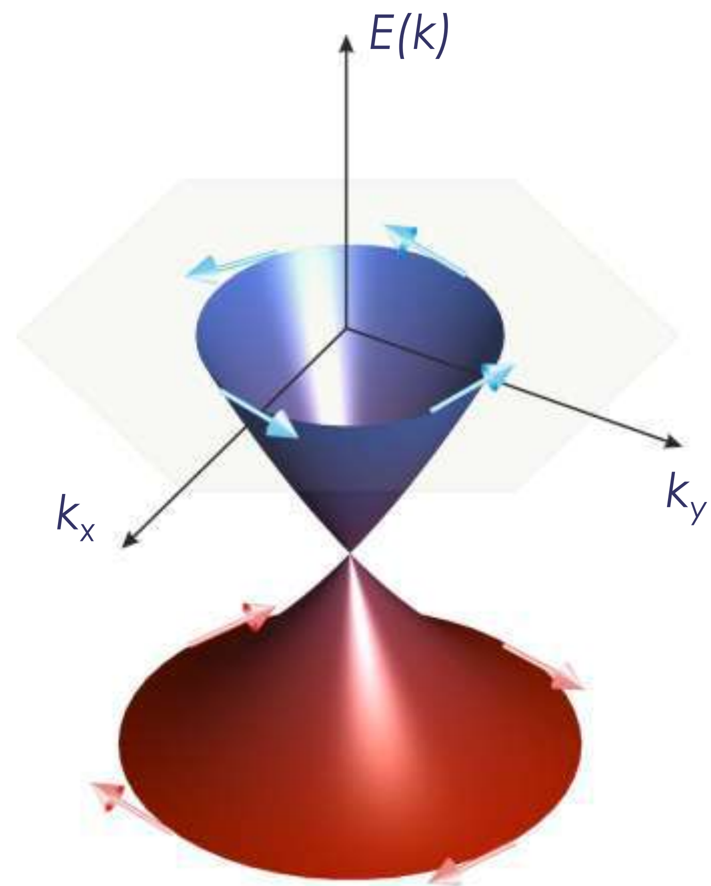

A. Soumyanarayanan *et al*, *Nature* **539**, 509 (2016)

Example: The Spin-Polarized Surface of α-Sn

- Previous experiments demonstrated spin-polarized surface states by ARPES

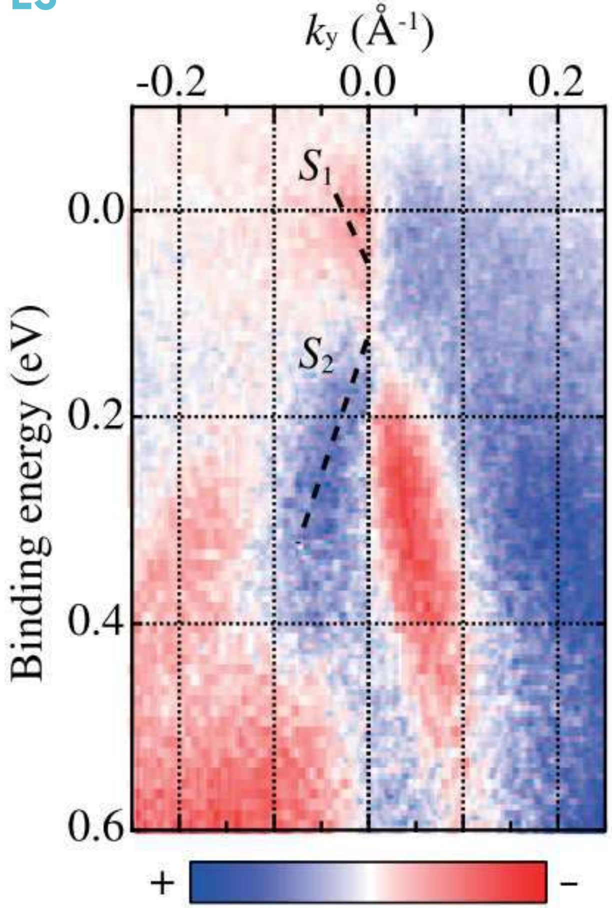

Y. Ohtsubo *et al*, *Phys. Rev. Lett.* **111**, 216401 (2013)

@ CASSIOPEE beamline

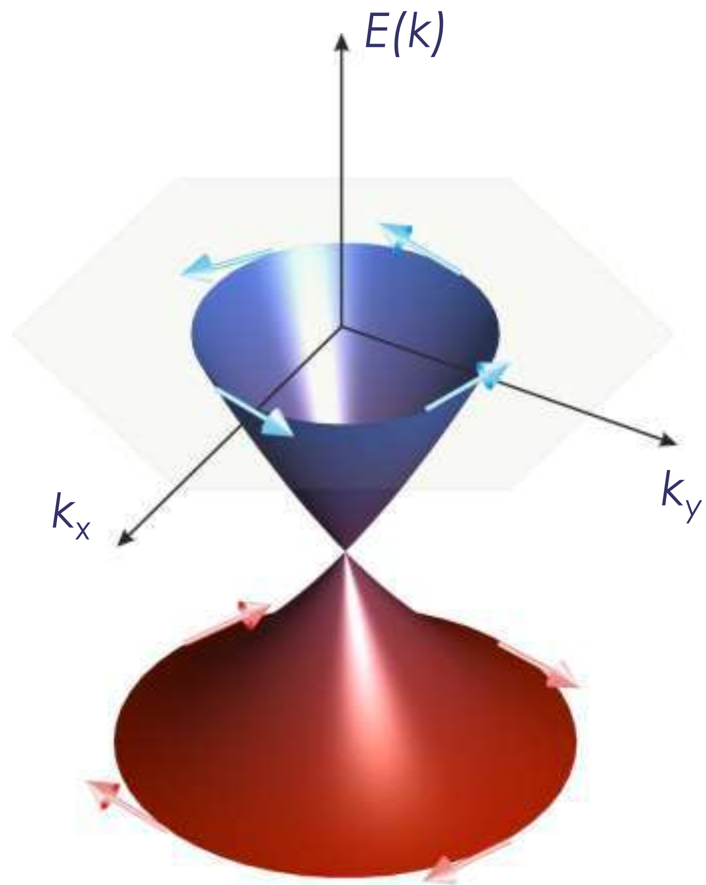

Change of helicity with Fermi level

How to use these Surface States for Spintronics?

Surface states of topological insulators can be very efficient for charge to spin "conversion"

Similarly:

$$q_{\mathrm{EE}} = \frac{J_s^{3D}}{J_c^{2D}}$$

Edelstein length, analog of SHA, is a new parameter characterizing the efficiency at surfaces:

$$\lambda_{\mathrm{IEE}} = \frac{J_c^{2D}}{J_s^{3D}}$$

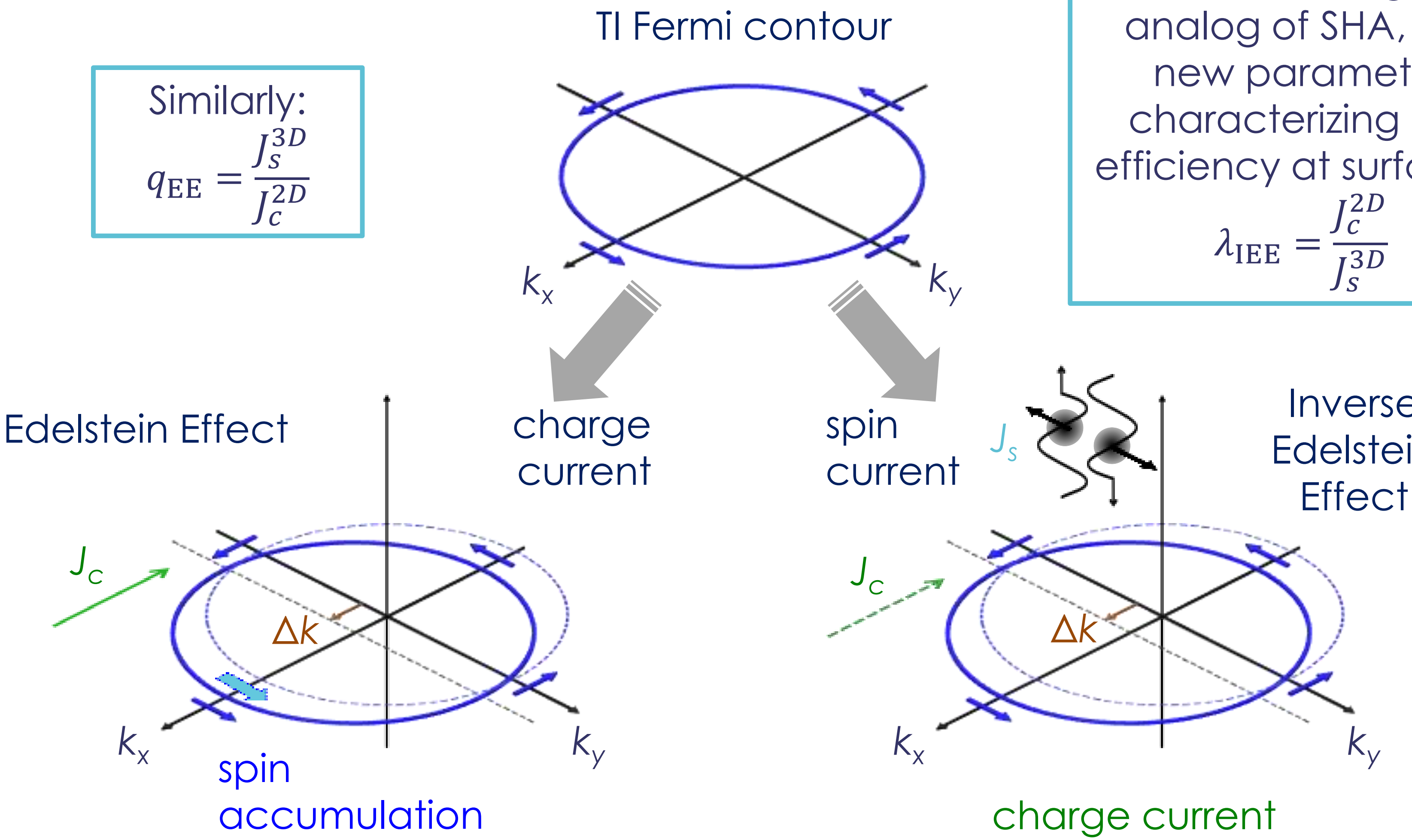

See, e.g., S. Zhang and A. Fert, *Phys. Rev. B* **94**, 184423 (2016)

How to preserve the Surface States?

- **To make any use of the surface states, you need to connect them without destroying them…**
  - How are the surface state evolving with metals in contact?
  - Spin-to-charge conversion at the interface depending on the surface states?

- **We need both growth facility and ARPES**
  - This combination is found on CASSIPEE beamline at SOLEIL SYNCHROTRON

- **We select the α-Sn, which growth was already realized at SOLEIL.**

Strained α-Sn – a Peculiar Type of Topological Insulator

Theoretically predicted in 2007

by L. Fu and C. L. Kane, *Phys. Rev. B* **76**, 045302 (2007)

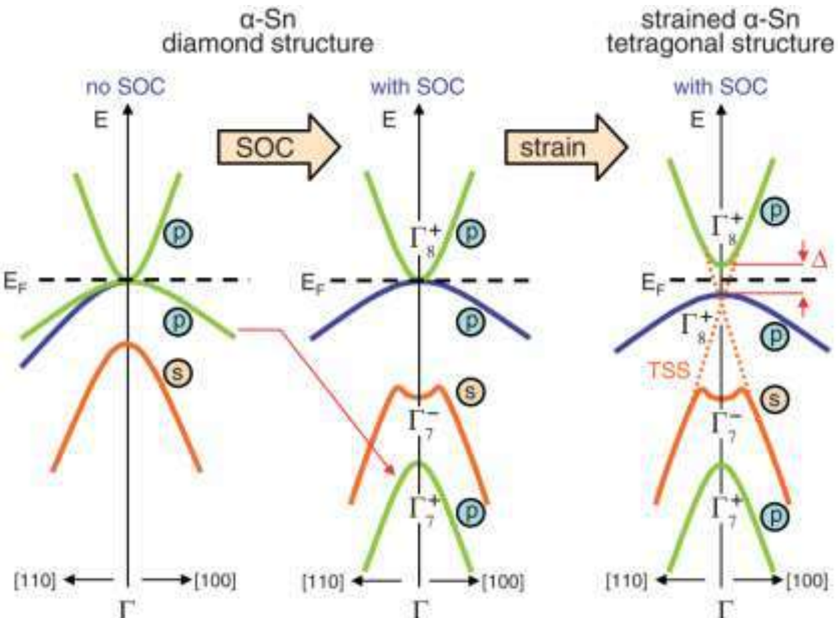

A. Barfuss *et al*, *Phys. Rev. Lett.* **111**, 157205 (2013)

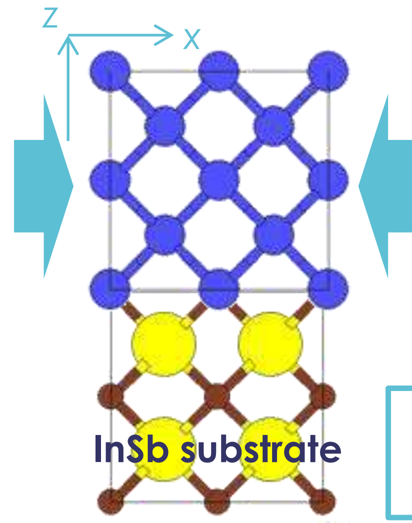

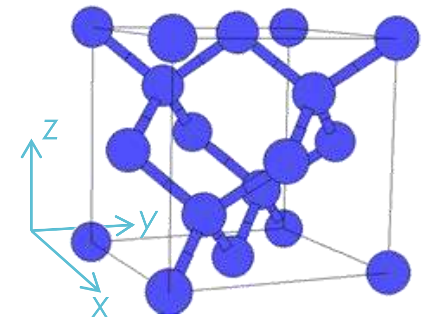

Compressive strain: 0.16%

Finite size effect: Quantification of the energy levels

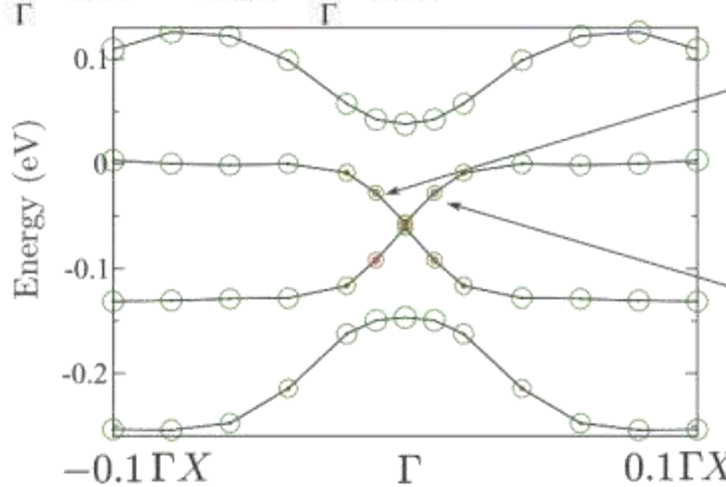

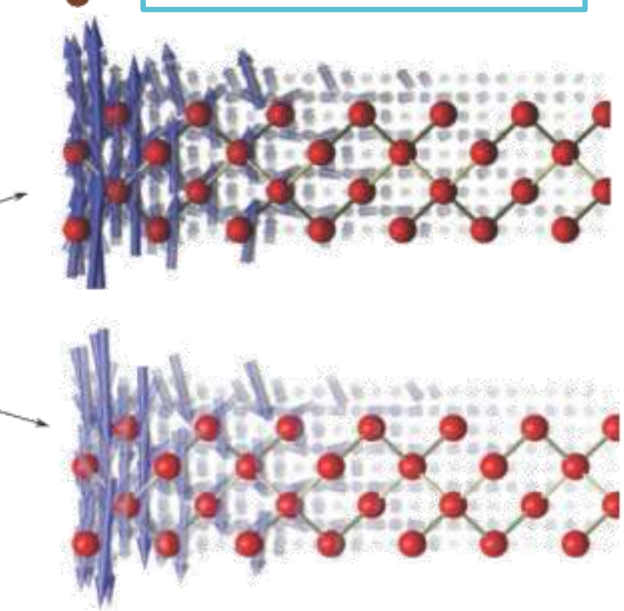

S. Küfner *et al*, *Phys. Rev. B* **90**, 125312 (2014)

CASSIOPEE Beamline Overview

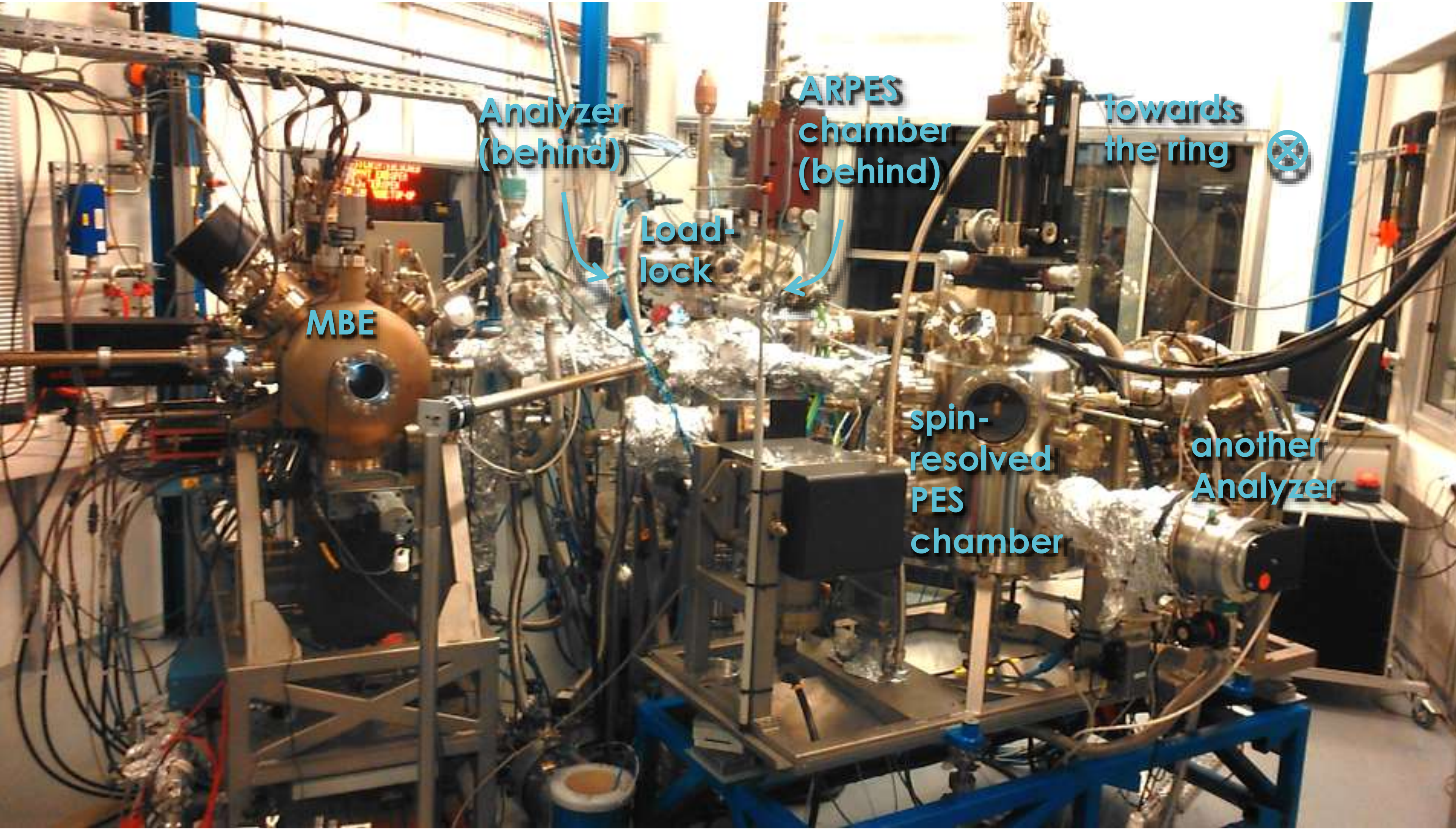

ARPES Measurements

Fe deposition: $v_F \approx 5-6 \cdot 10^5$ m/s $\quad H_{TI} = \hbar v_F (\hat{z} \wedge \vec{k}) \cdot \vec{\sigma}$

Ag deposition:

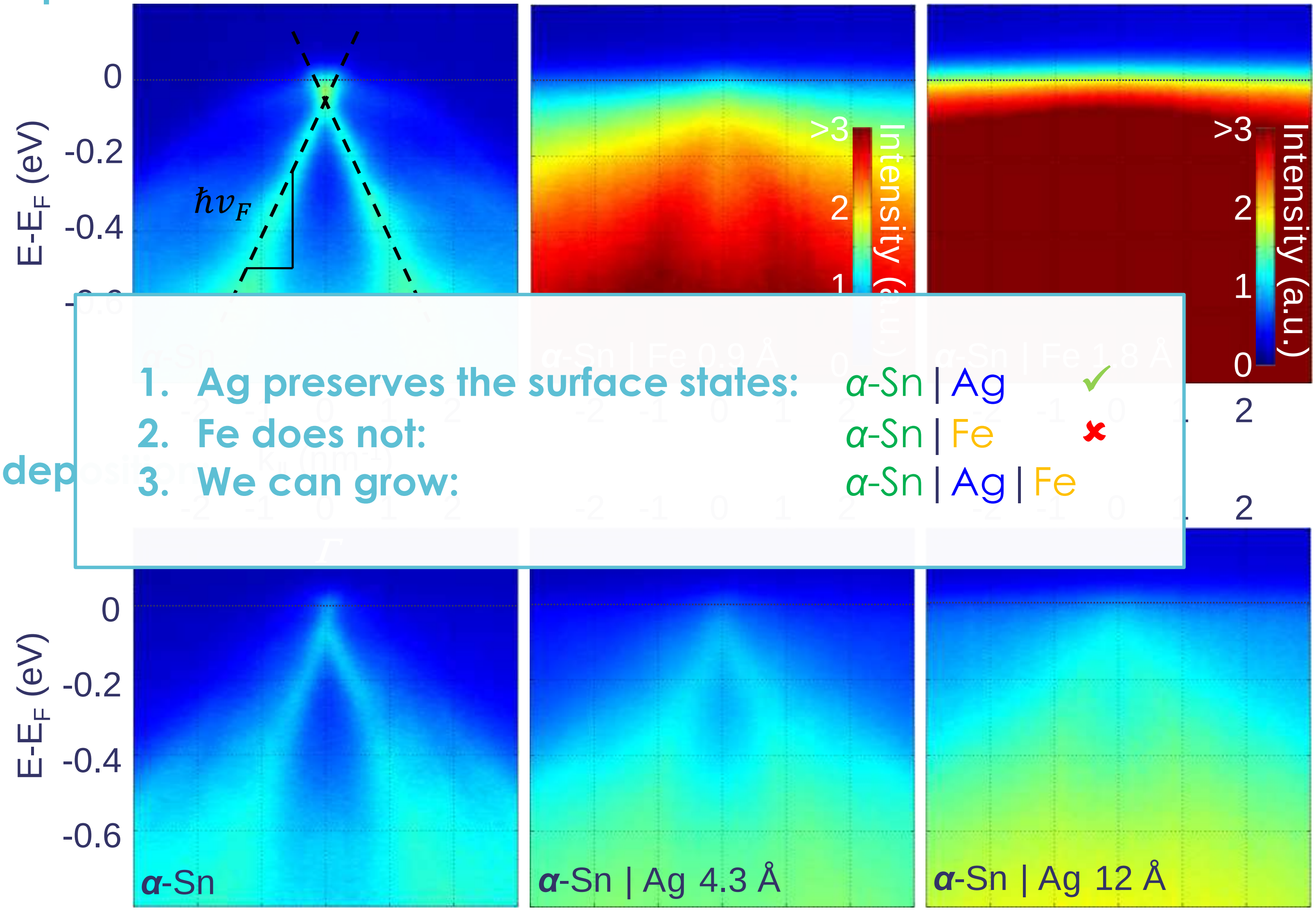

1. Ag preserves the surface states: α-Sn | Ag ✓
2. Fe does not: α-Sn | Fe ✗
3. We can grow: α-Sn | Ag | Fe

J.-C. Rojas-Sánchez *et al*, *Phys. Rev. Lett.* **116**, 096602 (2016)

Spin to Charge Conversion Technique: Spin-Pumping

Spin-pumping – IEE: a technique of choice

- Pure spin current (no charge current associated)
- Easy lithography (if any)
- Spin to charge ➔ easy voltage detection

…but difficulties are also present!

- Many variables must be determined to evaluate the spin current

$$j_S = \frac{g_{\text{eff}}^{\uparrow\downarrow}\gamma^2\hbar\, h_{\text{rf}}^2}{8\pi\,\alpha^2}\left[\frac{4\pi M_{\text{eff}}\gamma + \sqrt{(4\pi M_{\text{eff}}\gamma)^2 + 4\omega^2}}{(4\pi M_{\text{eff}}\gamma)^2 + 4\omega^2}\right]\left(\frac{2e}{\hbar}\right)$$

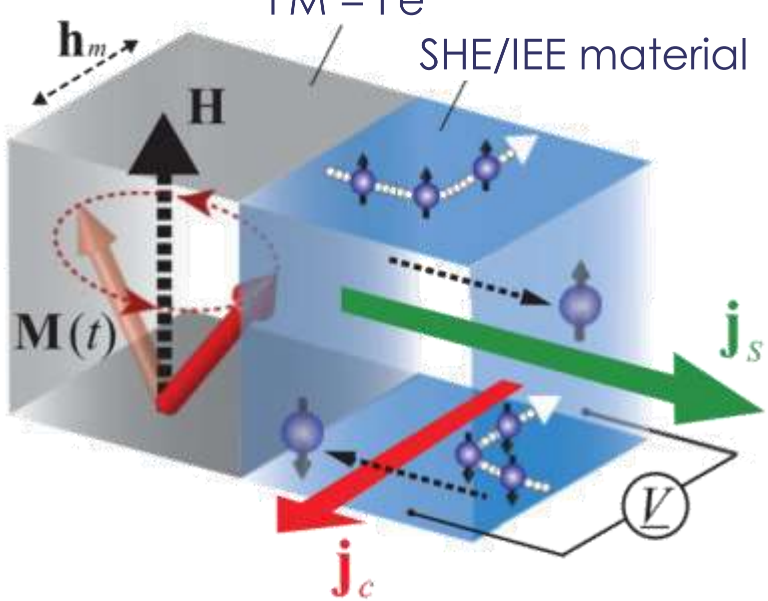

FMR	spin accumulation
↓	
Spin current	relaxation in nearby material
↓	
IEE	conversion through SOC
↓	
Voltage	charge accumulations

H. Nakayama *et al*, *Phys. Rev. B* **85**, 144408 (2012)

Ferromagnetic resonance: determination of the spin current

- From absorption curve:
  - fixed rf frequency f
  - peak-to-peak line-width ΔH_{pp}
  - resonant field H_{res}

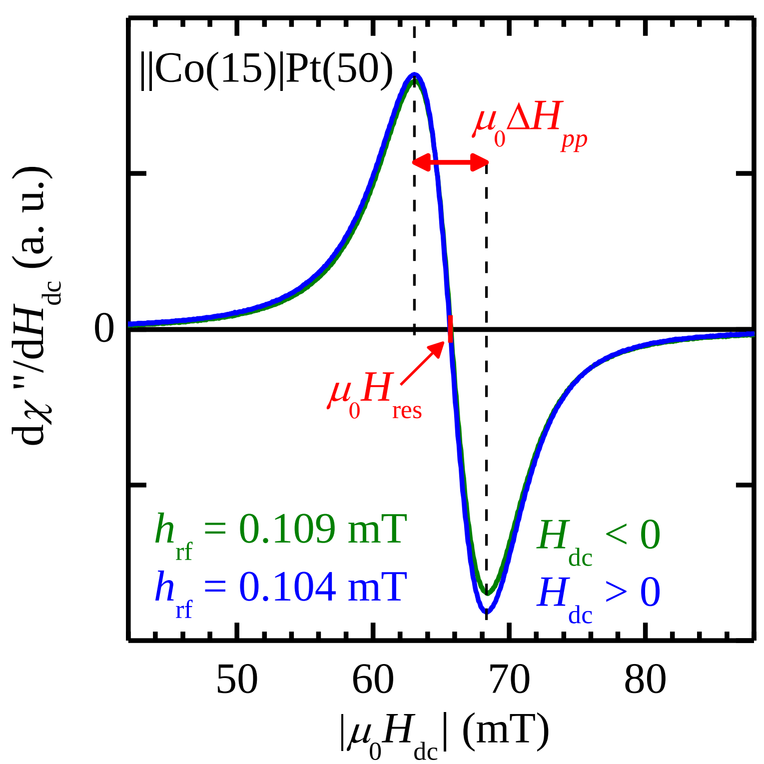

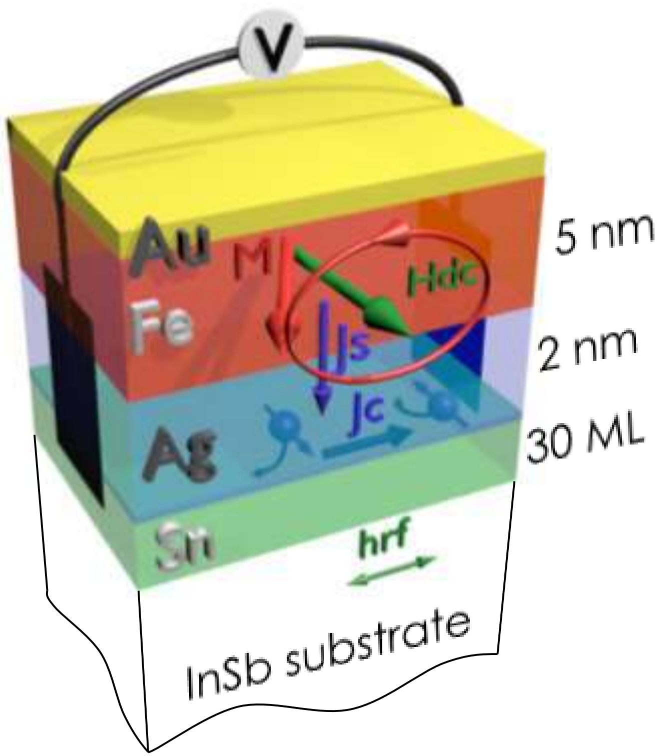

Determination of the Spin Current from FMR

Ferromagnetic resonance: determination of the spin current

$$j_s = \frac{g_{\text{eff}}^{\uparrow\downarrow}\gamma^2\hbar\, h_{\text{rf}}^2}{8\pi\,\alpha^2}\left[\frac{4\pi M_{\text{eff}}\gamma + \sqrt{(4\pi M_{\text{eff}}\gamma)^2 + 4\omega^2}}{(4\pi M_{\text{eff}}\gamma)^2 + 4\omega^2}\right]\left(\frac{2e}{\hbar}\right)$$

$$\Delta H_{pp} = \Delta H_0 + \frac{2}{\sqrt{3}}\left(\frac{\omega}{\gamma}\right)\alpha \qquad \left(\frac{\omega}{\gamma}\right)^2 = (B + \mu_0 H_K)(B + \mu_0 H_K + \mu_0 M_{\text{eff}})$$

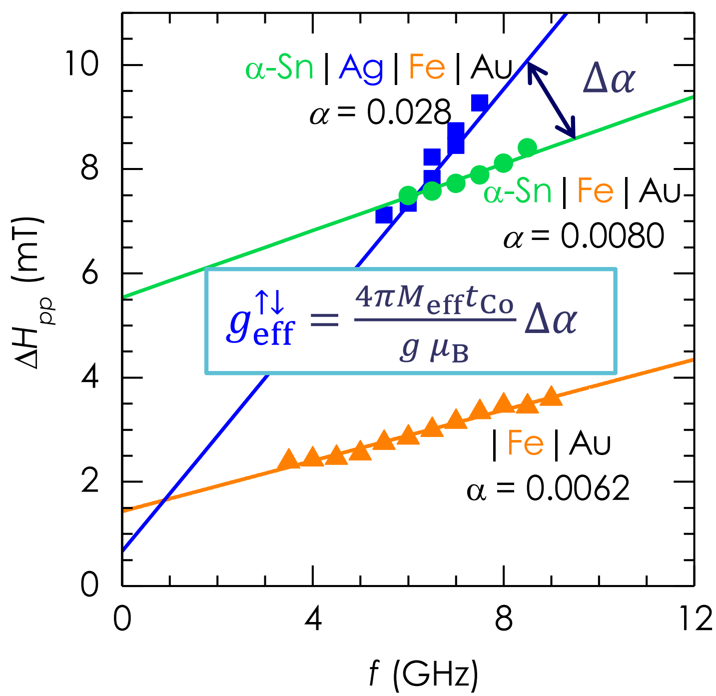

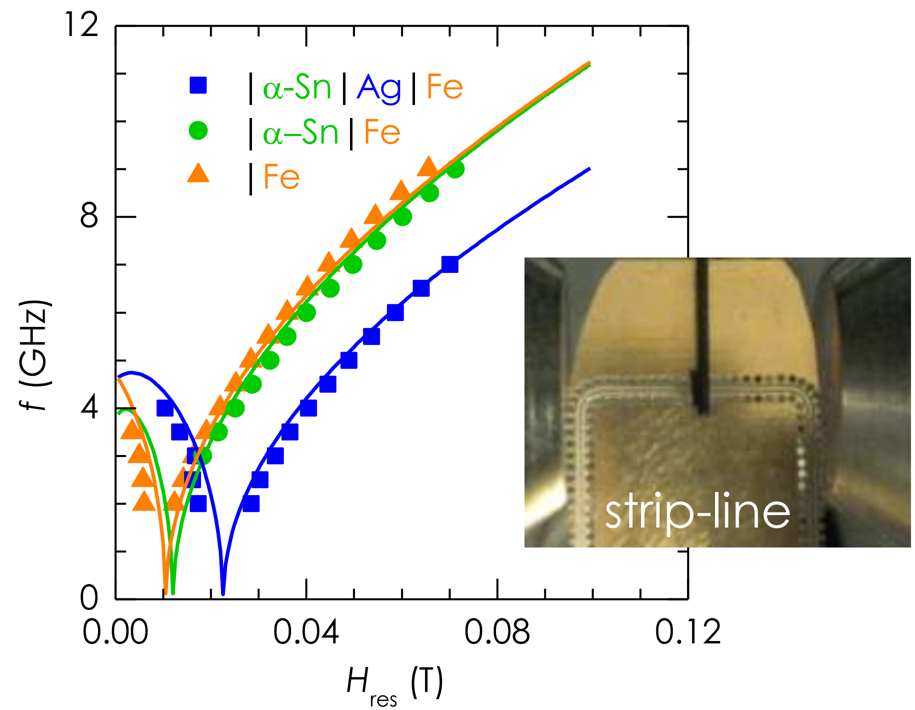

Experimental Configuration for Spin Pumping and ISHE

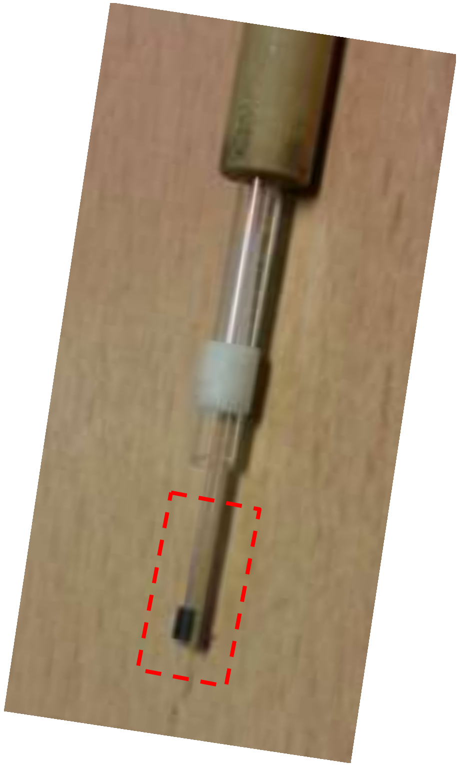

h_{rf} determined using cavity Q factor with sample inside cavity.

inside a split-cylinder resonant cavity.

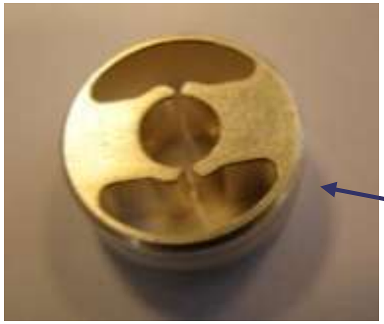

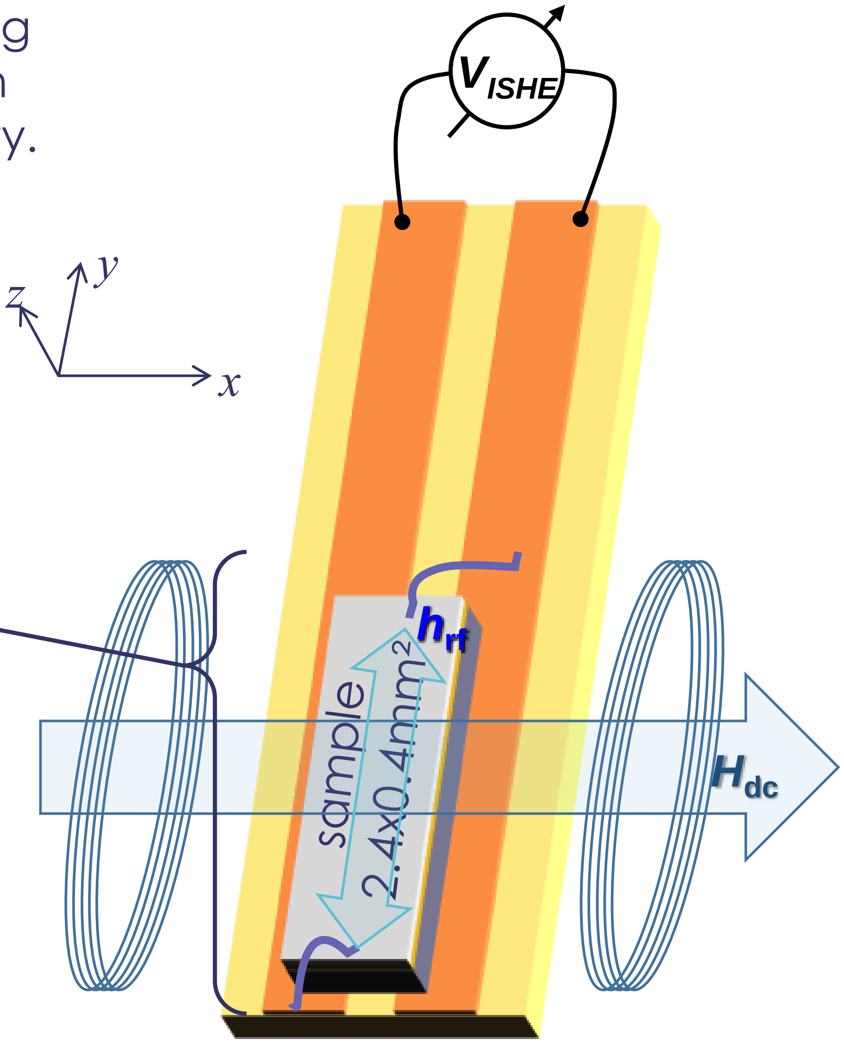

(Commercial Bruker EPR)

Inverse Edelstein Effect/Spin-Pumping Results on α-Sn Samples

- Reference sample InSb | Fe | Au
- Sample with Fe in direct contact: InSb | α-Sn | Fe | Au
- With Ag interlayer, preserving the surface state: InSb | α-Sn | Ag | Fe | Au

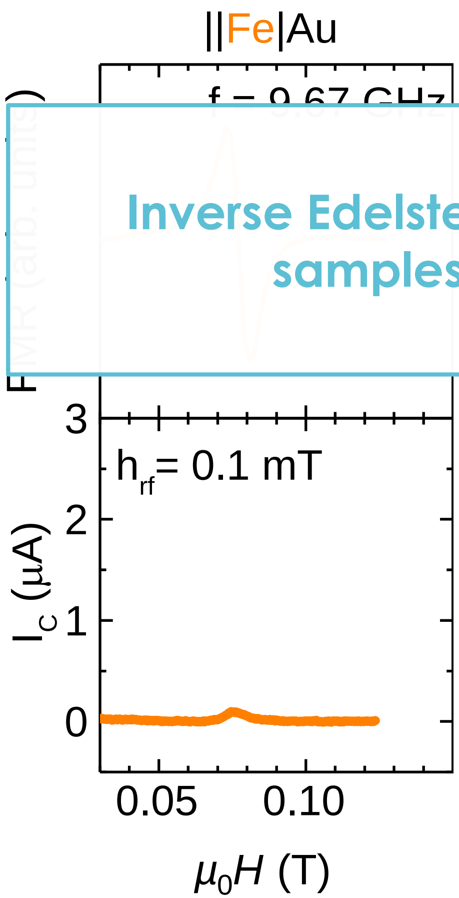

Inverse Edelstein effect (IEE) is only observed for samples with preserved Dirac cone

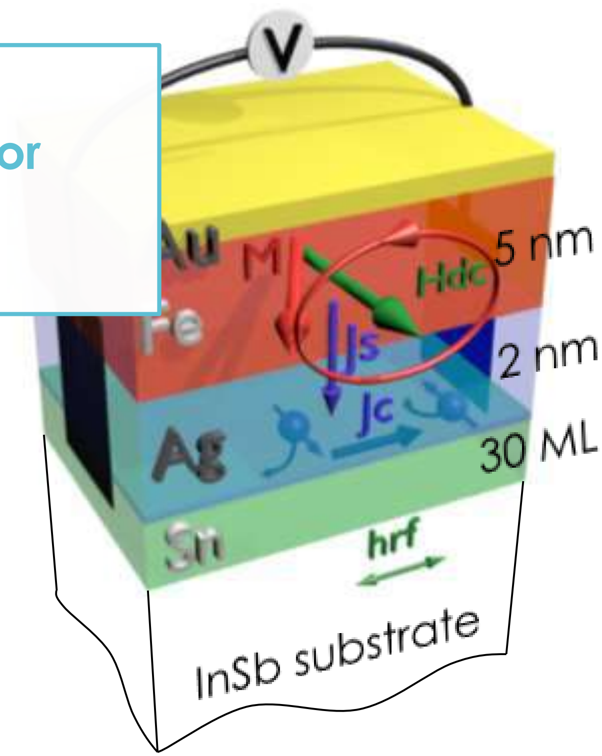

J.-C. Rojas-Sánchez *et al*, *Phys. Rev. Lett.* **116**, 096602 (2016)

Spin-Orbit at Surfaces and Interfaces – the Rashba Effect

Tunable Rashba and IEE at $SrTiO_3$ | $LaAlO_3$ interface

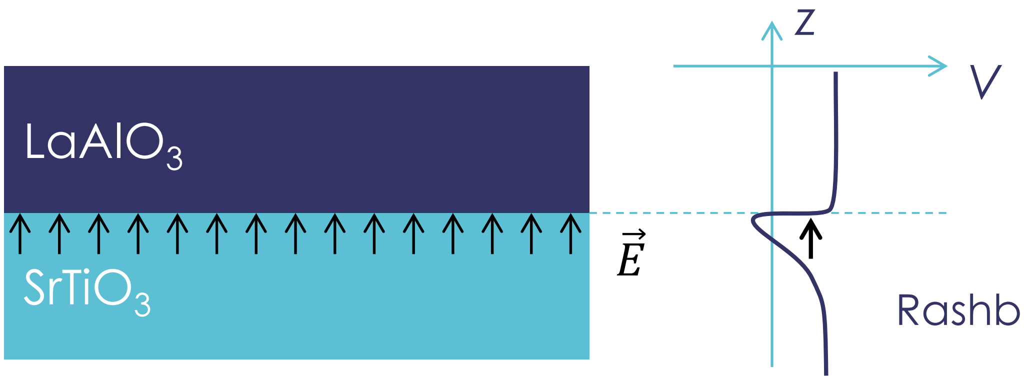

Rashba Hamiltonian: $H_R \propto (\hat{z} \wedge \vec{k}) \cdot \vec{\sigma}$

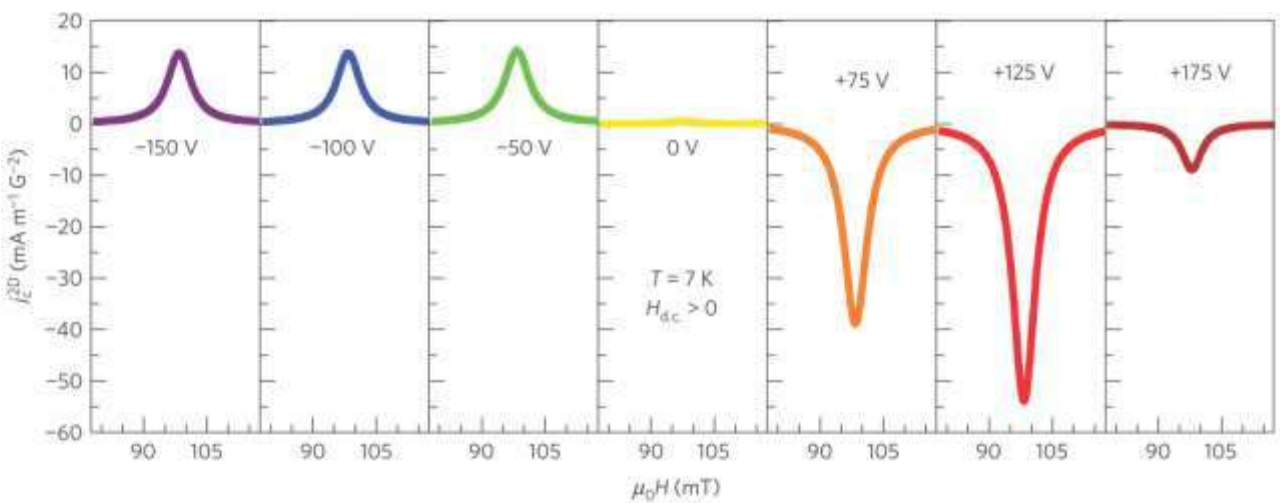

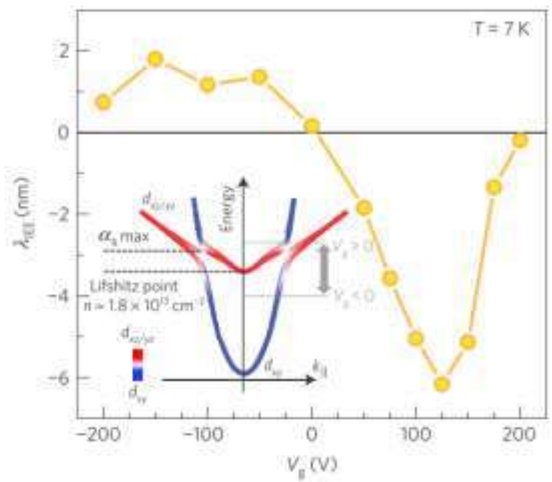

E. Lesne *et al*, *Nat. Mater.* **15**, 1261 (2016)

Results: Record Values for the Conversion Efficiency!

Spin-to-charge conversion $\lambda_{\text{IEE}} = \frac{J_s}{J_c}$

- Topological insulator surface state

  α-Sn: $\lambda_{\text{IEE}} \approx 2.1$ nm

  J.-C. Rojas-Sánchez *et al*, *Phys. Rev. Lett.* **116**, 096602 (2016)

- Rashba interfaces:

  Ag | Bi: $\lambda_{\text{IEE}} \approx 0.3$ nm

  J.-C. Rojas-Sánchez *et al*, *Nat. Comm.* **4**, 2944 (2013)

  $LaAlO_3$ | $SrTiO_3$: $\lambda_{\text{IEE}} \approx 2 \leftrightarrow -6$ nm

  E. Lesne *et al*, *Nat. Mater.* **15**, 1261 (2016)

- Bulk materials:

  Pt, Ta, W, … $\lambda^* = \theta_{\text{SHE}} \ell_{sf} \leq 0.2 - 0.4$ nm

J.-C. Rojas-Sánchez *et al*, *Phys. Rev. Lett.* **116**, 096602 (2016)
J.-C. Rojas-Sánchez & A. Fert, *Phys. Rev. Appl.* **11**, 054049 (2019)

Question session

?

Magnetization textures and DMI

Dzyaloshinskii-Moriya Interaction

Antisymmetric exchange term:

$$H_{H+DM} = -J\sum(\vec{S}_i \cdot \vec{S}_j) - \sum \vec{d}_{ij} \cdot (\vec{S}_i \times \vec{S}_j)$$

Exchange DMI

I. Dzyaloshinskii, *J. Phys. Chem. Solids* **4**, 241 (1958)
T. Moriya, *Phys. Rev. Lett.* **4**, 228 (1960)

How to obtain such a term?

- Spin-orbit inte
- Break the inve

SP-STM of a Mn monolayer on W(110):

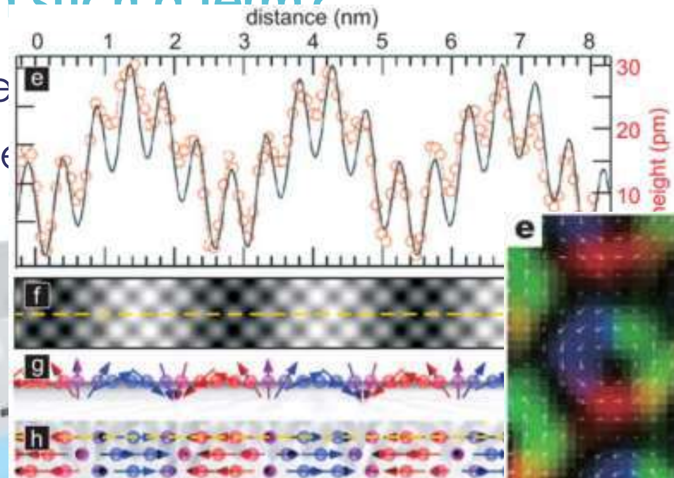

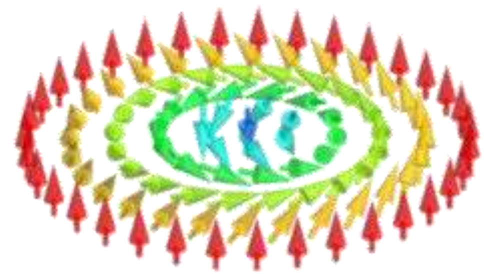

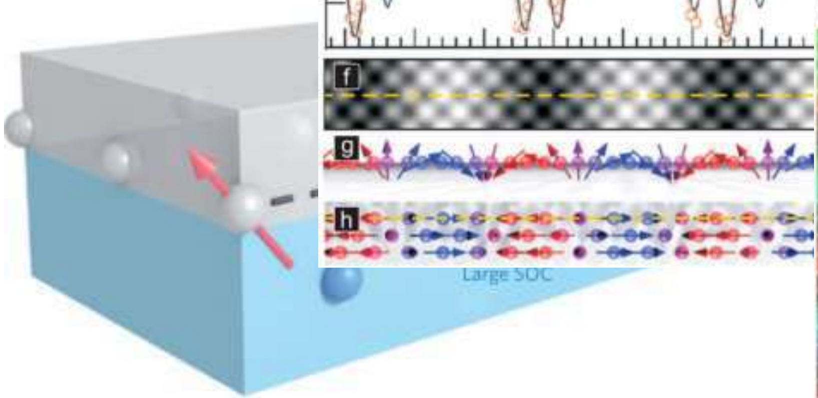

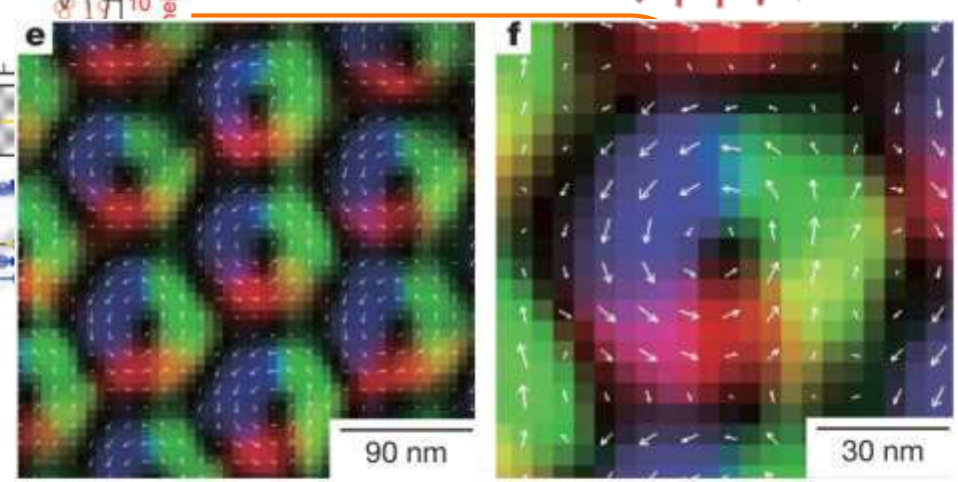

A. Fert *et al*, *Nature Nanotechnol.* **8**, 152 (2013)

A. Fert, *Mater. Sci. Forum* **59-60**, 439 (1990)

Bloch skyrmions in $Fe_{0.5}Co_{0.5}Si$ X. Z. Yu *et al*, *Nature* **465**, 901 (2010)

Dzyaloshinskii-Moriya Interaction

What can you expect from interfacial DMI in a simple magnetic stripe with PMA?

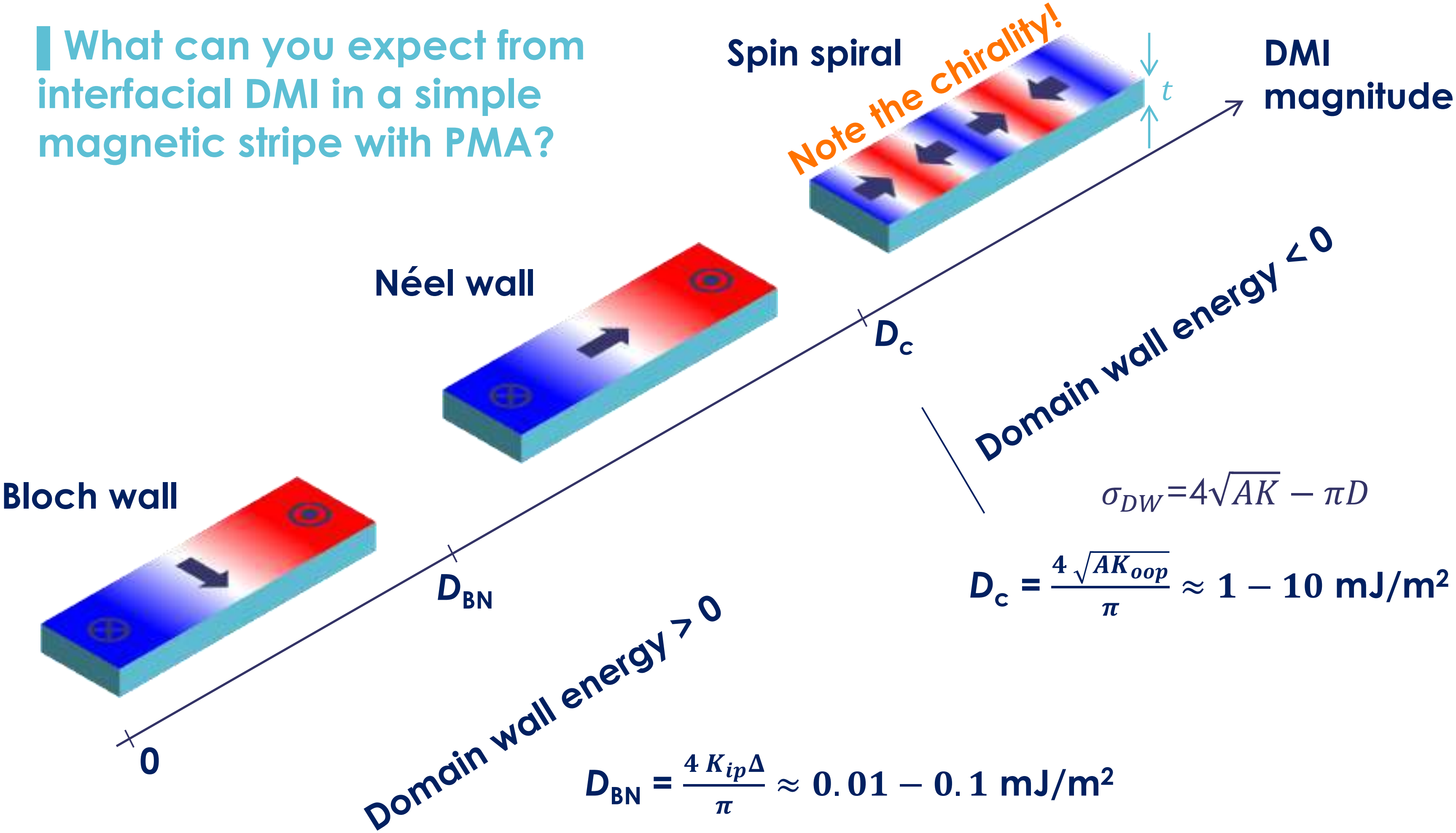

$$\sigma_{DW} = 4\sqrt{AK} - \pi D$$

$$D_c = \frac{4\sqrt{AK_{oop}}}{\pi} \approx 1 - 10 \text{ mJ/m}^2$$

$$D_{BN} = \frac{4K_{ip}\Delta}{\pi} \approx 0.01 - 0.1 \text{ mJ/m}^2$$

micromagnetic quantity:

$$D \propto d_{ij}/(a\,t)$$

$$A \propto J/a$$

Dzyaloshinskii-Moriya Interaction

What can you expect from interfacial DMI in a simple magnetic stripe with PMA?

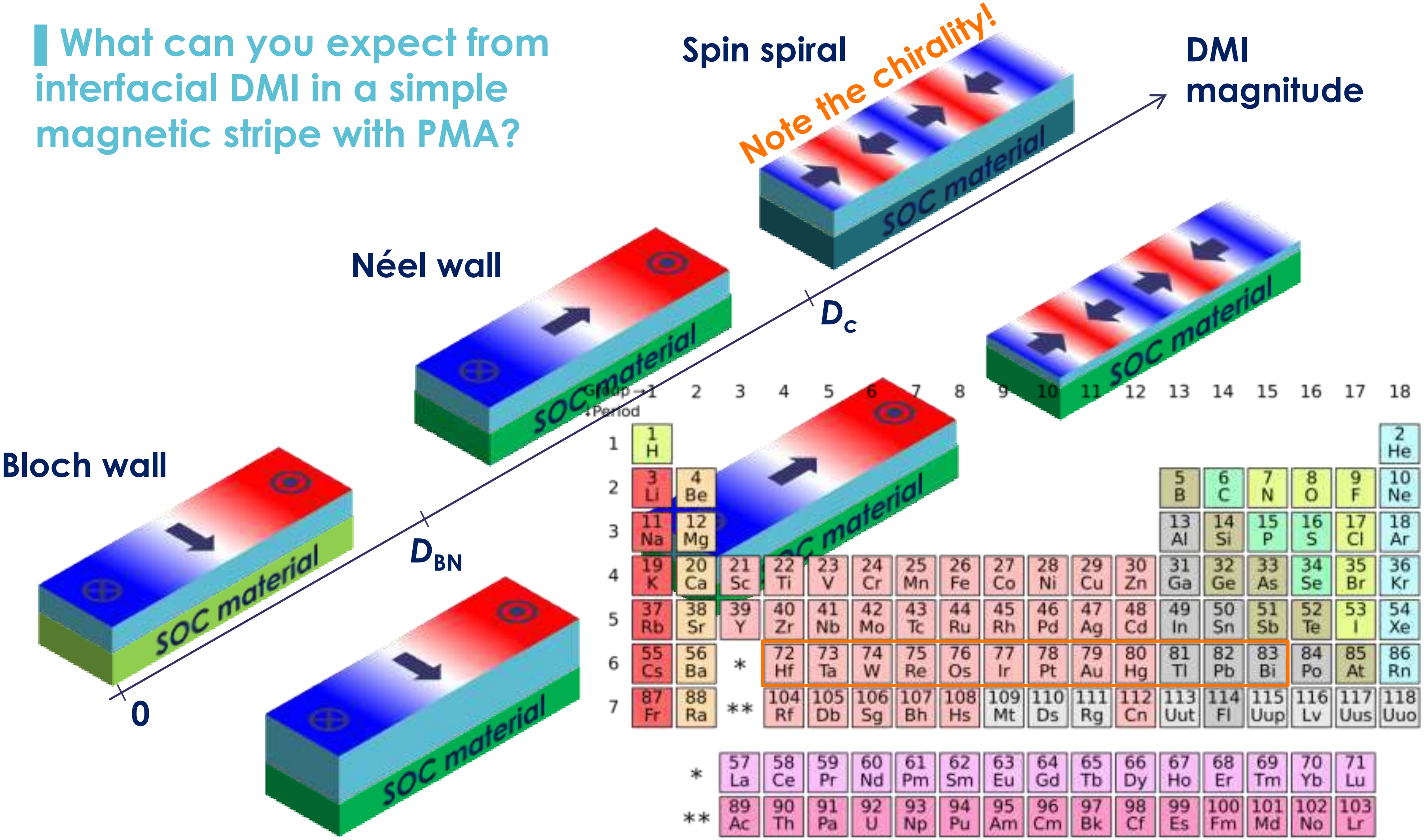

Wikipedia.org

Dzyaloshinskii-Moriya Interaction (moderate case)

What can you expect from interfacial DMI in a simple magnetic stripe with PMA?

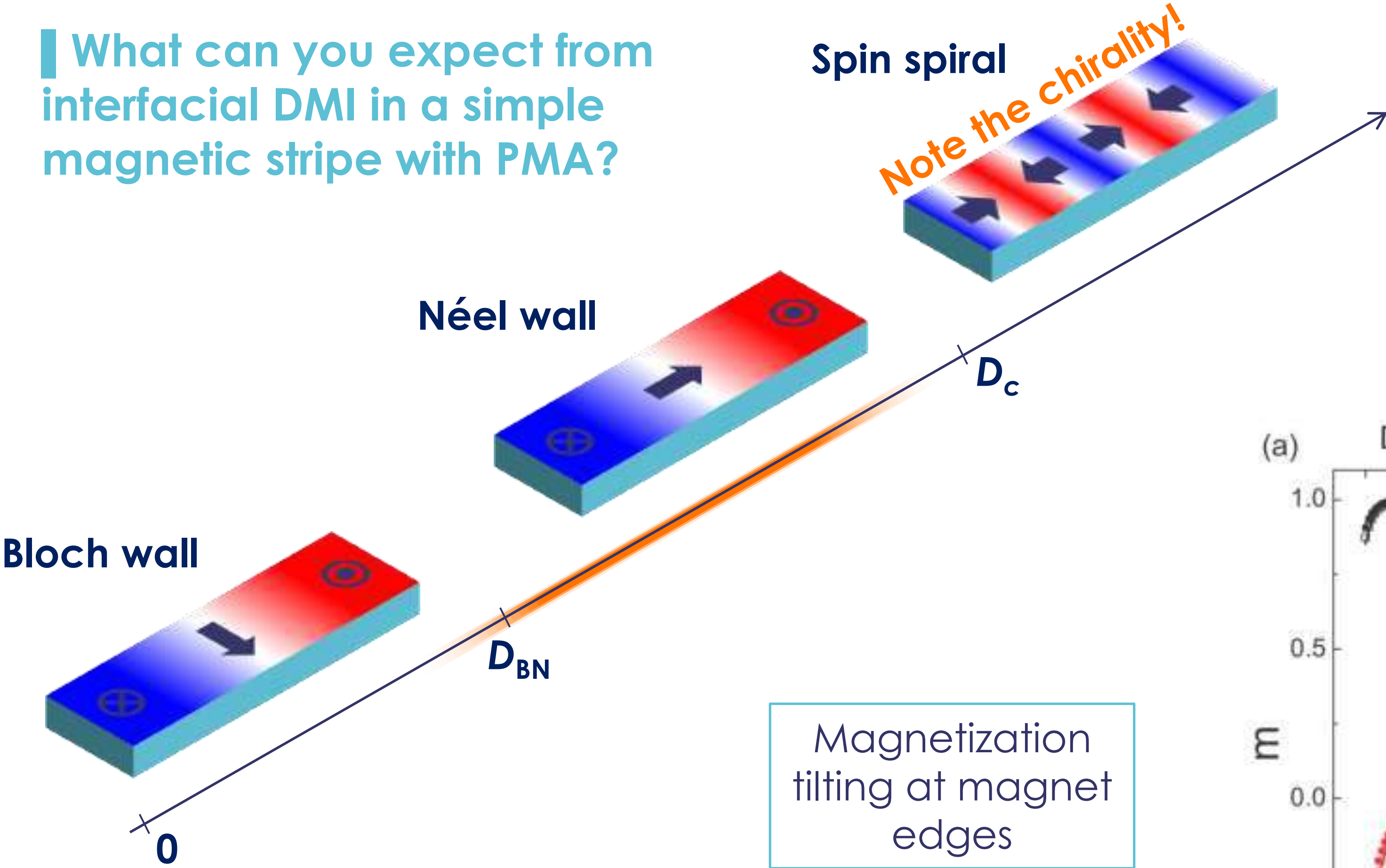

Magnetization tilting at magnet edges

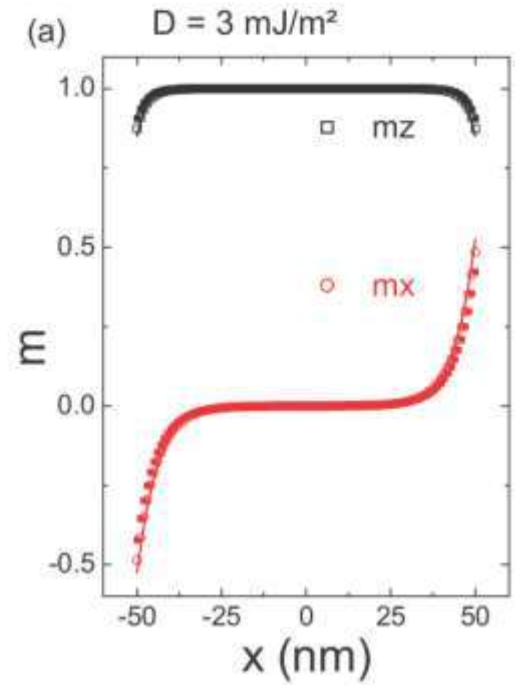

S. Rohart and A. Thiaville, *Phys. Rev. B* **88**, 184422 (2013)

Consequences of the DMI

Moderate DMI: still positive domain wall energy: $\sigma_{DW} = 4\sqrt{AK} - \pi D > 0$

- Favors Néel domain walls
- Tilts the magnetization at the edges of patterned structures

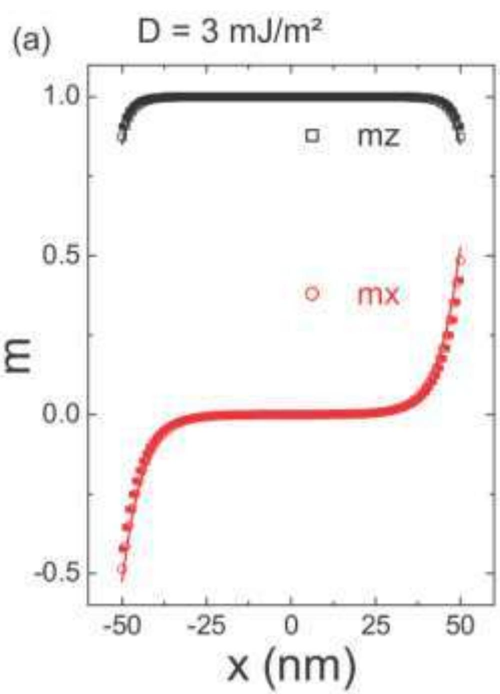

S. Rohart and A. Thiaville, *Phys. Rev. B* **88**, 184422 (2013)

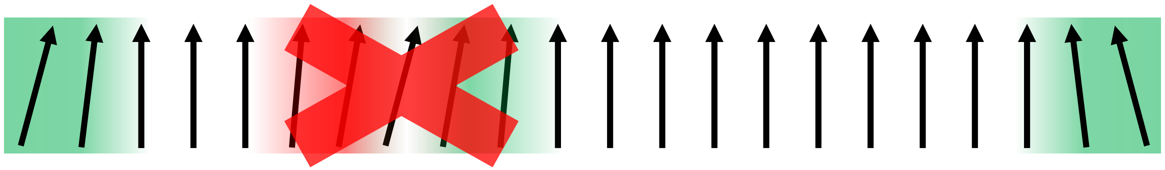

(Top view)

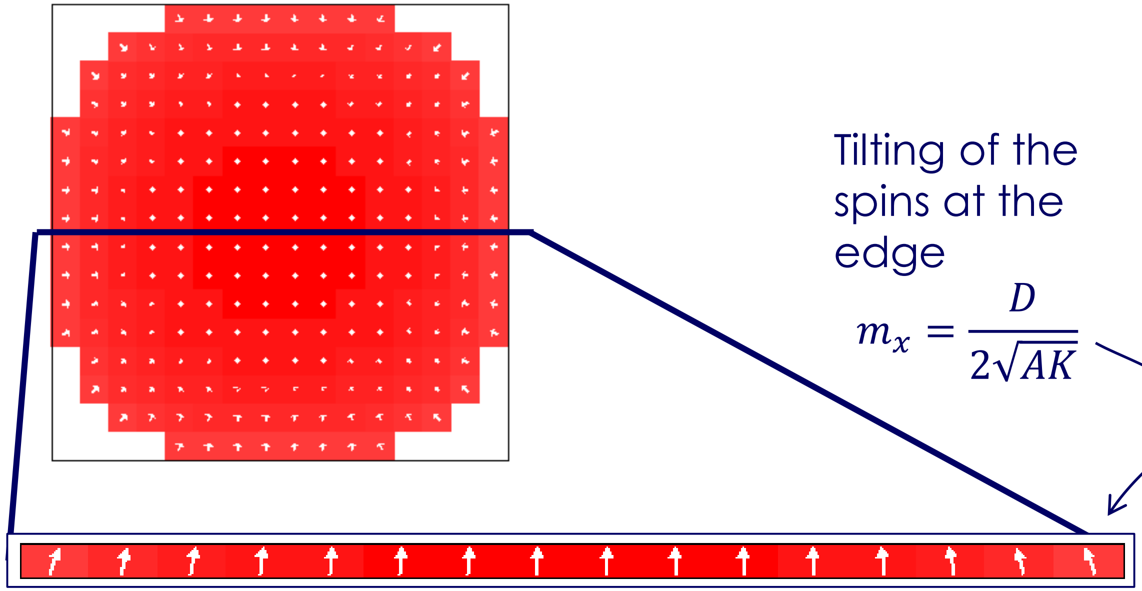

(Side view)

Tilting of the spins at the edge

$$m_x = \frac{D}{2\sqrt{AK}}$$

Dzyaloshinskii-Moriya Interaction (moderate case)

What can you expect from interfacial DMI in a simple magnetic stripe with PMA?

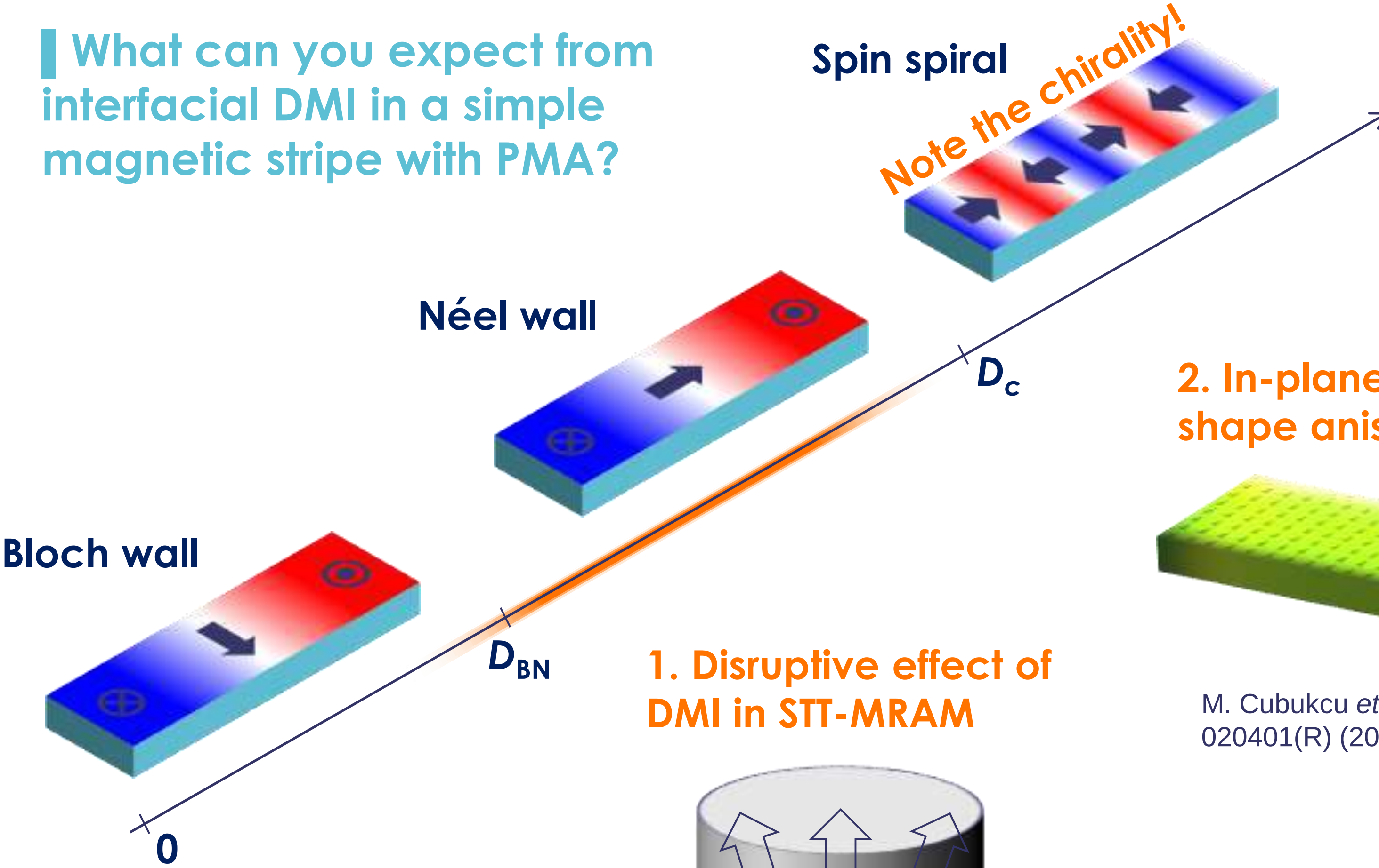

2. In-plane DM shape anisotropy

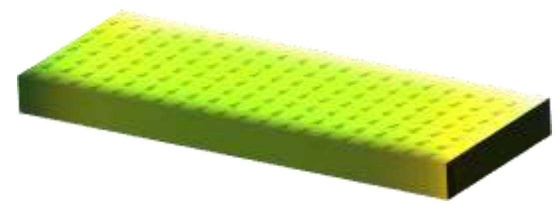

M. Cubukcu *et al*, *Phys. Rev. B* **93**, 020401(R) (2016)

1. Disruptive effect of DMI in STT-MRAM

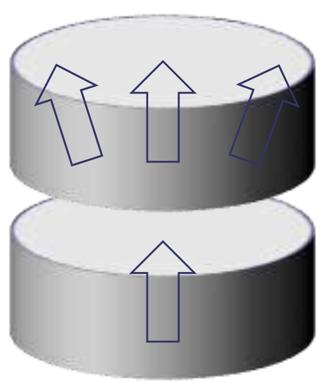

J. Sampaio *et al*, *Appl. Phys. Lett.* **108**, 112403 (2016)

3. Domain wall motion using spin-orbit torques

Dzyaloshinskii-Moriya Interaction (strong case)

What can you expect from interfacial DMI in a simple magnetic stripe with PMA?

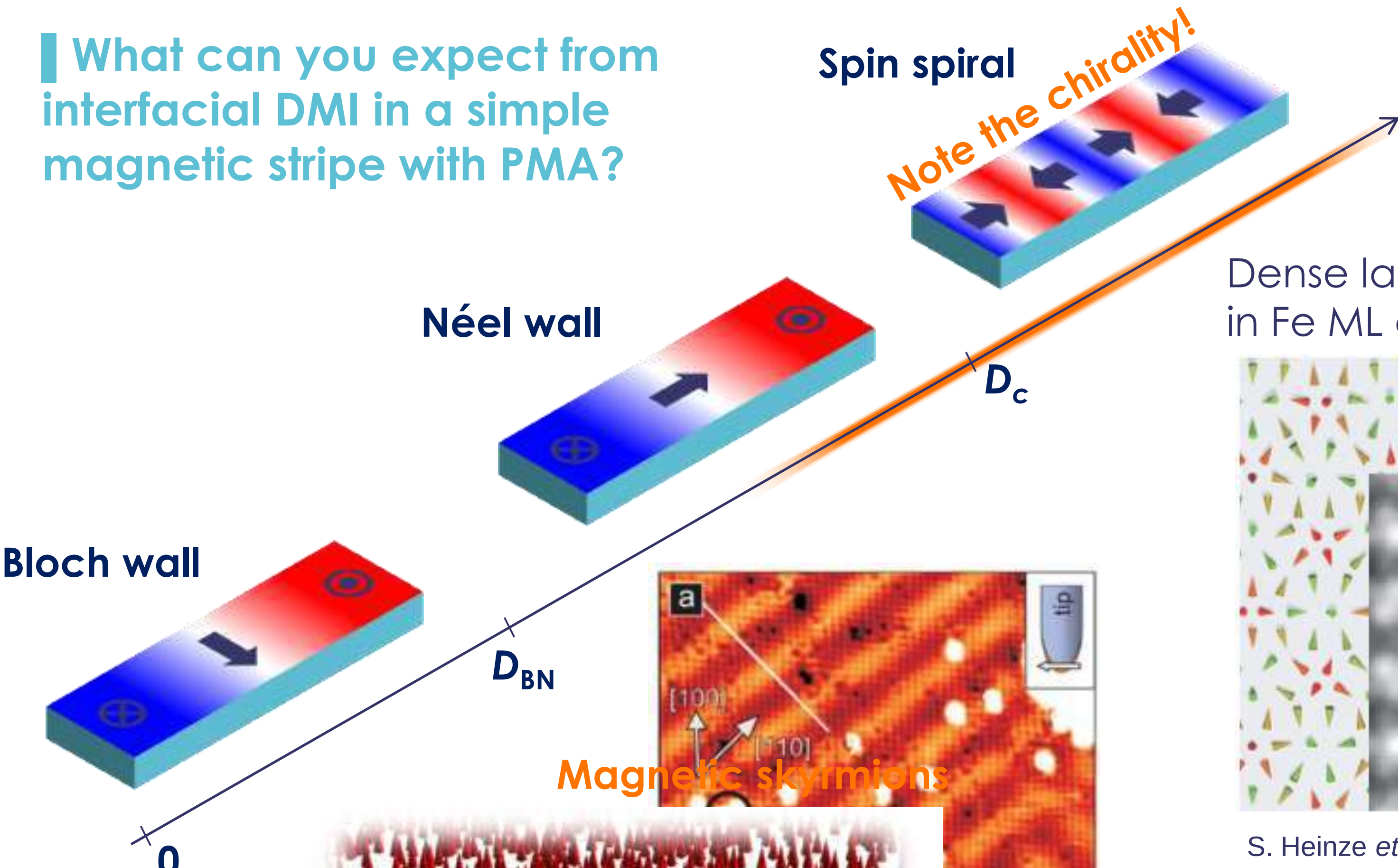

Dense lattice of skyrmions in Fe ML on Ir (111)

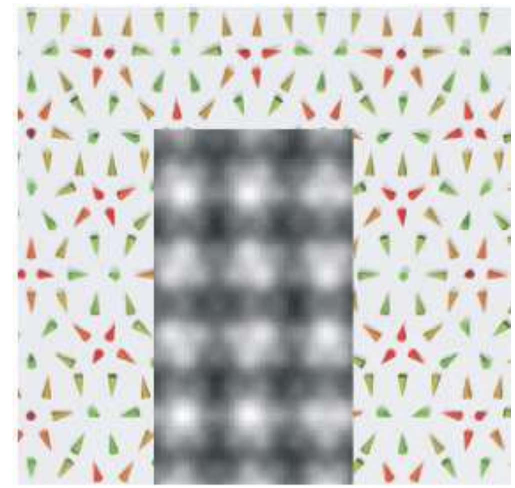

S. Heinze *et al*, *Nat. Phys.* **7**, 713 (2011)

Magnetic skyrmions

SP

mo

C. Moreau-Luchaire, *Nature Nanotechnol.* **11**, 444 (2016)
W. Legrand *et al*, *Nano Lett.* **17**, 2703 (2017)
A. Fert *et al*, *Nature Review Materials* **2**, 17031 (2017)
D. Maccariello *et al*, *Nature Nanotechnol.* **13**, 233 (2018)
J.-Y. Chauleau *et al*, *Phys. Rev. Lett.* **120**, 037202 (2018)
W. Legrand *et al*, *Science Adv.* **4**, eaat0415 (2018)
W. Legrand *et al*, arXiv:**1807**.04935
Rev. Lett. **101**, 027201 (2008)

Role of Intermixing at Interfaces

In sputtered samples: intermixing is present

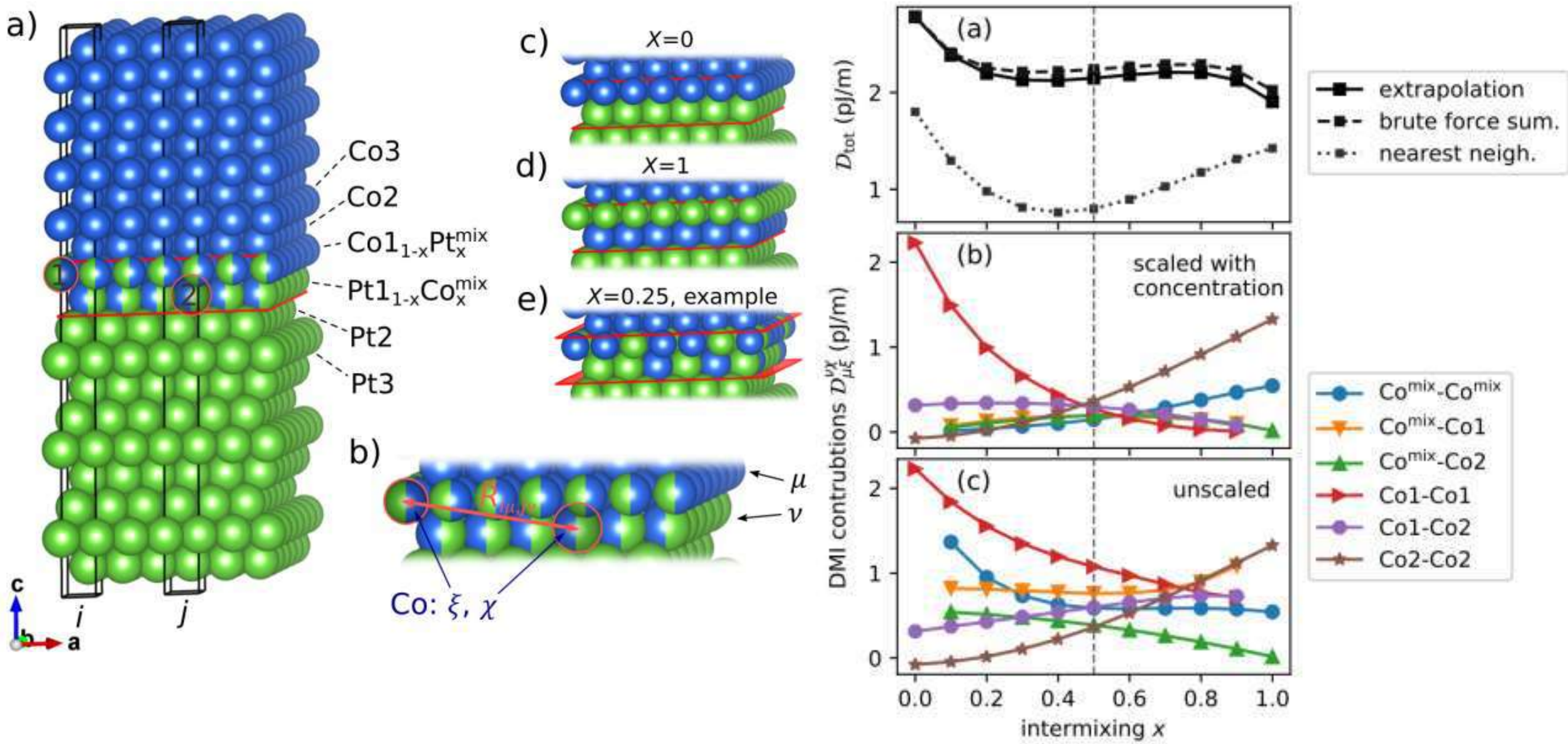

DMI is robust against intermixing!

B. Zimmermann *et al*, *Appl. Phys. Lett*, **113**, 232403 (2018)

Means of DMI Measurements

Direct measurement of the magnetic texture

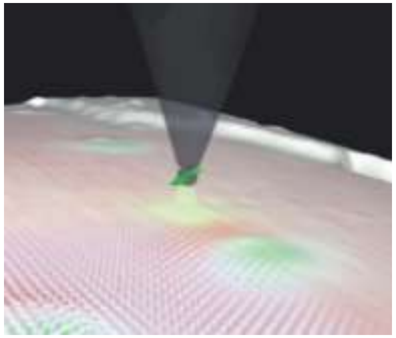

Scanning transmission microscopy (STM) with a spin-polarized probe

SP-STM of a Mn monolayer on W(110):

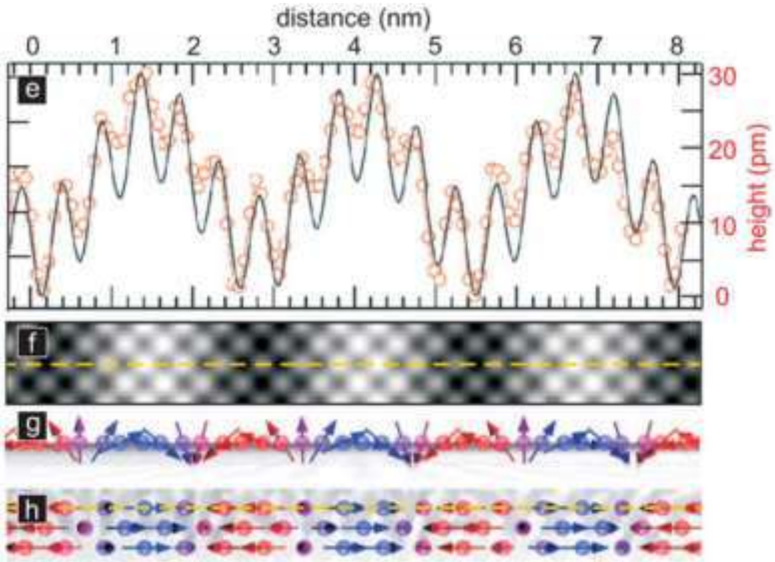

M. Bode *et al*, *Nature* **447**, 190 (2007)
P. Ferriani *et al*, *Phys. Rev. Lett.* **101**, 027201 (2008)

Spin polarized low-energy electron microscopy (SPLEEM)

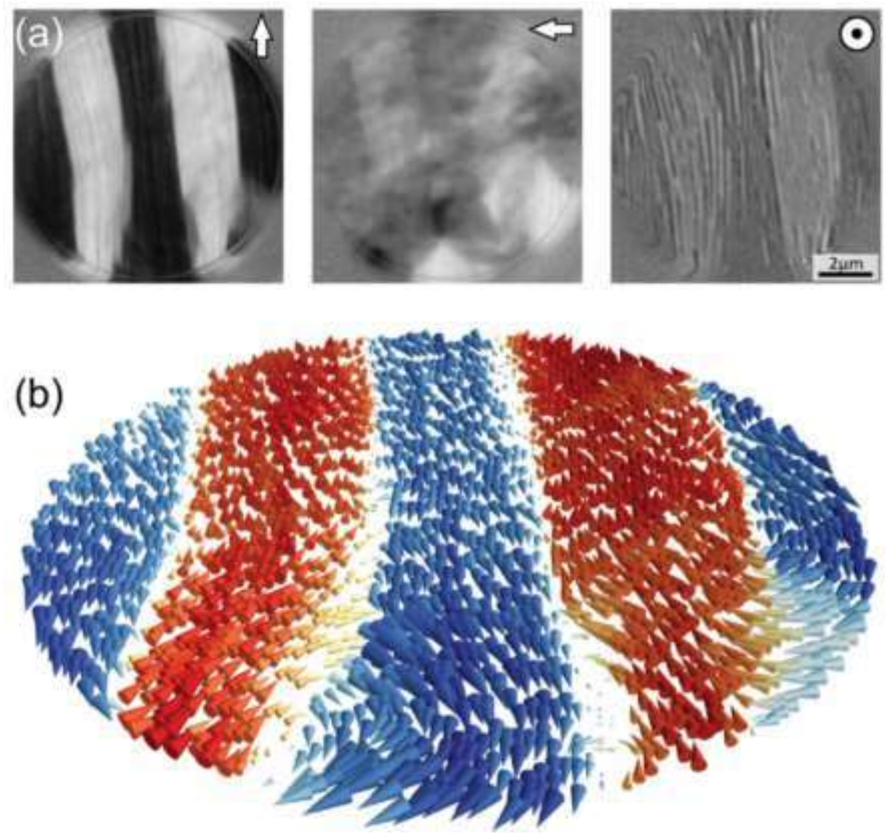

G. Chen & A. K. Schmid, *Adv. Matter.* **27**, 5738 (2015)

Means of DMI Measurements

Brillouin light scattering (BLS)

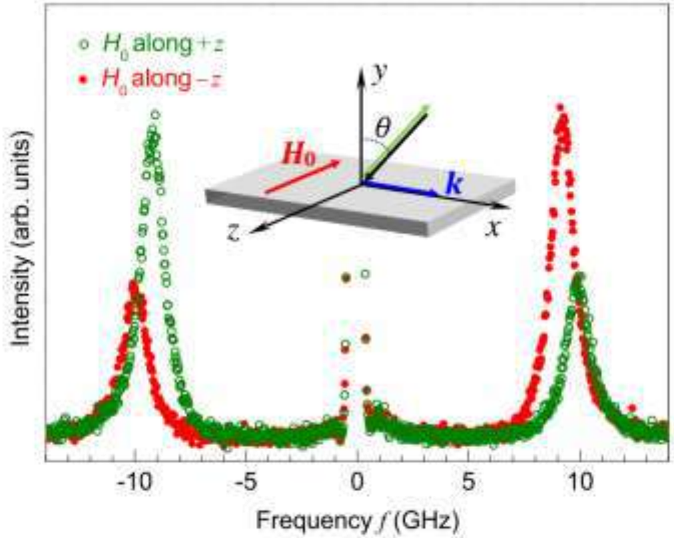

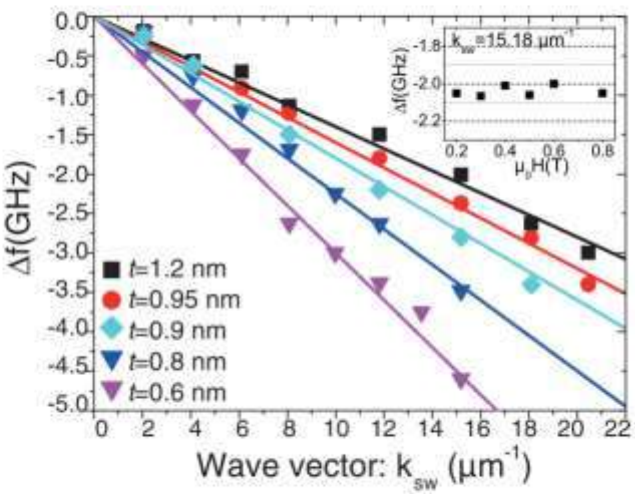

K. Di *et al*, *Phys. Rev. Lett.* **114**, 047201 (2015)
M. Belmeguenai, *Phys. Rev. B* **91**, 180405(R) (2015)

Usually used in Damon-Eshbach geometry:

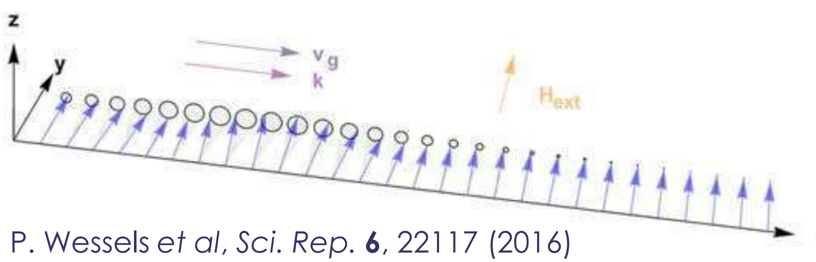

P. Wessels *et al*, *Sci. Rep.* **6**, 22117 (2016)

Surface spin waves are excited by shining light (typically green laser with $\lambda \approx 500$ nm) with incidence θ. Using energy and momentum conservation:

$$k_{\mathrm{sw}} = \frac{4\pi \sin(\theta)}{\lambda}$$

In the ultrathin film limit:

$$\frac{\Delta f}{k_{\mathrm{sw}}} = \frac{f_S - f_{AS}}{k_{\mathrm{sw}}} = \frac{2\gamma}{\pi M_s} D_{\mathrm{eff}} = \frac{2\gamma}{\pi M_s t} D_s$$

Purely interfacial case

Means of DMI Measurements

Brillouin light scattering (BLS)

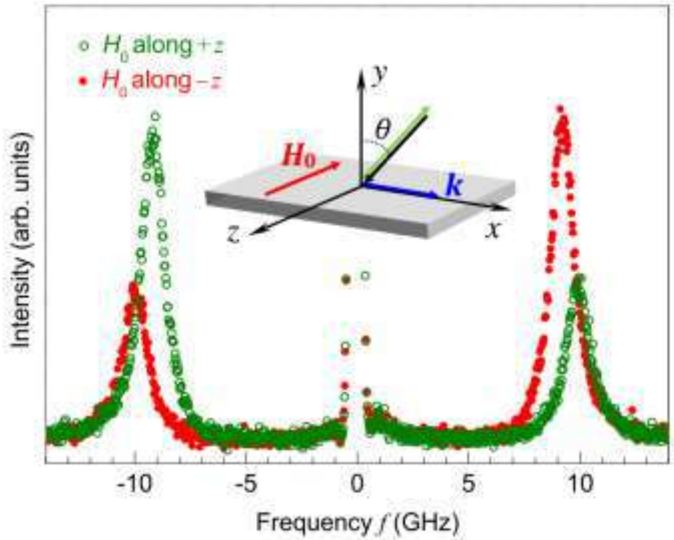

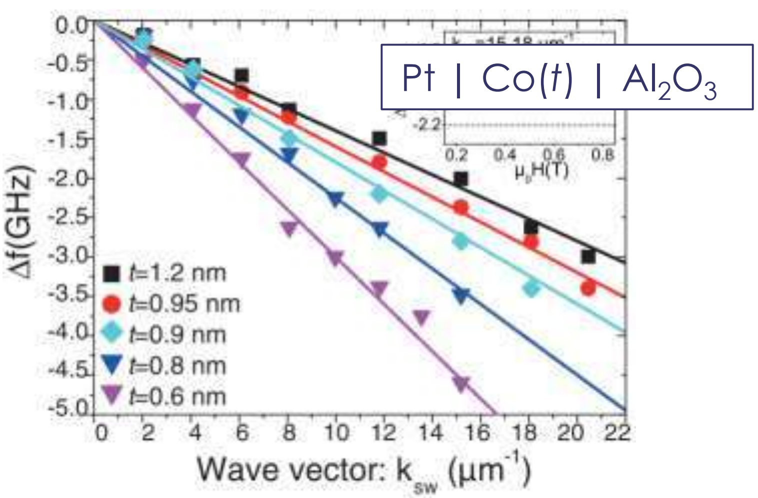

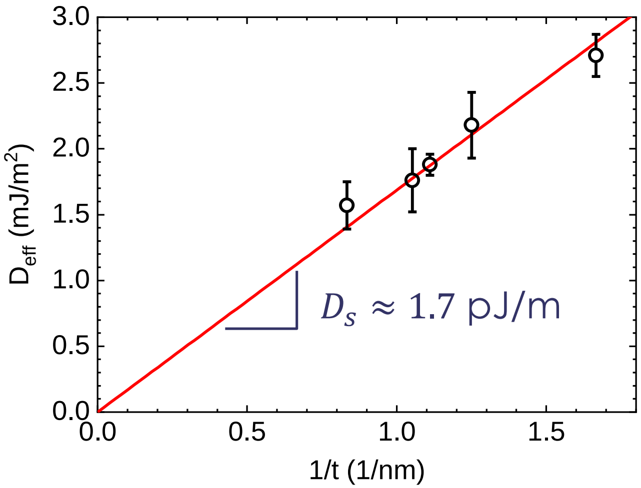

Results are compatible with a purely interfacial DMI effect.

K. Di *et al*, *Phys. Rev. Lett.* **114**, 047201 (2015)
M. Belmeguenai, *Phys. Rev. B* **91**, 180405(R) (2015)

Means of DMI Measurements

Asymmetric magnetic domain extension

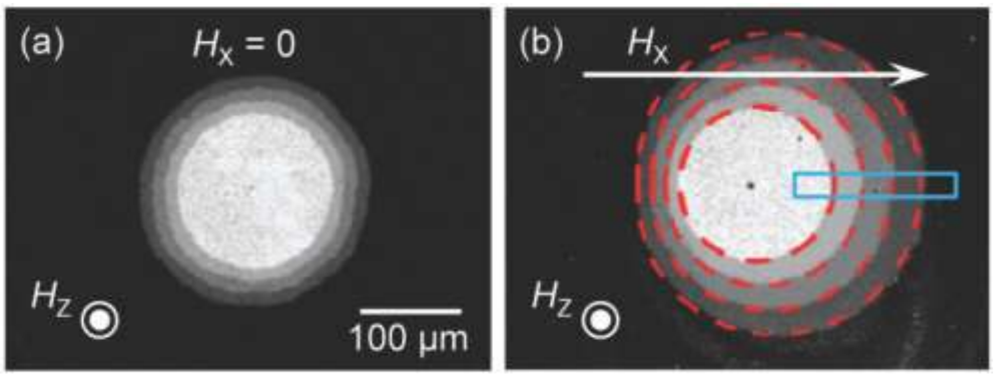

S.-G. Je *et al*, *Phys. Rev. B* **88**, 214401 (2013)

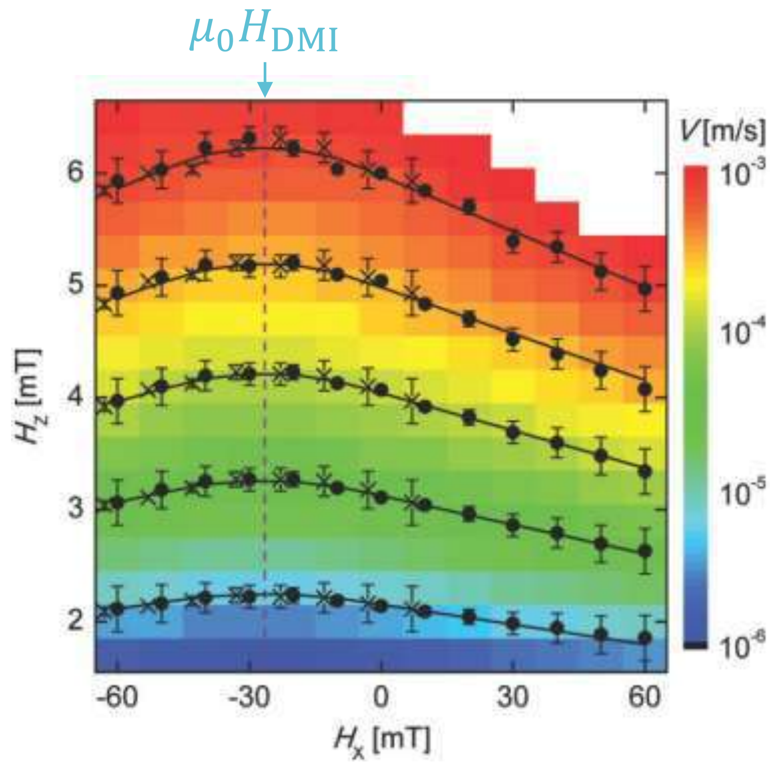

In the large DMI limit:

$$\mu_0 H_{\mathrm{DMI}} = \frac{D}{M_s \Delta}$$

Note that limit DW velocity (Walker breakdown) is increased by DMI:

$$v_W = \frac{\gamma_0 \Delta}{\alpha} H_W \approx \frac{\pi}{2} \gamma_0 H_{\mathrm{DMI}} \Delta = \frac{\pi}{2} \gamma_0 \frac{D}{M_s}$$

Means of DMI Measurements

Asymmetric nucleation

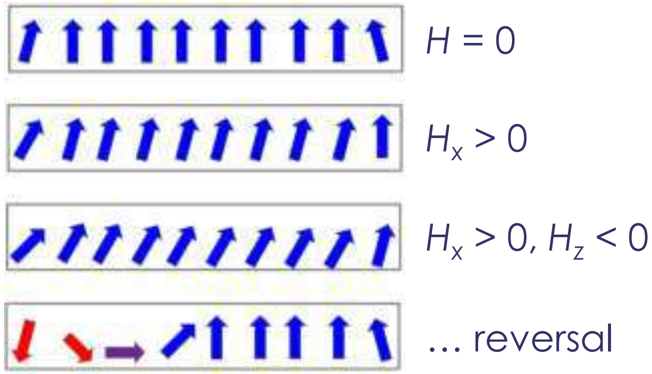

S. Pizzini *et al*, *Phys. Rev. Lett.* **113**, 047203 (2014)

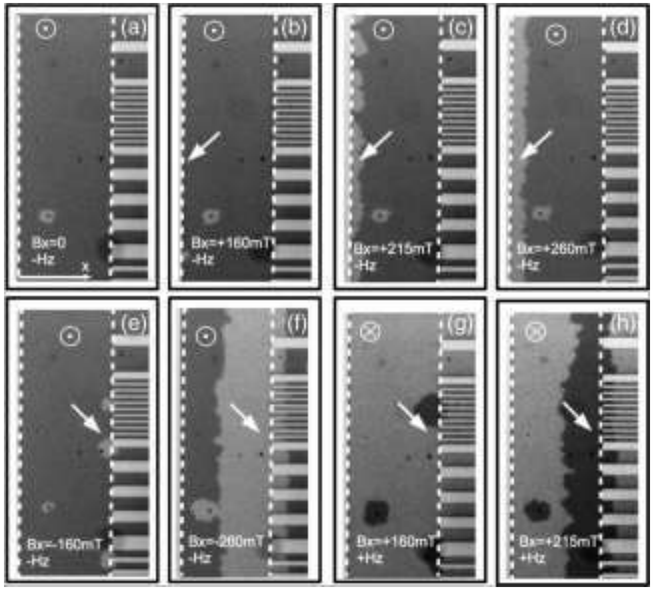

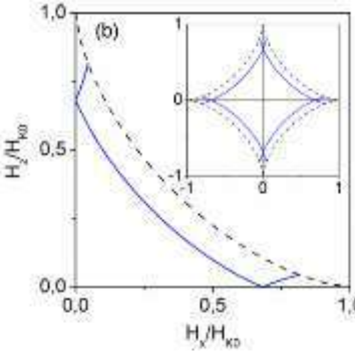

Asymmetric hysteresis in triangular-shaped magnets

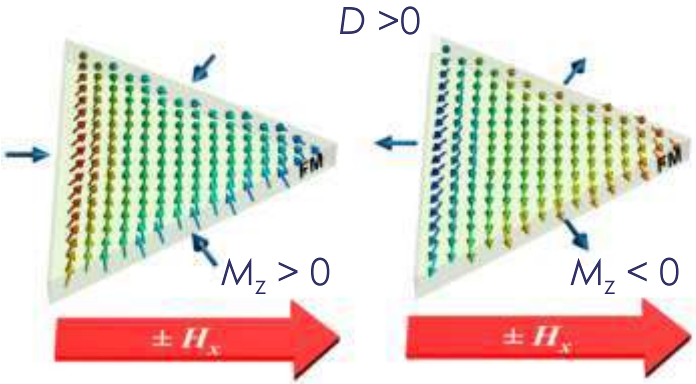

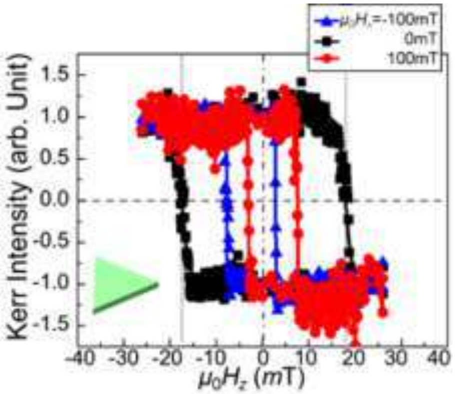

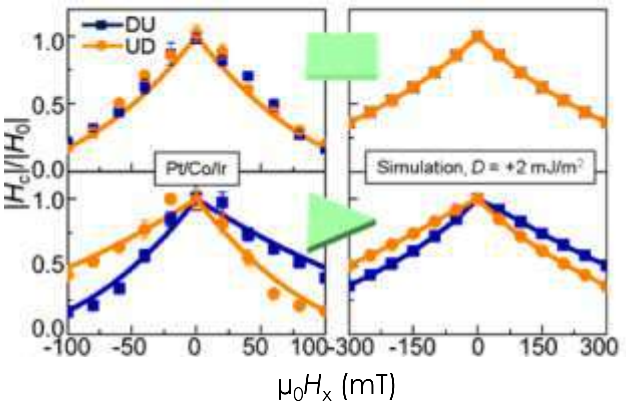

D.-S. Han *et al*, *Nano Lett.* **16**, 4438 (2016)

Means of DMI Measurements

Quantitative magnetometry

- NV center magnetometry

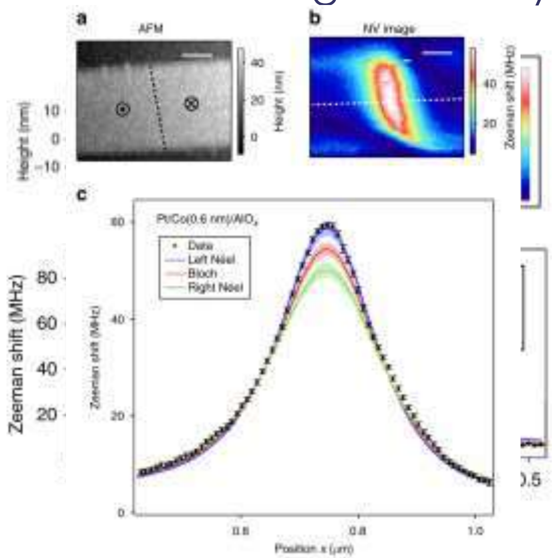

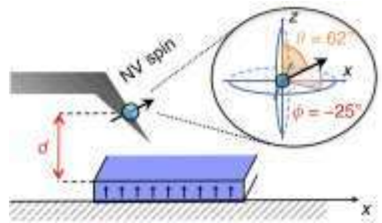

MgO AlO$_x$
CoFeB
Pt Ta

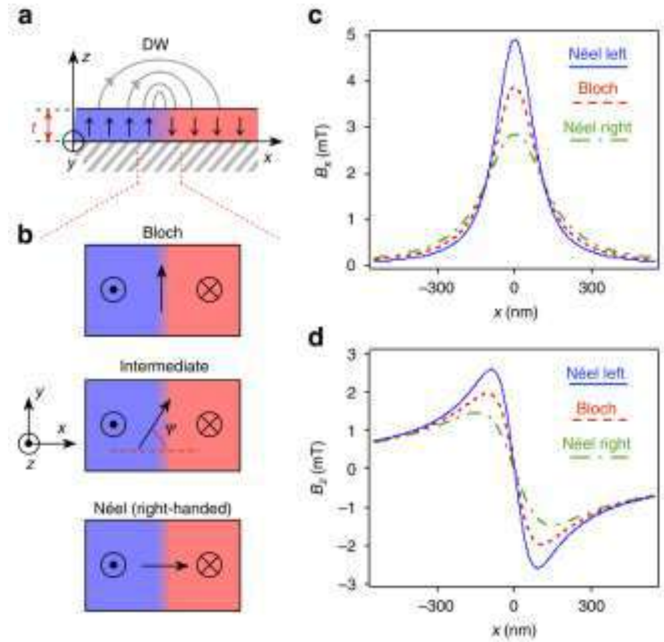

J.-P. Tetienne *et al*, *Nat. Commun.* **6**, 6733 (2015)

- (Quantitative) MFM

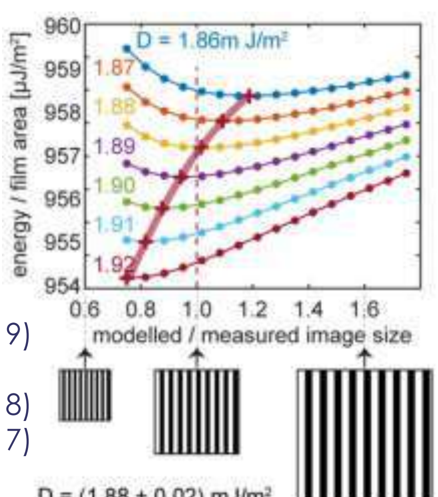

M. Baćani *et al*, *Sci. Rep.* **9**, 3114 (2019)

W. Legrand *et al*, *Sci. Adv.* **4**, eaat0415 (2018)
I. Lemesh *et al*, *Phys. Rev. B* **95**, 174423 (2017)

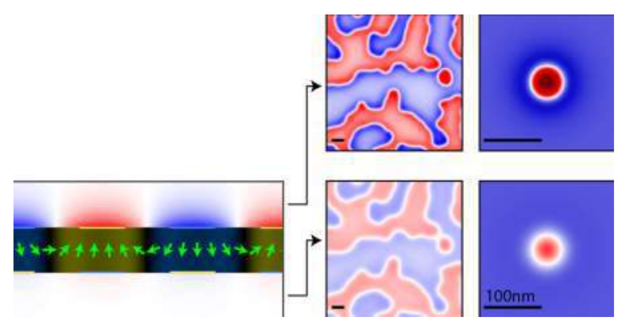

M. A. Marioni *et al*, *Nano Lett.* **18**, 2263 (2018)
F. Ajejas *et al*, in preperation

X-ray Resonant Magnetic Scattering probes the Wall Structures

Synchrotron technique: probe magnetism using photons at the Co L_3-edge energy

- 2D detector on SEXTANTS beamline at Synchrotron SOLEIL: get real-space periodicity of the domains
- Circular dichroism: get the chirality of the structure

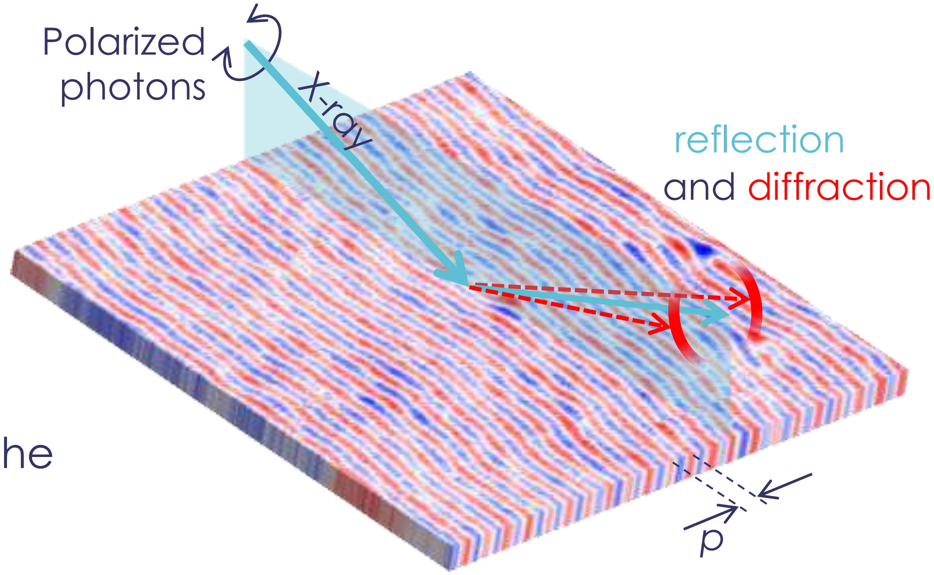

(CL-CR)/(CL+CR)

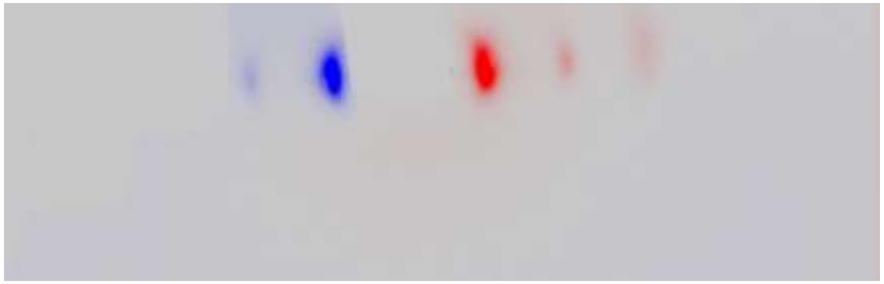

CCD signal (CL+CR)

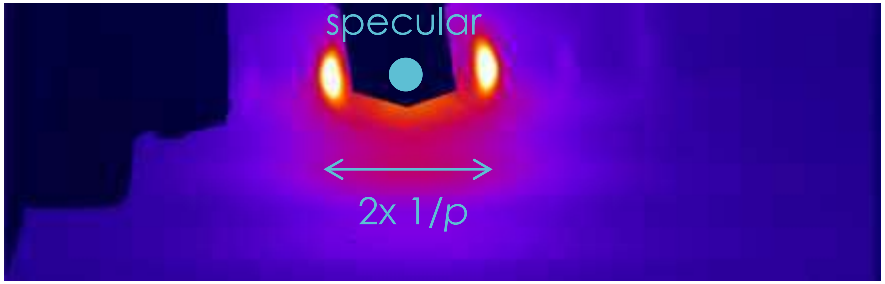

Strong circular dichroism of the XRMS diffraction peaks in our multilayers

H. A. Dürr *et al*, *Science* **284**, 2166 (1999)
J.-Y. Chauleau *et al*, *Phys. Rev. Lett.* **120**, 037202 (2018)

Definite Determination of the Chirality of the Multilayers

Domain wall texture is determined by XRMS

- Néel/Bloch character
- CW or CCW

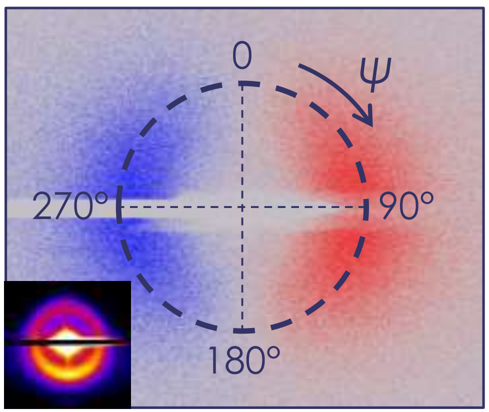

[Ir(1) | Co(0.8) | Pt(1)]$_{x5}$

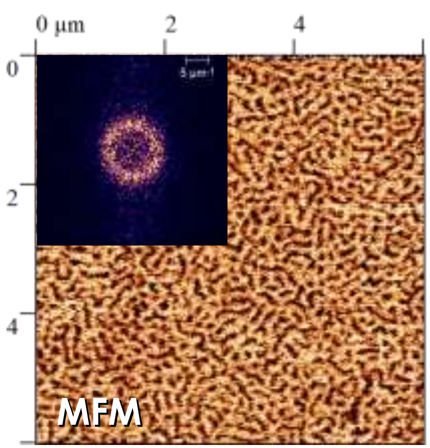

Calculations for sinusoidal magnetization textures:

$$I(\mathbf{Q}) \propto \Big|\sum_n f_n \exp(i\mathbf{Q}\cdot\mathbf{r}_n)\Big|^2$$

$$\mathbf{Q} = \mathbf{k}_f - \mathbf{k}_i$$

$$f_n = f_0 + f_m^1 + f_m^2$$

$$f_m^1 \propto -i(\hat{e}\times\hat{e}')\cdot\mathbf{m}_n,$$
$$f_m^2 \propto (\hat{e}'\cdot\mathbf{m}_n)(\hat{e}\cdot\mathbf{m}_n),$$

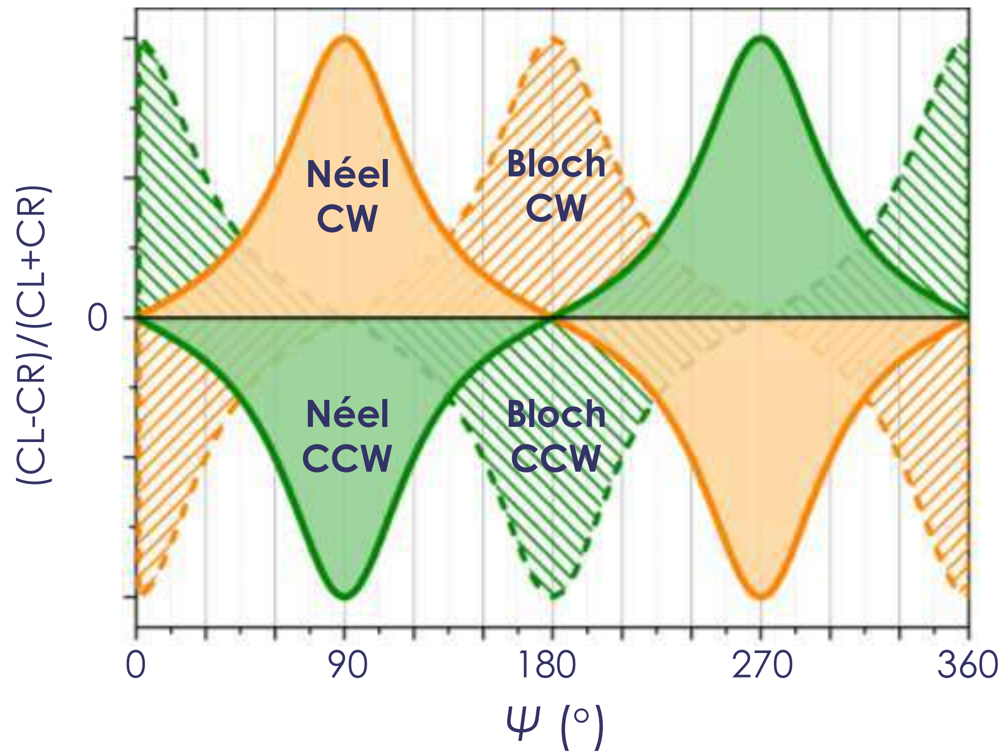

J.-Y. Chauleau *et al*, *Phys. Rev. Lett.* **120**, 037202 (2018)

Definite Determination of the Chirality of the Multilayers

Domain wall texture is determined by XRMS

- We have pure Néel DW
- The chirality is fixed (CW)

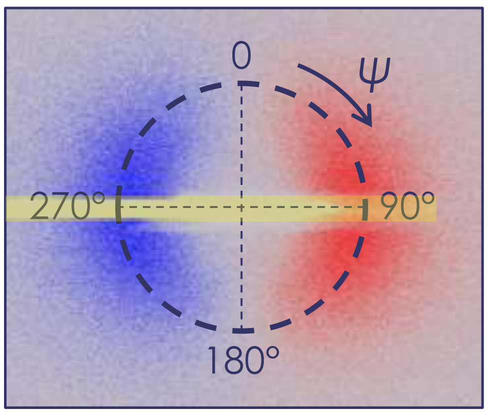

[Ir(1) | Co(0.8) | Pt(1)]$_{x5}$

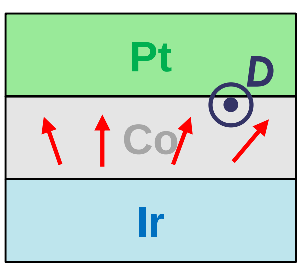

Calculations for sinusoidal magnetization textures:

$$I(\boldsymbol{Q}) \propto \left|\sum_n f_n \exp(i\boldsymbol{Q}\cdot\boldsymbol{r}_n)\right|^2, \quad \boldsymbol{Q} = \boldsymbol{k}_f - \boldsymbol{k}_i, \quad f_n = f_0 + f_m^1 + f_m^2$$

$$f_m^1 \propto -i(\hat{e}\times\hat{e}')\cdot\boldsymbol{m}_n,$$
$$f_m^2 \propto (\hat{e}'\cdot\boldsymbol{m}_n)(\hat{e}\cdot\boldsymbol{m}_n),$$

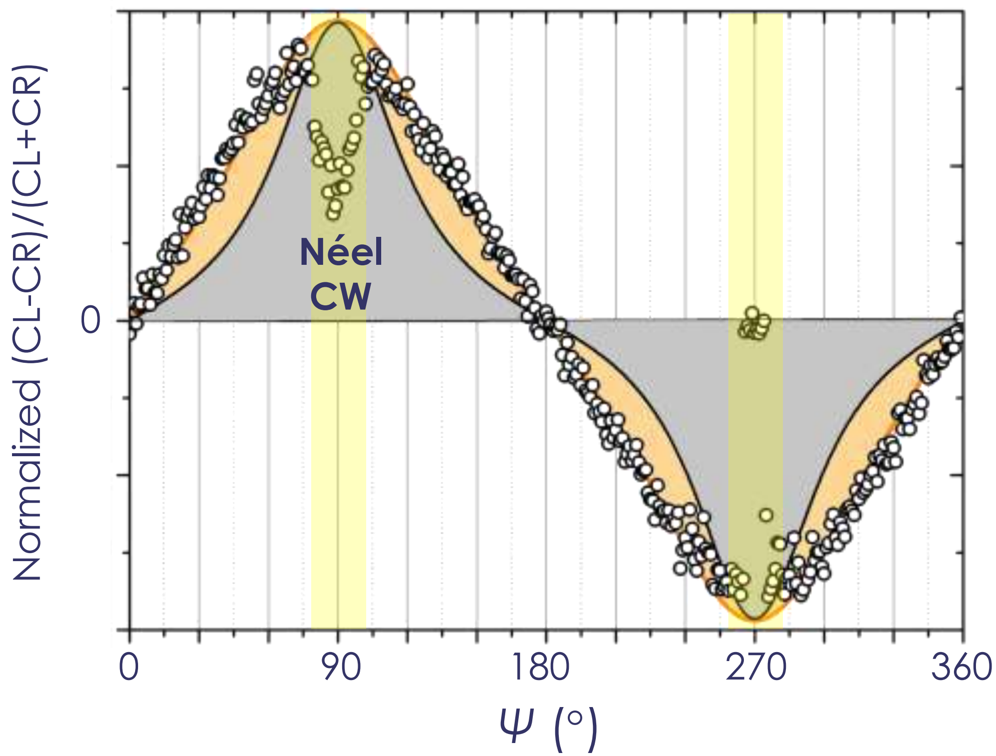

J.-Y. Chauleau *et al*, *Phys. Rev. Lett.* **120**, 037202 (2018)

Definite Determination of the Chirality of the Multilayers

Inversion of the multilayer stack

- Pure Néel walls in both case
- Inverted chirality: CCW for Co on top of Pt, CW for Pt on top of Co

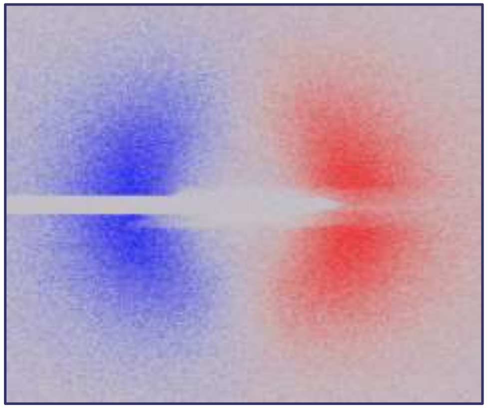

[Ir(1) | Co(0.8) | Pt(1)]$_{x5}$

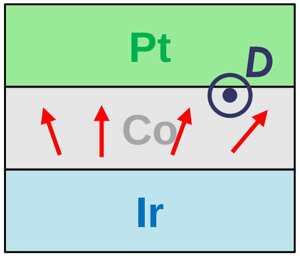

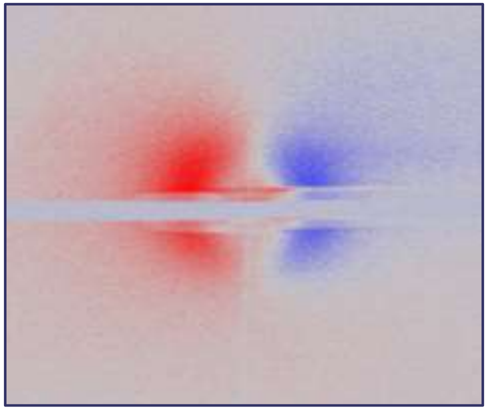

[Pt(1) | Co(0.8) | Ir(1)]$_{x5}$

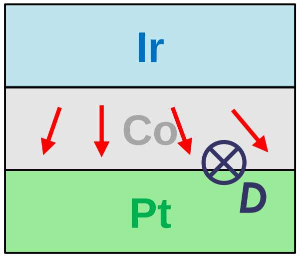

Just *looking* at a couple of XRMS images without analysis directly reveals the domain structure!

- Fast (10 minutes)
- No need to pattern
- No parameter to know
- Probe under a capping layers
- Sensitive to few nm of magnetic materials
- No effect on magnetization
- Possibility to apply field
- Possibility to probe insulating sample ($BiFeO_3$)
- …

J.-Y. Chauleau *et al*, *Phys. Rev. Lett.* **120**, 037202 (2018)

So, we understood everything?

Something happens at large repetition number…

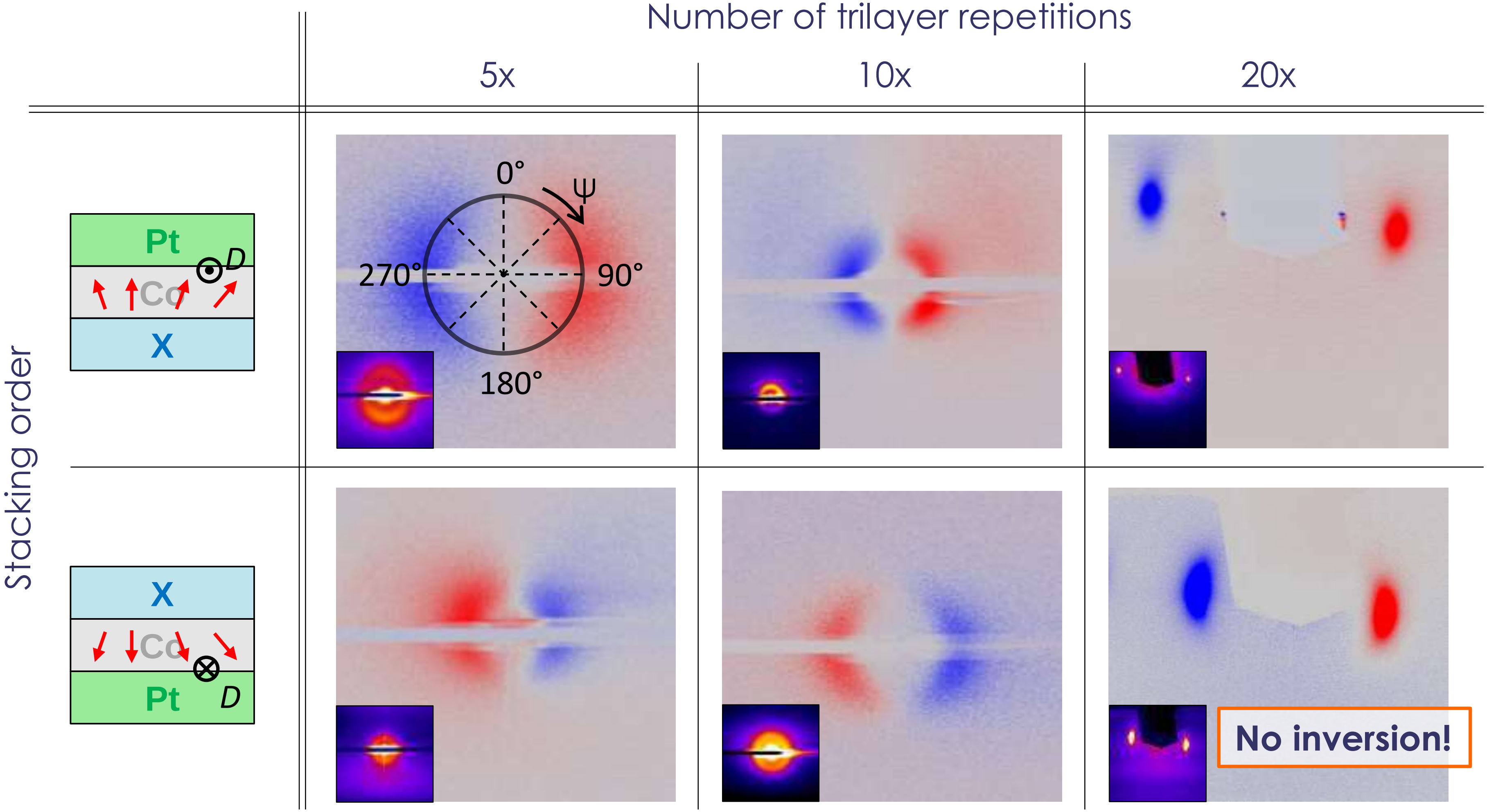

W. Legrand *et al*, *Science Adv.* **4**, eaat0415 (2018)

Recently reproduced in W. Li *et al*, *Adv. Mater.* **31**, 1807683 (2019)

Competition between Dipolar Energy and DMI in the DW

Evolution of the domain wall texture

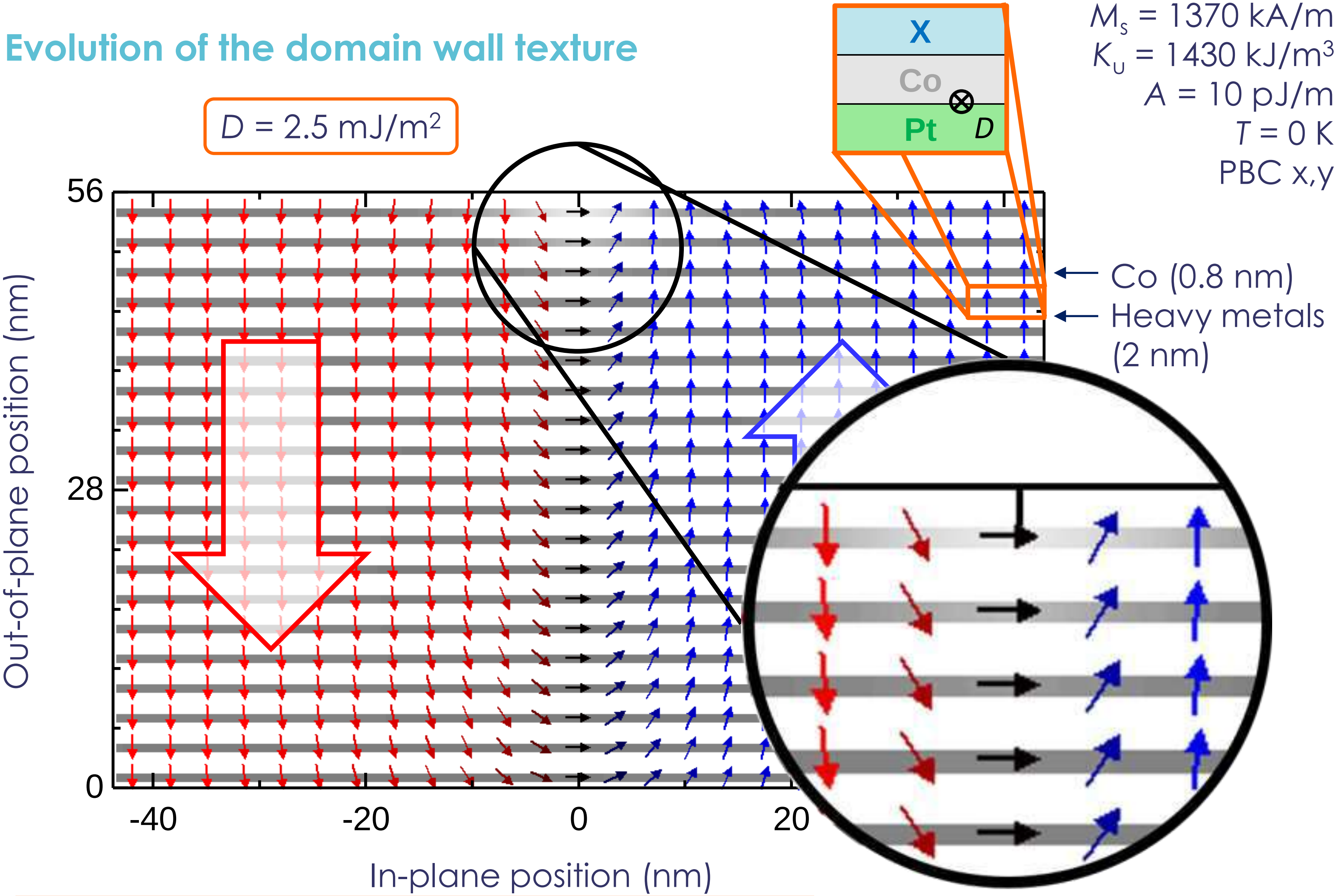

DMI stronger than 'demag': CCW Néel wall

W. Legrand *et al*, *Science Adv.* **4**, eaat0415 (2018)

Competition between Dipolar Energy and DMI in the DW

Evolution of the domain wall texture

M_s = 1370 kA/m
K_U = 1430 kJ/m^3
A = 10 pJ/m
T = 0 K
PBC x,y

D = 2.0 mJ/m^2

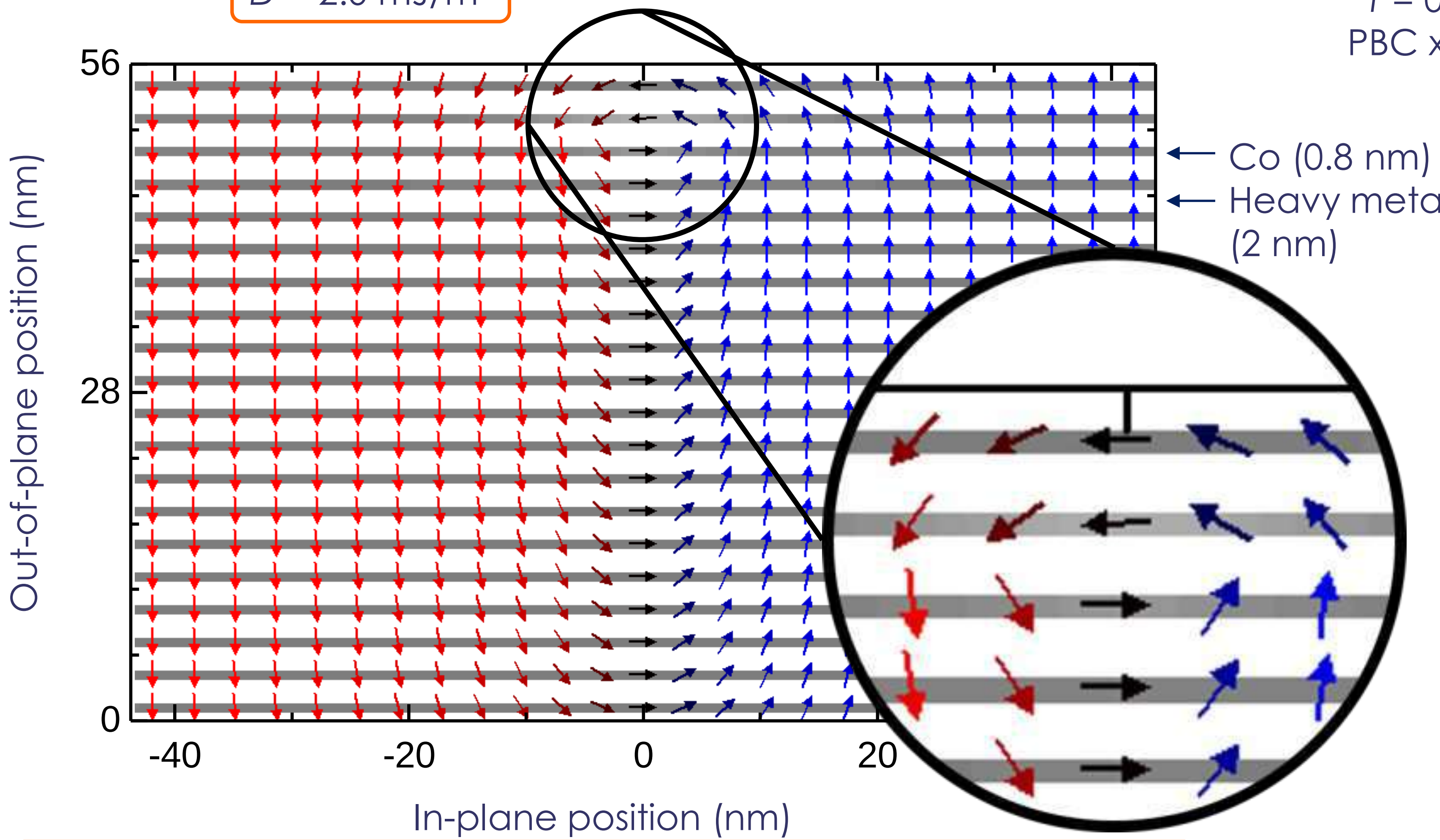

DMI smaller than 'demag' in top two layers: CW Néel wall

W. Legrand et al, Science Adv. **4**, eaat0415 (2018)

Competition between Dipolar Energy and DMI in the DW

M_s = 1370 kA/m
K_U = 1430 kJ/m^3
A = 10 pJ/m
T = 0 K
PBC x,y

Evolution of the domain wall texture

D = 1.0 mJ/m^2

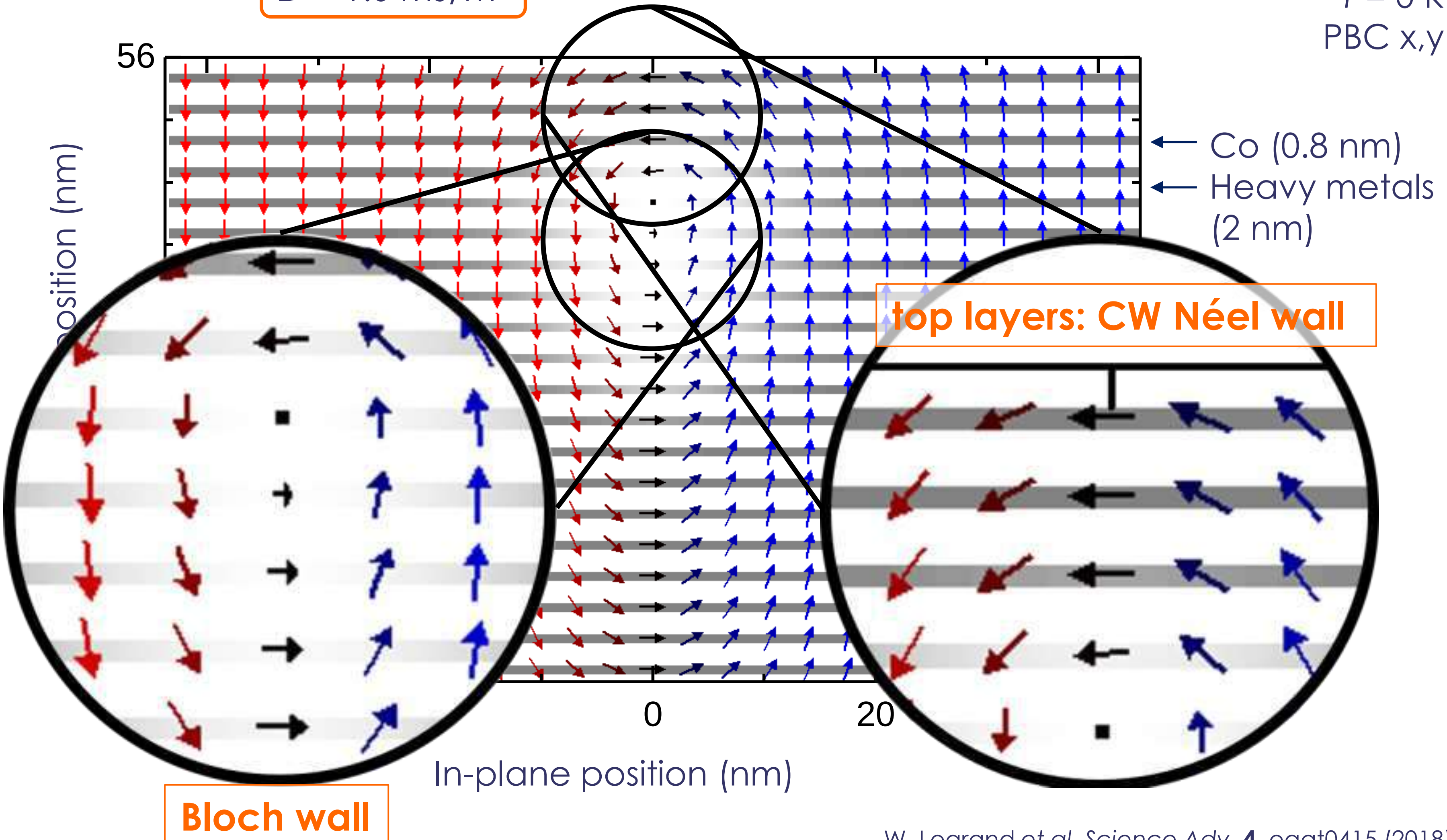

W. Legrand *et al*, *Science Adv.* **4**, eaat0415 (2018)

Competition between Dipolar Energy and DMI in the DW

Evolution of the domain wall texture

M_s = 1370 kA/m
K_U = 1430 kJ/m^3
A = 10 pJ/m
T = 0 K
PBC x,y

D = 0 mJ/m^2

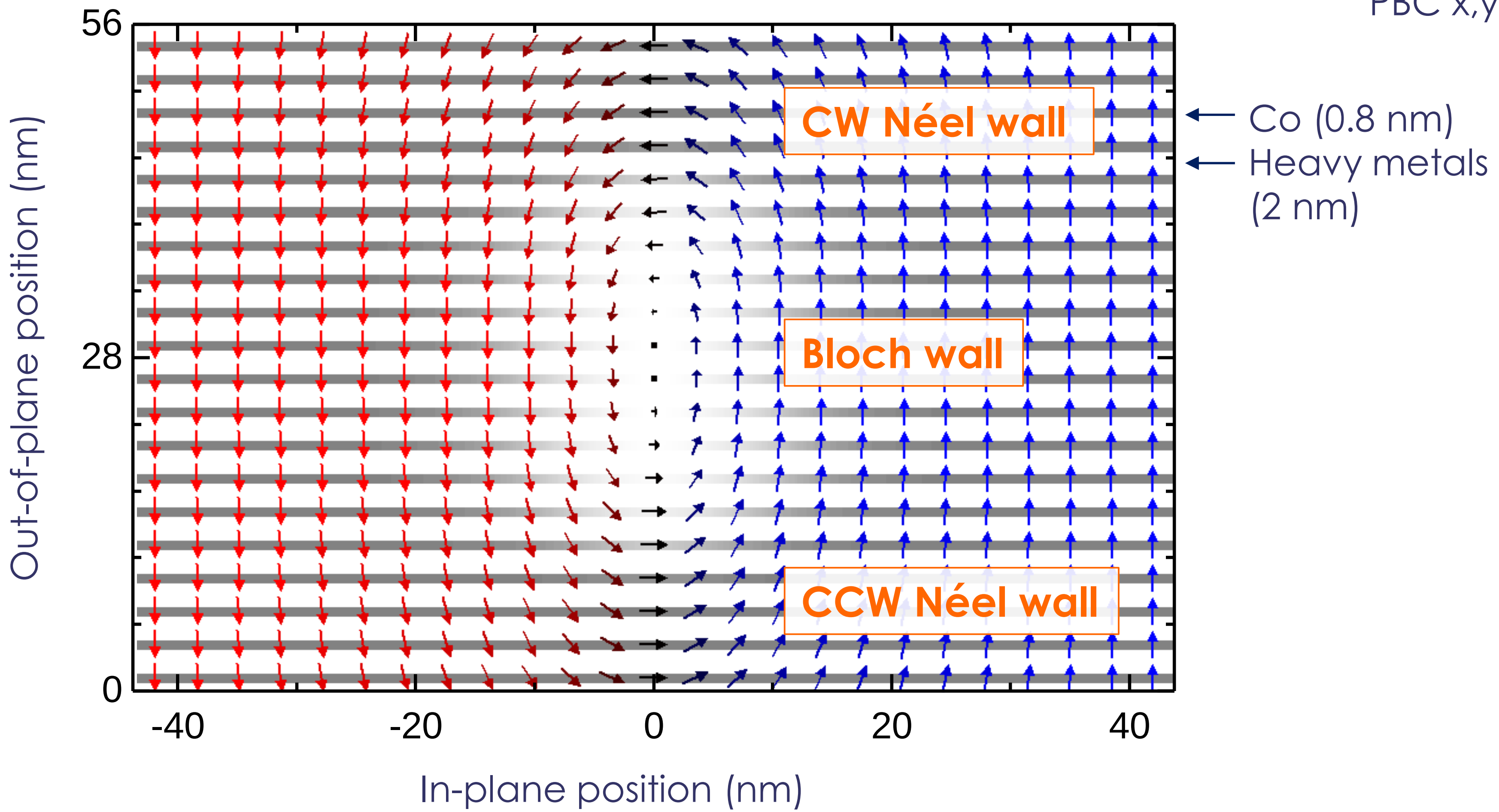

W. Legrand *et al*, *Science Adv*. **4**, eaat0415 (2018)

Explanation of the XRMS

M_s = 1370 kA/m
K_U = 1430 kJ/m^3
A = 10 pJ/m
D = 1.0 mJ/m^2

Resonant X-rays at Co L_3 edge penetrate only the first nm

- XRMS corresponds to a few topmost layers with reversed chirality.

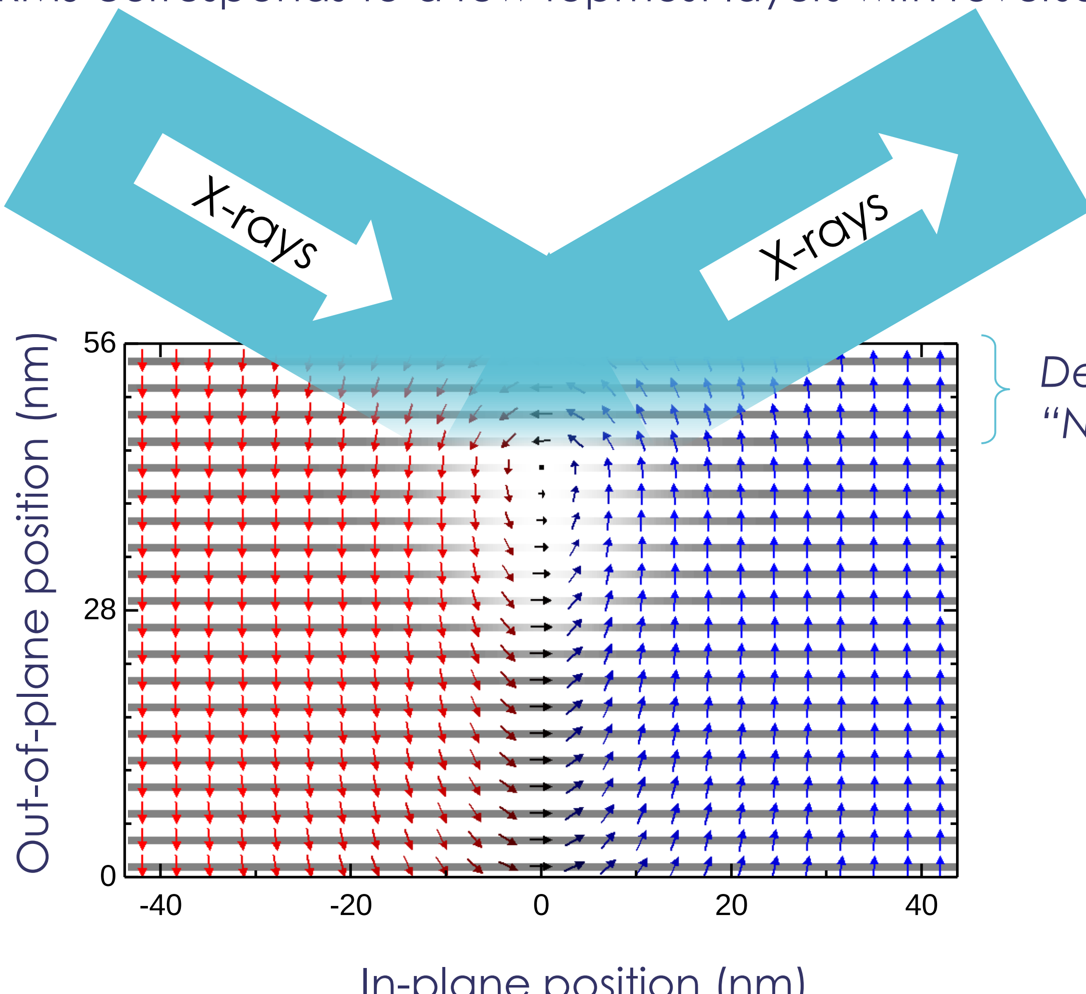

Detection of the "Néel cap" only.

Domain wall texture (including chirality) changes through the different Co layers.

W. Legrand *et al*, *Science Adv*. **4**, eaat0415 (2018)

Lorentz-TEM Confirms and Quantify the Hybrid Texture

Simulation of the signal for "pure Néel" DW vs. hybrid ones

- Néel walls only revealed is sample is tilted
- Bloch walls produce signal at normal incidence
- Hybrid walls produce … hybrid signals!

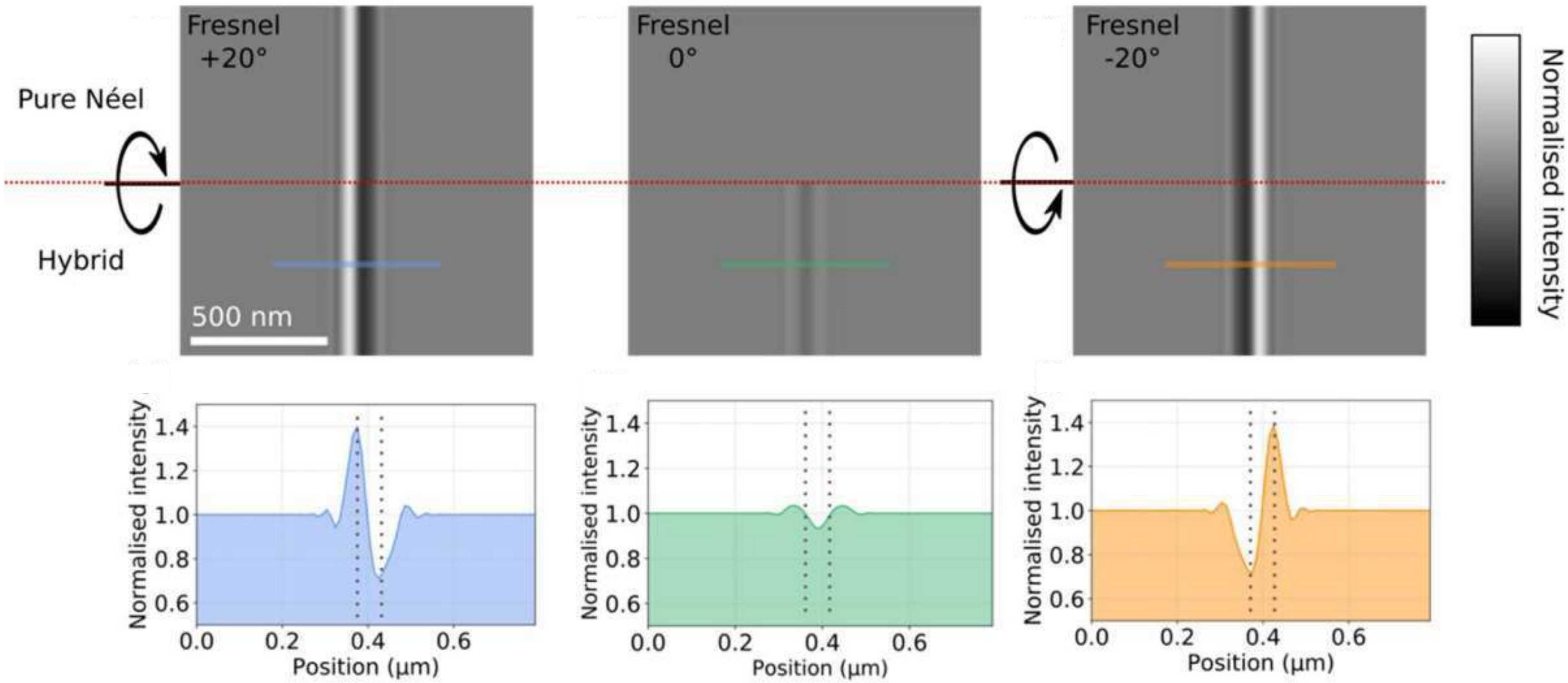

K. Fallon *et al*, arXiv: **1901**.03652

Lorentz-TEM Confirms and Quantify the Hybrid Texture

Comparison with experimental data allows to fit Δ and Bloch/Néel ratio.

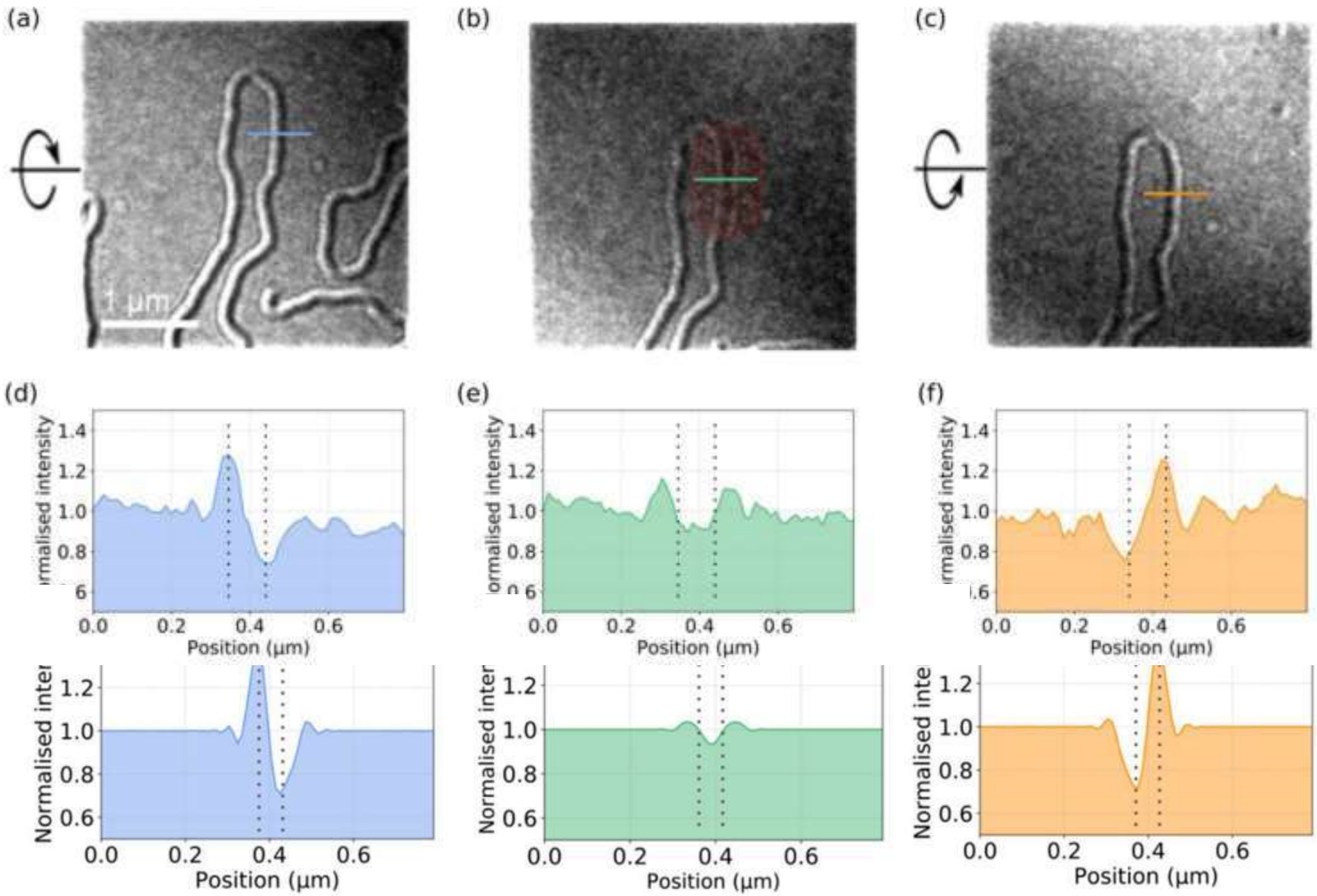

K. Fallon *et al*, arXiv: **1901**.03652

Lorentz-TEM Confirms and Quantify the Hybrid Texture

Comparison with experimental data allows to fit Δ and Bloch/Néel ratio

- Estimation of A = 12 pJ/m

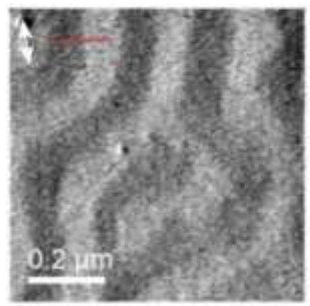

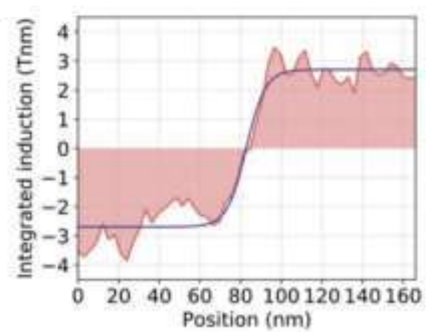

- Quantitative confirmation of the model (explained in next section)

Sample	Experiment		Calculation	
	Δ (nm)	t_{Bloch}/t	Δ (nm)	t_{Bloch}/t
5x	n.a.	n.a.	4	0.04
10x	5 ± 1	0.16 ± 0.02	5	0.16
15x	11 ± 1	0.18 ± 0.02	10	0.19

K. Fallon *et al*, arXiv: **1901**.03652

Question session

?

Examples: DM-MRAM & DM anisotropy

Use of DMI in perpendicular STT-MRAM?

Can the DMI be used to reduce the “incubation time”?

- Idea: Thanks to the initial tilt, the spin transfer torque is efficient since the beginning of the pulse.

Torque $\vec{\Gamma} = a\,\vec{M} \times (\vec{P} \times \vec{M})$

Perpendicular STT-MRAM configuration (no DMI)

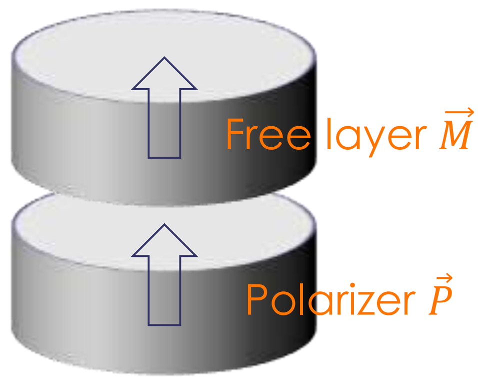

$\Rightarrow$ Need to wait for stochastic thermal fluctuations

$\Rightarrow$ Increase the writing error rate (WER)

Per

co

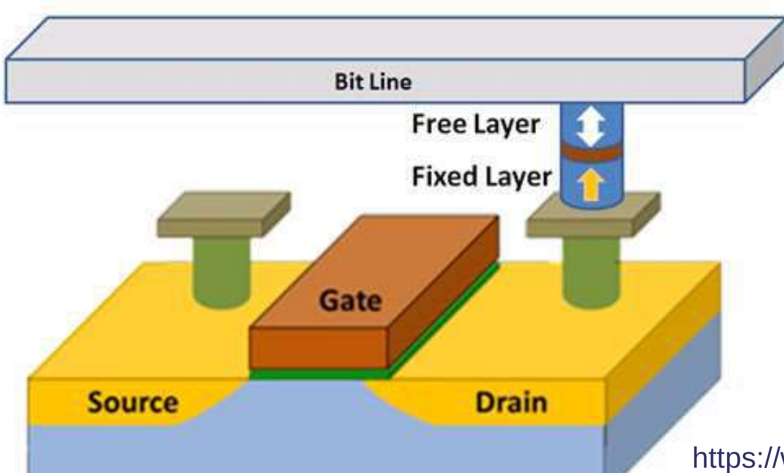

erface(s)

$\Rightarrow$ Torque efficient at start? (DW nucleation and propagation)

https://www.eetimes.com/document.asp?doc_id=1280508

Evaluation of the Energy Barrier Height

Nudged Elastic Band method (FastMag)

- 32nm disks, calculation of the lowest energy path for different *D*
- Reversal through nucleation and propagation (even down to 30nm!)

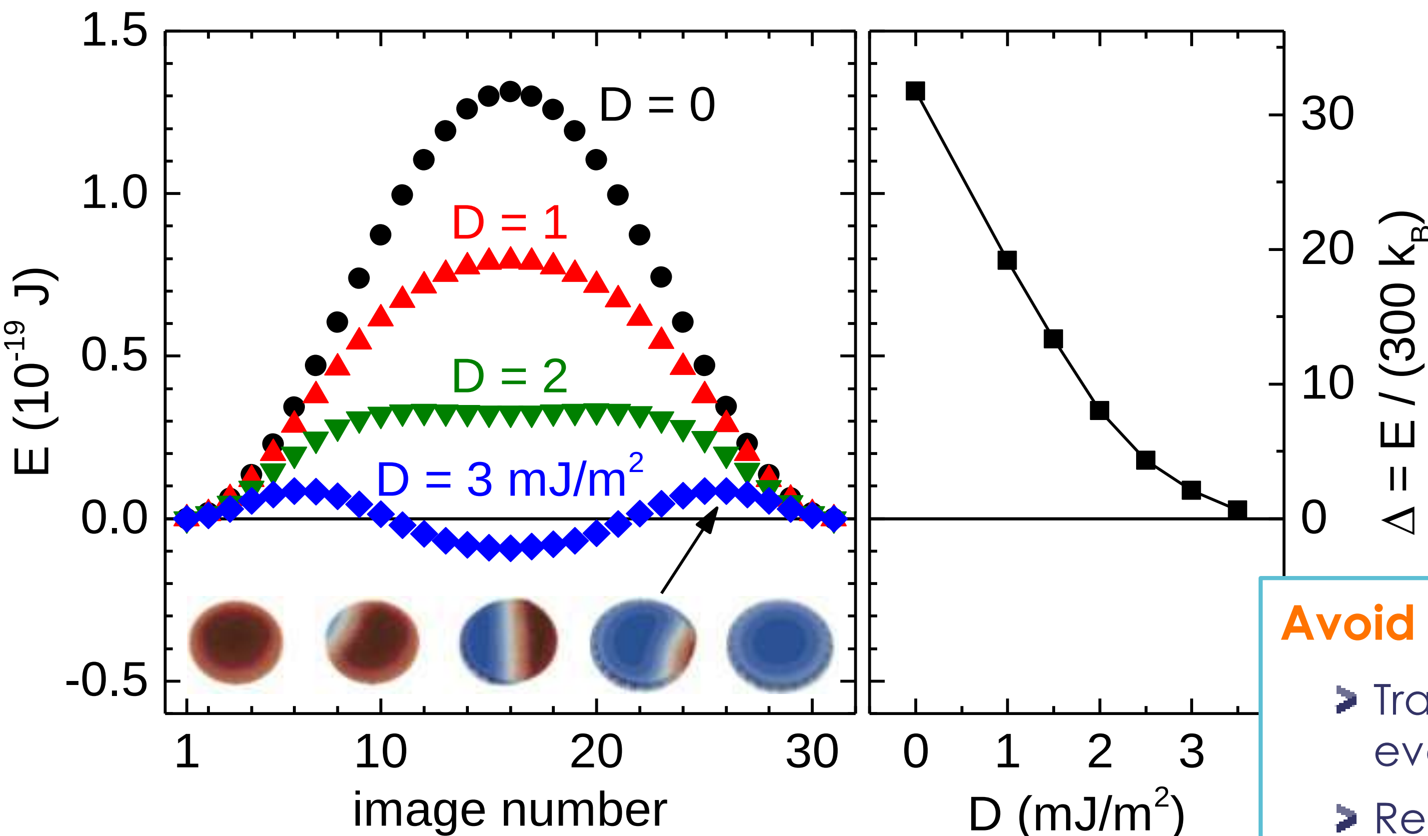

Geometry:
Ø = 32 nm
t = 1 nm

CoFeB parameters:
M_s = 1.03 MA/m
A = 10 pJ/m
K_u = 0.77 MJ/m^3
α = 0.01

Avoid too large DMI!

- Trapped states or even not binary
- Reduced stability

J. Sampaio *et al*, *Appl. Phys. Lett.* **108**, 112403 (2016)

Dynamics – Switching Currents, J_{c0} at Zero Temperature

- J_{c0} : The extrapolated switching current for “infinitely long” STT current pulses

$$J_{c0} = J_c(1/\tau_{sw} \rightarrow 0)$$

J_{c0} is increasing with the DMI

DMI is detrimental for power consumption

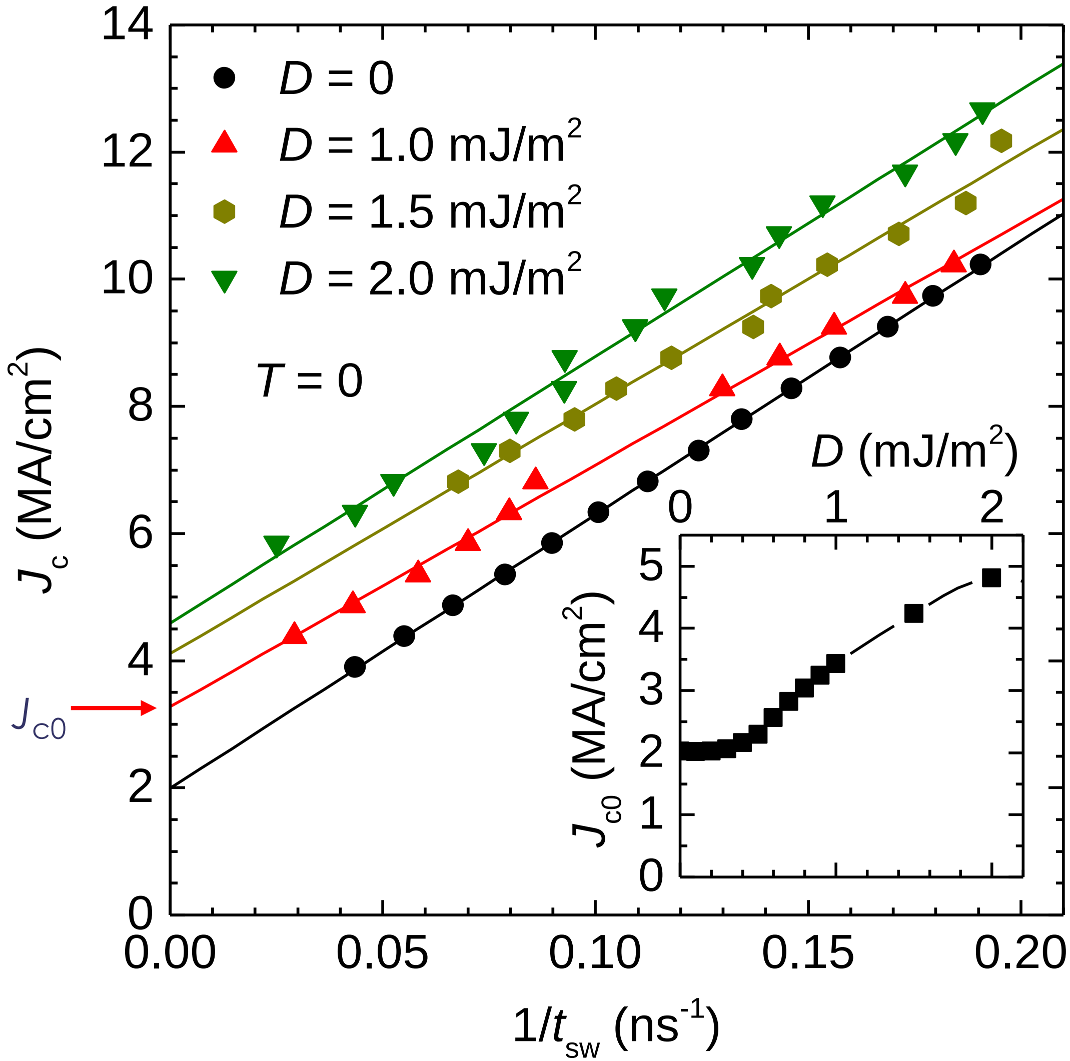

J. Sampaio *et al*, *Appl. Phys. Lett.* **108**, 112403 (2016)

Avoid DMI in pSTT-MRAM!

DMI *is detrimental* to STT-MRAM even for *D* as low as 0.25 mJ/m²

J. Sampaio *et al*, *Appl. Phys. Lett.* **108**, 112403 (2016)

P.-H. Jang *et al*, *Appl. Phys. Lett.* **107**, 202401 (2015)

What solutions?

- Avoid large SOC materials such as 5*d* metals (problem with PMA)
- Compensate at the other interface (problem with MgO)
- Mix metals with DMI of opposite sign

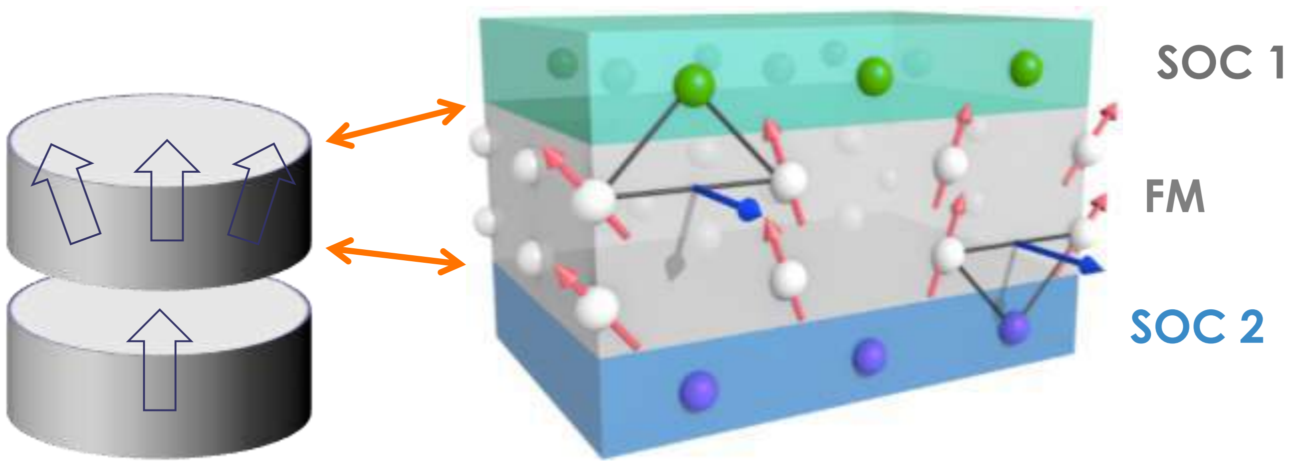

DMI in Nanomagnets with in-Plane Magnetization

DMI tilts the magnetization at the edges perpendicular to the magnetization

$$H_{H+DM} = -J\sum(\vec{S}_i \cdot \vec{S}_j) - \sum \vec{d}_{ij} \cdot (\vec{S}_i \times \vec{S}_j)$$

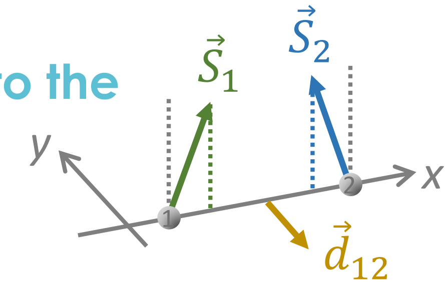

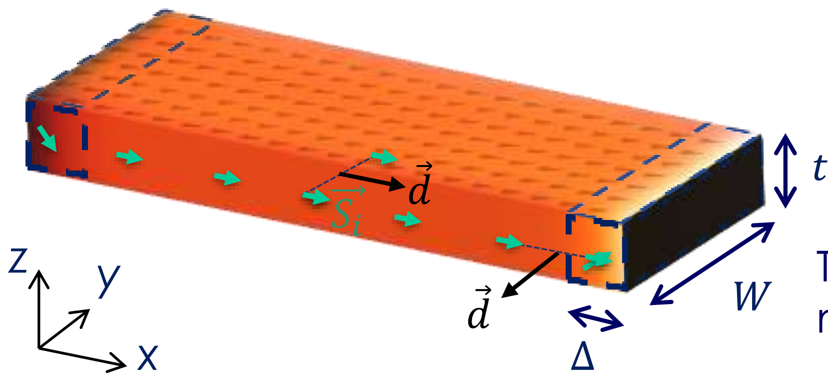

Tilted magnetization

Gain energy with D and K_U in these volumes:

$$E_{\text{tilt}} = -\frac{D^2}{4\sqrt{AK_{xz}}}tW$$

$$K_{xz} = \frac{1}{2}\mu_0 M_s^2(N_z - N_x) - K_u$$

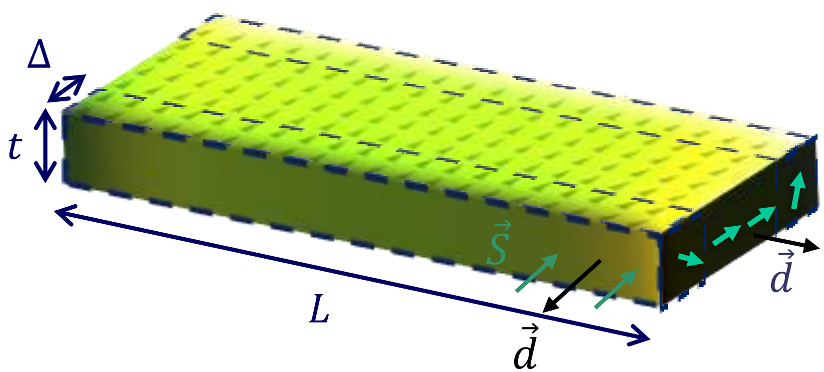

In some cases, the energy gain with magnetization along the short-axis configuration is large enough to change the ground-state!

$$E_{\text{tilt}} = -\frac{D^2}{4\sqrt{AK_{yz}}}tL$$

M. Cubukcu *et al*, *Phys. Rev. B* **93**, 020401(R) (2016)

Analytic Toy Model

Toy-model with parallelepipedic (box) nanomagnet:

- Difference of energy between the two states: E() – E()

$$E_x - E_y = \Delta E_{\text{demag}} + \Delta E_{\text{tilt}} = -K_{xy}LWt - \frac{D^2 t}{4\sqrt{A}}\left(\frac{2W}{\sqrt{K_{xz}}} - \frac{2L}{\sqrt{K_{yz}}}\right)$$

$$\approx \left(\boxed{K_{xy}} + \underbrace{\boxed{\frac{D^2}{2\sqrt{AK_{xz}}}}\,\boxed{\frac{L-W}{LW}}}_{K_{\text{DM}}}\right) LWt$$

Usual shape anisotropy related to demagnetization field

Mainly material dependent term (t-dependence hidden in K_{xz} and D)

Geometrical term

$$K_{xy} = 1/2\,\mu_0 M_s^2 (N_y - N_x)$$
$$K_{xz} = 1/2\,\mu_0 M_s^2 (N_z - N_x) - K_u$$
$$K_{yz} = 1/2\,\mu_0 M_s^2 (N_z - N_y) - K_u$$

Analytical expression for the N_i form factors (assuming a uniform magnetization):

$$\pi D_z = \frac{b^2-c^2}{2bc}\ln\left(\frac{\sqrt{a^2+b^2+c^2}-a}{\sqrt{a^2+b^2+c^2}+a}\right) + \frac{a^2-c^2}{2ac}\ln\left(\frac{\sqrt{a^2+b^2+c^2}-b}{\sqrt{a^2+b^2+c^2}+b}\right) + \frac{b}{2c}\ln\left(\frac{\sqrt{a^2+b^2}+a}{\sqrt{a^2+b^2}-a}\right) + \frac{a}{2c}\ln\left(\frac{\sqrt{a^2+b^2}+b}{\sqrt{a^2+b^2}-b}\right)$$
$$+ \frac{c}{2a}\ln\left(\frac{\sqrt{b^2+c^2}-b}{\sqrt{b^2+c^2}+b}\right) + \frac{c}{2b}\ln\left(\frac{\sqrt{a^2+c^2}-a}{\sqrt{a^2+c^2}+a}\right) + 2\arctan\left(\frac{ab}{c\sqrt{a^2+b^2+c^2}}\right) + \frac{a^3+b^3-2c^3}{3abc}$$
$$+ \frac{a^2+b^2-2c^2}{3abc}\sqrt{a^2+b^2+c^2} + \frac{c}{ab}\left(\sqrt{a^2+c^2}+\sqrt{b^2+c^2}\right) - \frac{(a^2+b^2)^{3/2}+(b^2+c^2)^{3/2}+(c^2+a^2)^{3/2}}{3abc}.$$

A. Aharoni, *J. Appl. Phys.* **83**, 3432 (1998)
M. Cubukcu *et al*, *Phys. Rev. B* **93**, 020401(R) (2016)

Critical DMI Magnitude for Magnetization Reorientation

Critical DMI magnitude $D_\perp$ for which the magnetization aligns either along the short axis or the long one when *E* () = *E* ()

$$D_\perp^2 \approx (N_x - N_y)\frac{WL}{W-L}\mu_0 M_s^2 \sqrt{AK_{xz}}$$

- Important role of the out-of-plane anisotropy
- Role of the shape
- Should be present in many nanoscale systems

M_s = 1 MA/m, A = 15 pJ/m, t = 1.5 nm

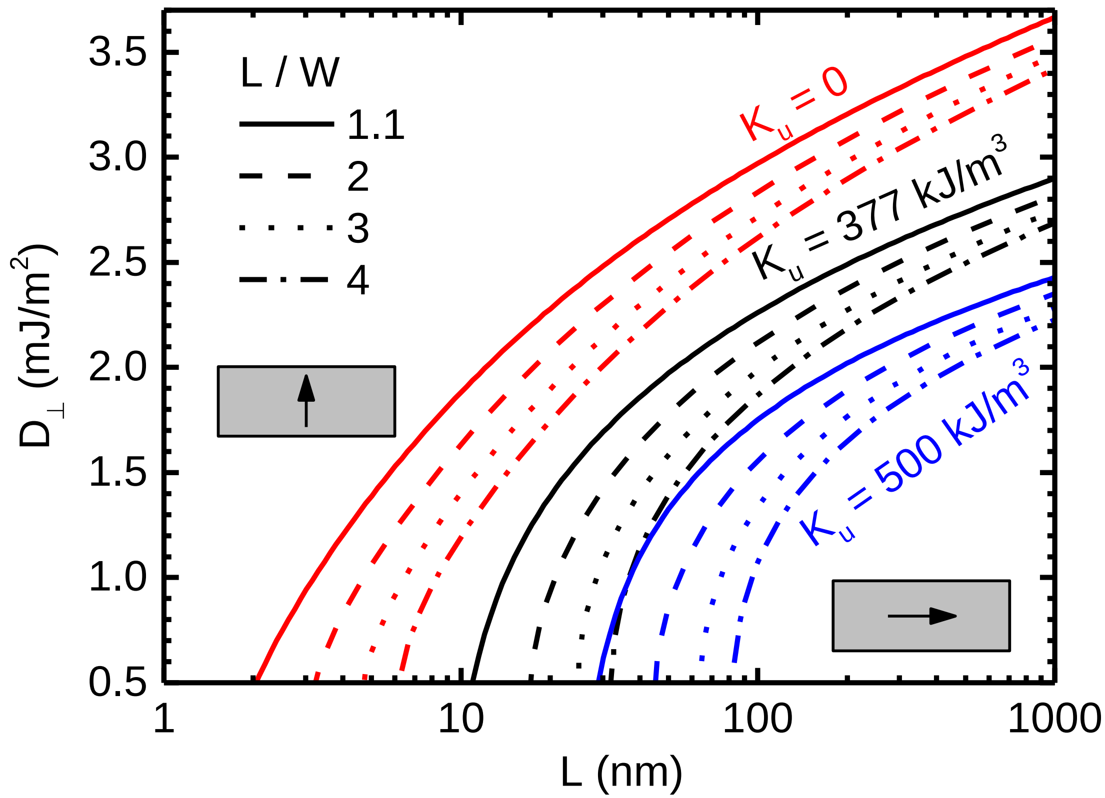

M. Cubukcu *et al*, *Phys. Rev. B* **93**, 020401(R) (2016)

Analytical Model *vs.* Micromagnetic Simulations

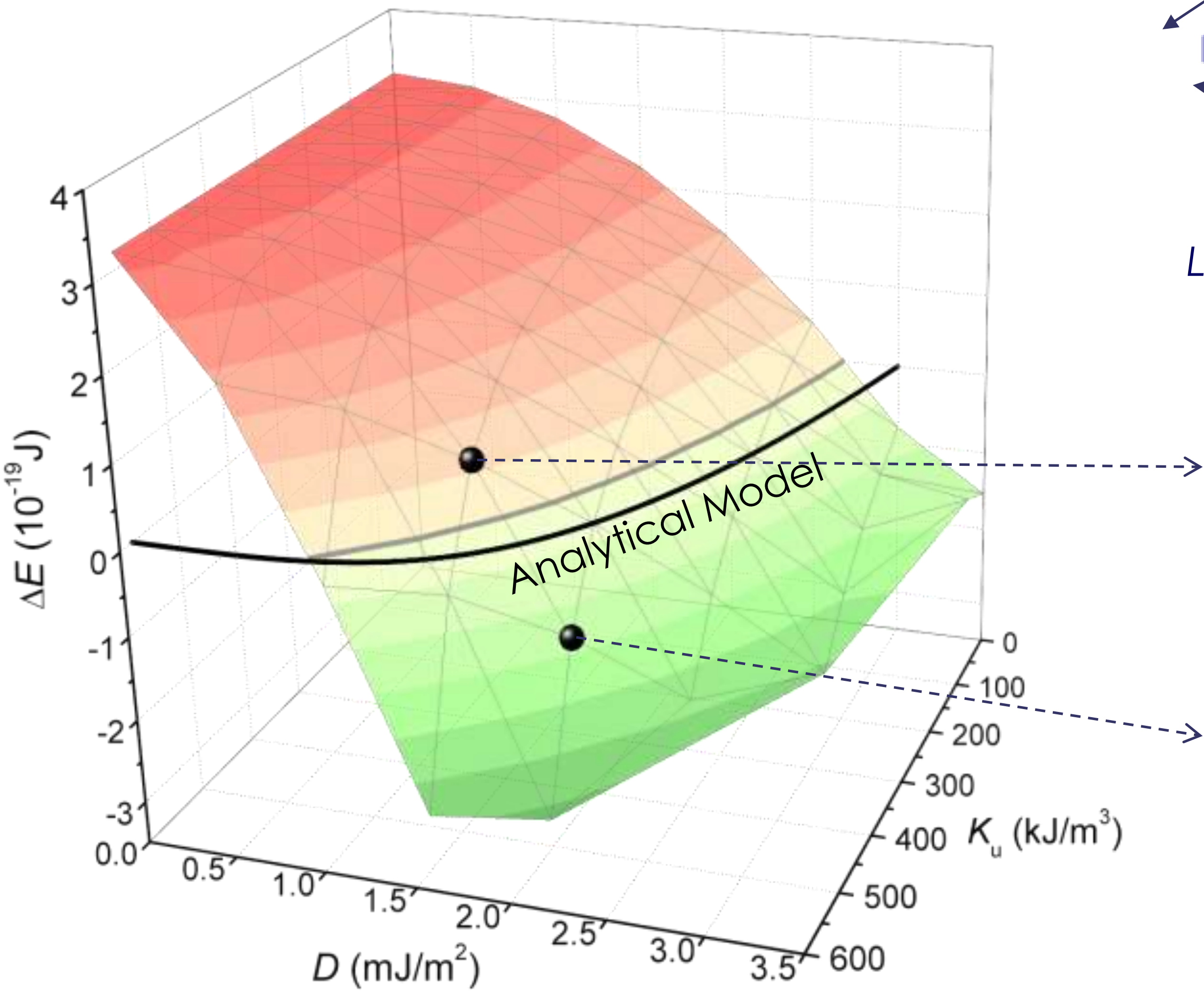

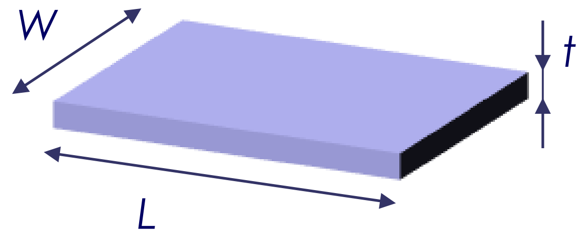

M_s = 1 MA/m, A = 15 pJ/m,
L = 210, W = 70 and t = 1.5 nm

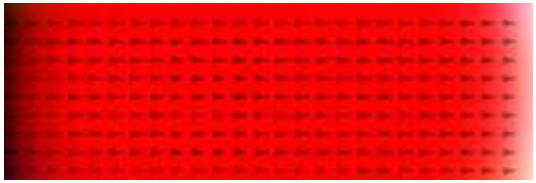

D = 1.5 mJ/m²

D = 2.0 mJ/m²

K_U = 440kJ/m³

M. Cubukcu *et al*, *Phys. Rev. B* **93**, 020401(R) (2016)

Experimental Observation of the DMI Anisotropy

‖ MgO | $Co_{20}Fe_{60}B_{20}$ (1.5 nm) | Pt (0.8 nm) | Ta (3 nm)

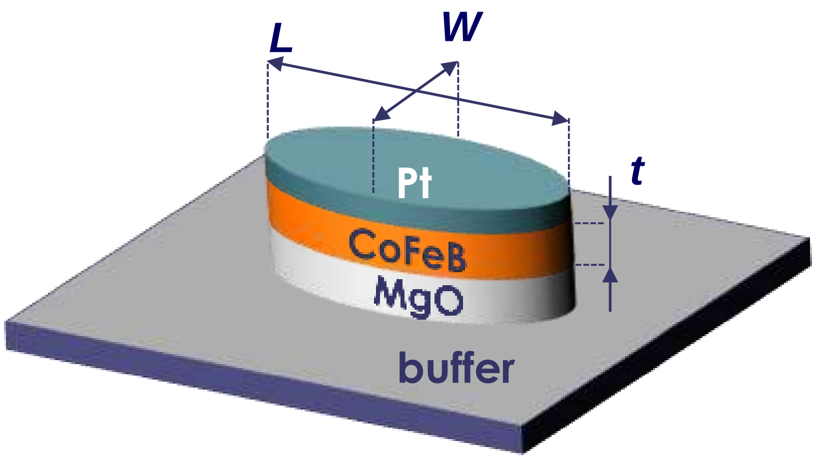

M. Cubukcu *et al*, *Phys. Rev. B* **93**, 020401(R) (2016)

Experimental Observation of the DMI Anisotropy

‖ MgO | $Co_{20}Fe_{60}B_{20}$ (1.5 nm) | Pt (0.8 nm) | Ta (3 nm)

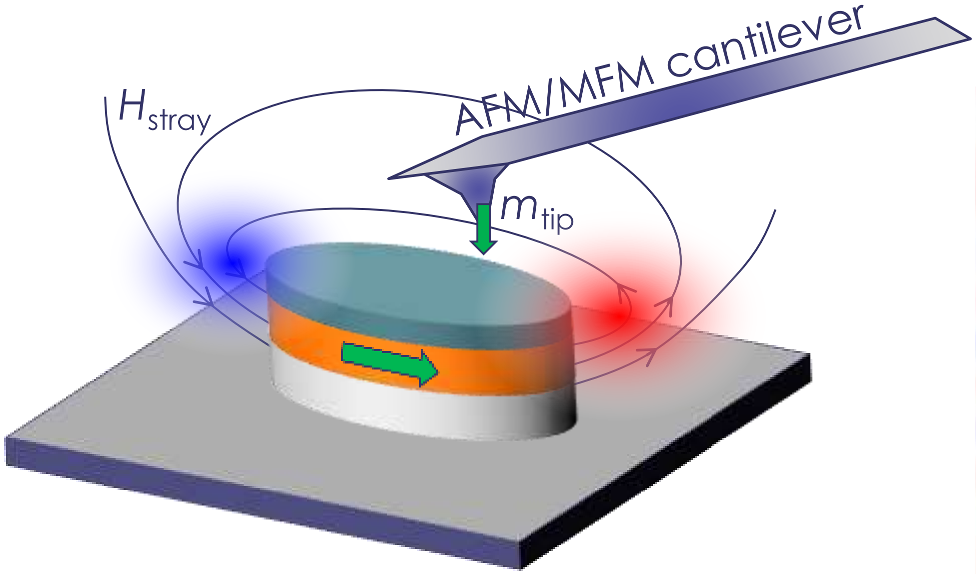

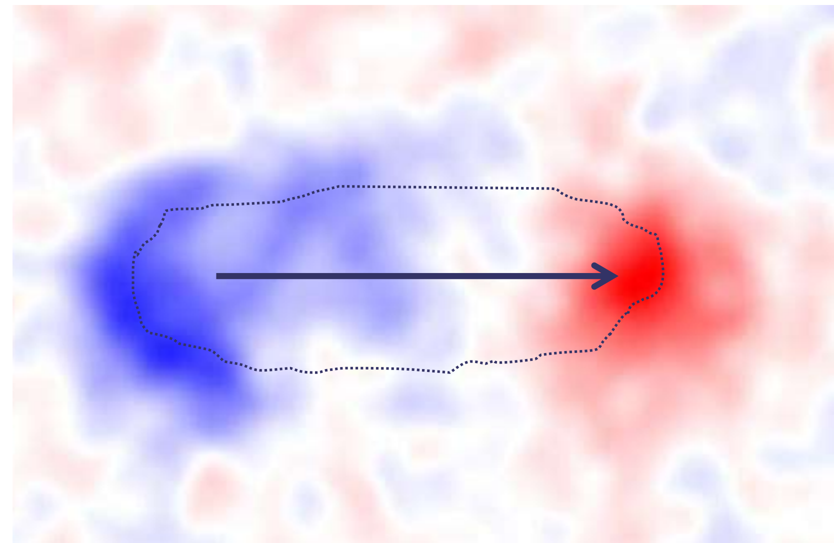

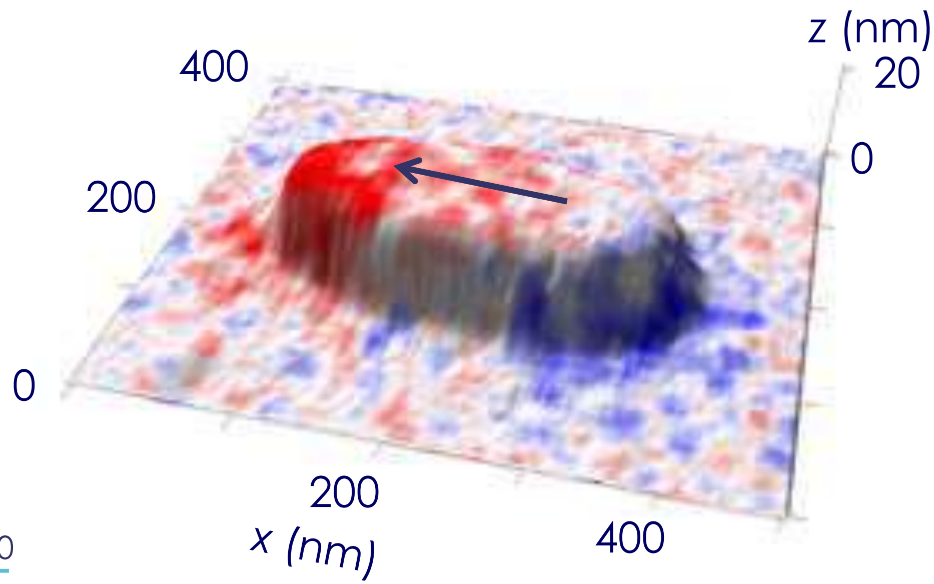

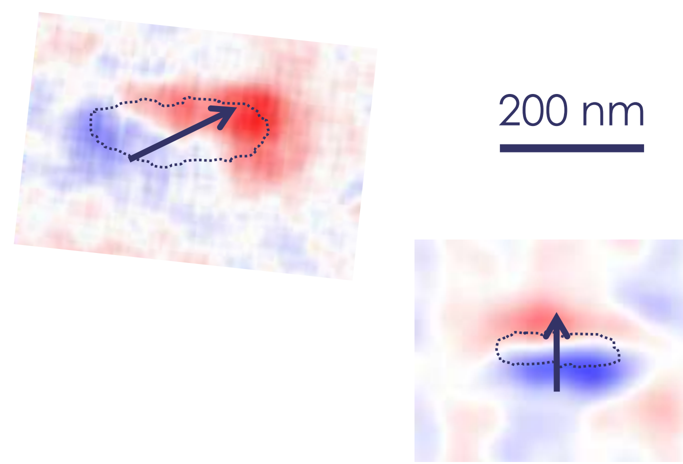

M. Cubukcu *et al*, *Phys. Rev. B* **93**, 020401(R) (2016)

Comparison with Micromagnetic Simulations

‖ MgO | $Co_{20}Fe_{60}B_{20}$ (1.5 nm) | Pt (0.8 nm) | Ta (3 nm)

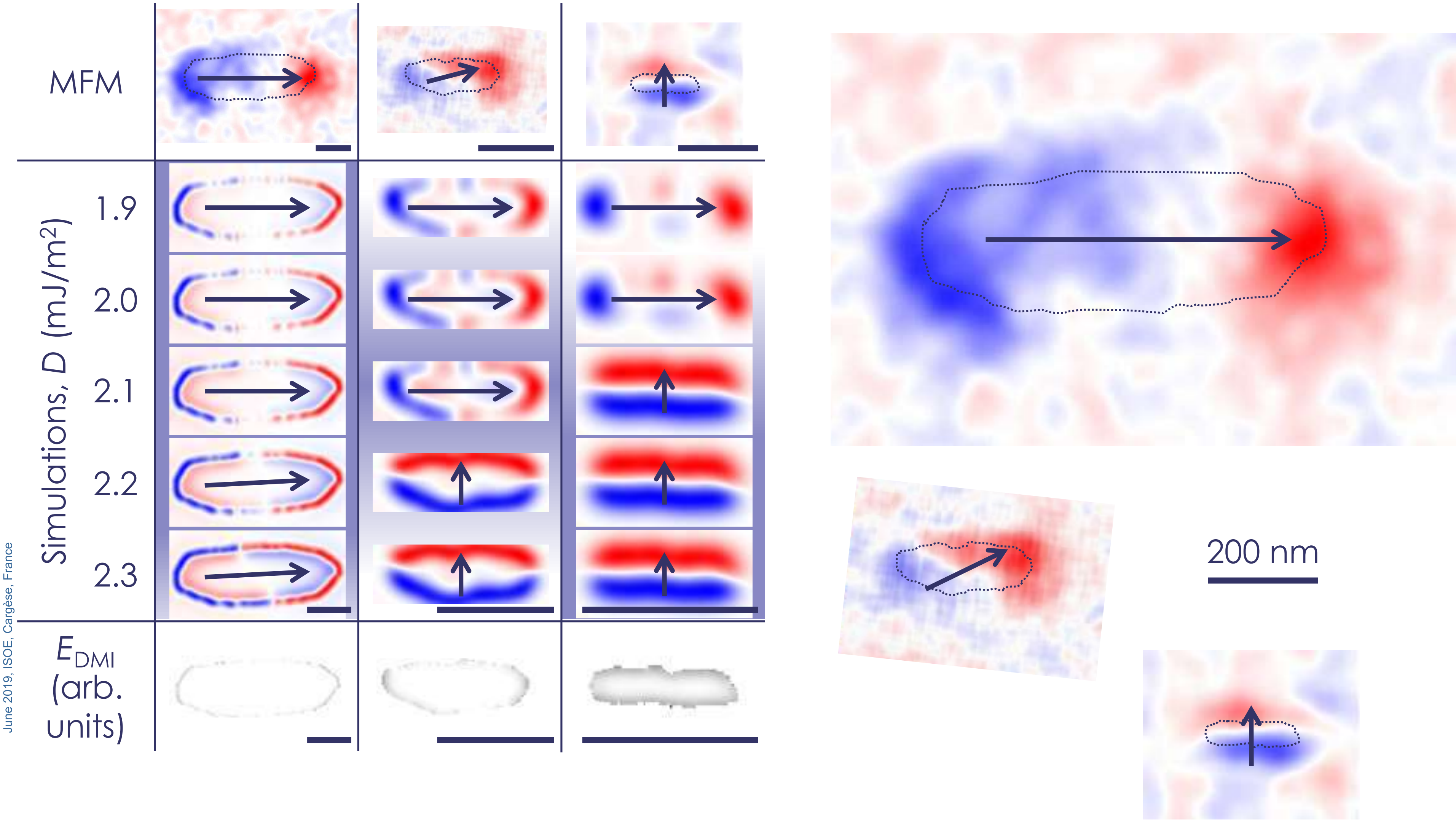

M. Cubukcu *et al*, *Phys. Rev. B* **93**, 020401(R) (2016)

Existence of a New in-Plane Anisotropy due to DMI

New type of shape anisotropy due the DMI-induced tilting of the magnetization at edges.

- Below about 100 nm this anisotropy should be rather common, as the necessary $D_{\perp} \approx 0.5$ mJ/m^2.
- Energy difference is large enough: With about 1 eV this state is stable at room temperature.
- Use for nanoscale magnetic field sensor in MTJ structure? …

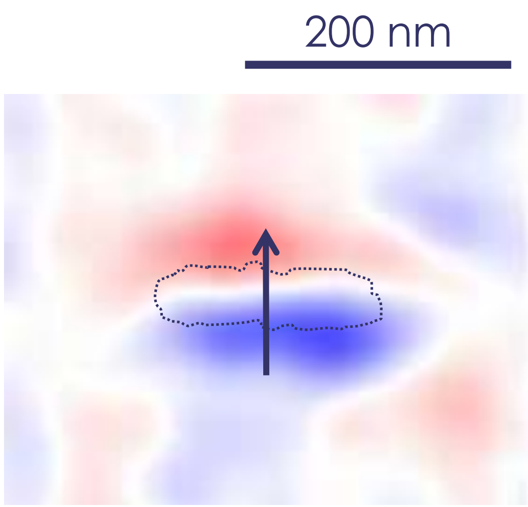

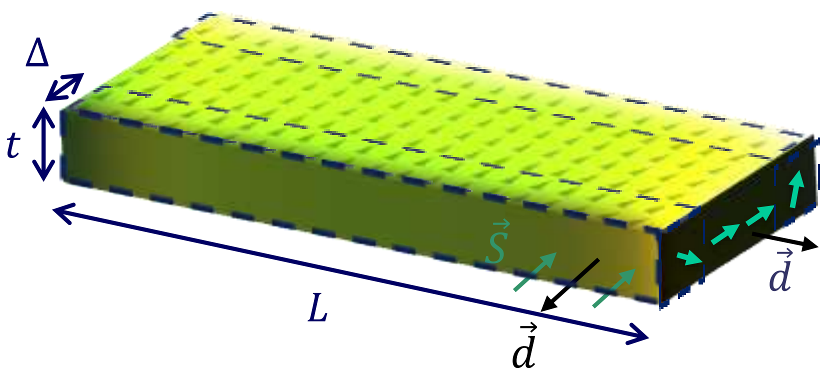

M. Cubukcu *et al*, *Phys. Rev. B* **93**, 020401(R) (2016)

Question session

?

Control of magnetization using SOT

SHE and DW motion (Bloch or Néel)

SHE
(spin Hall effect)

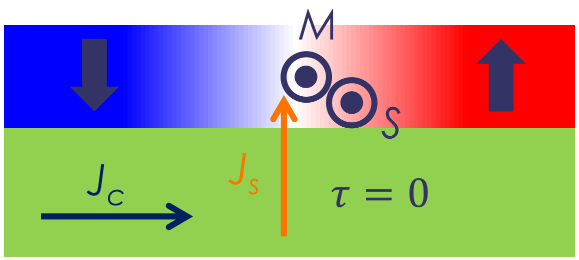

Bloch wall
No motion

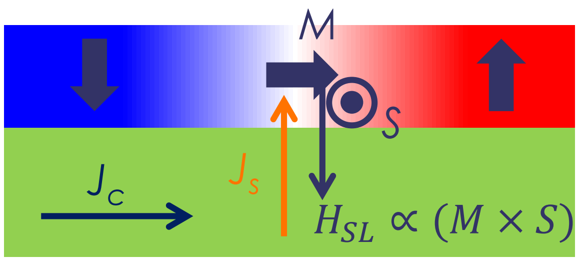

Néel wall
Motion towards the right

$\tau_{SL} \propto M \times (M \times S) = M \times H_{SL}$

Magnetization Switching using Charge Currents and Spin Hall Effect

What happens in micronic systems?

- Ferromagnetic film with PMA
- Spin torque acts on magnetization
- Spin current provided by heavy metal layer (*e.g.* Pt) through SHE

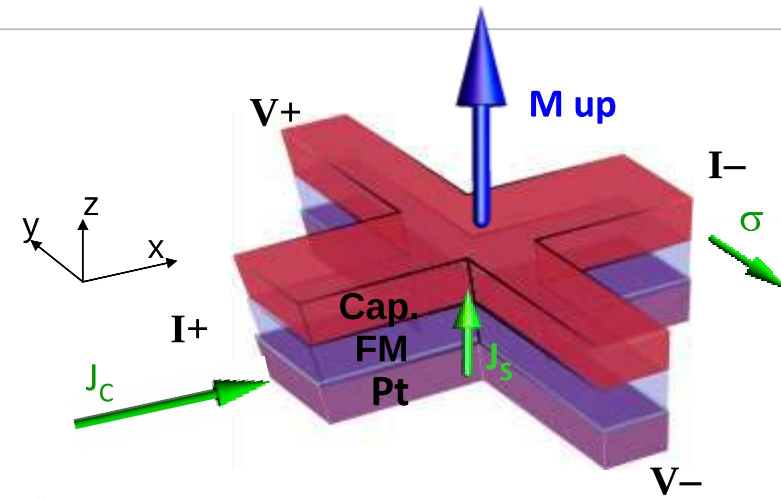

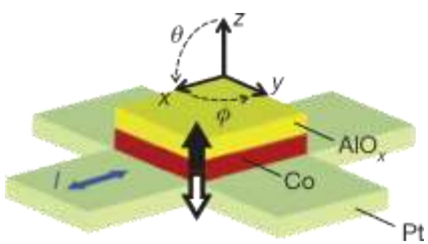

I. M. Miron *et al*, *Nature* **476**, 189 (2011)

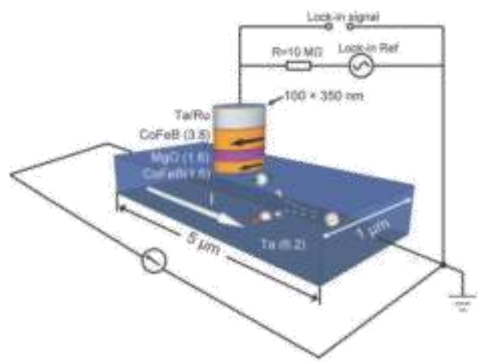

L. Liu *et al*, *Science* **336**, 555 (2012)

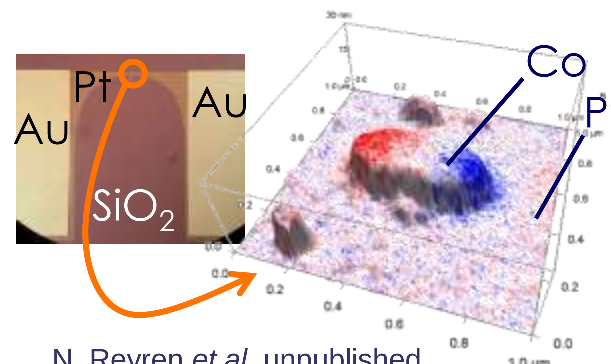

N. Reyren *et al*, unpublished

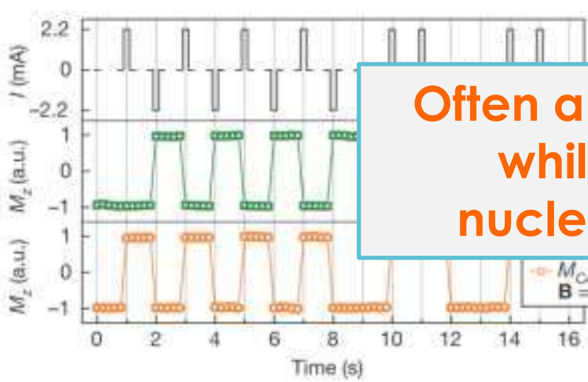

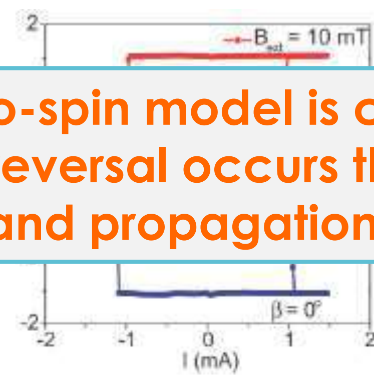

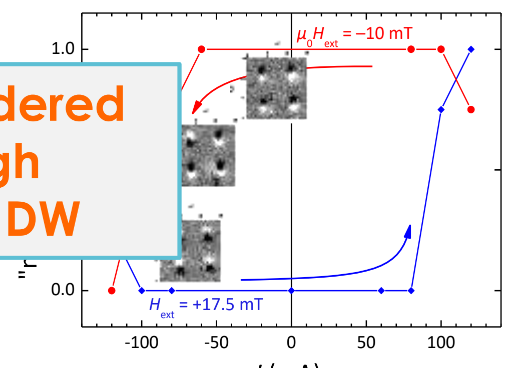

Often a macro-spin model is considered while the reversal occurs through nucleation and propagation of a DW

Current-induced Magnetization Switching - Device

Hall bar geometry

- ‖ Pt 6nm | { Co 0.2nm | Ni 0.6nm $\}_3$ | Al 5nm
- Anomalous Hall effect (AHE) allows the magnetic state to be determined using low current densities.

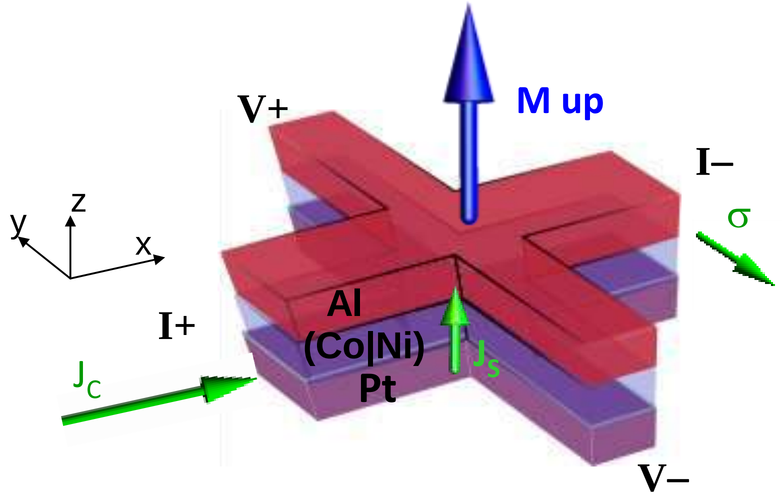

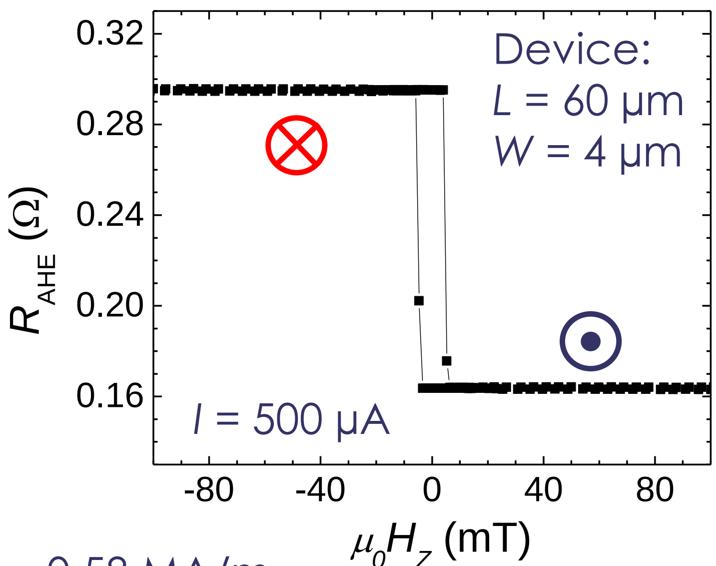

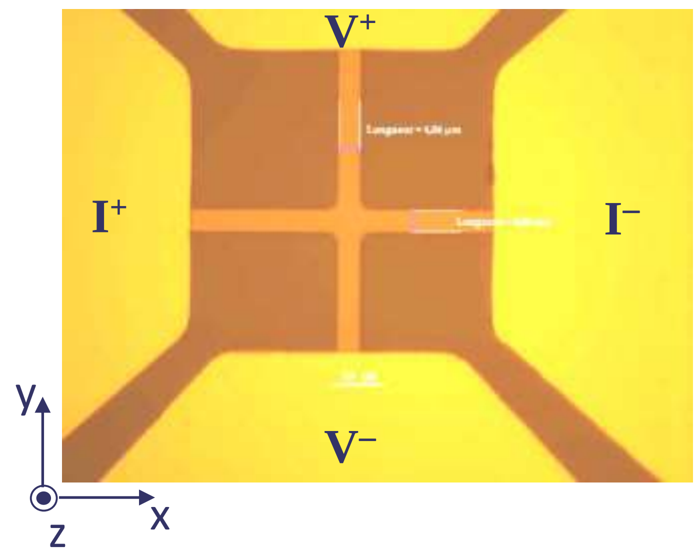

M_s = 0.58 MA/m
K_u = 3.8 MJ/m^3

Current-induced magnetization switching - device

Hall bar geometry

- ‖ Pt 6nm | { Co 0.2nm | Ni 0.6nm $\}_3$ | Al 5nm
- Using "large" current pulses, magnetization can be switched.

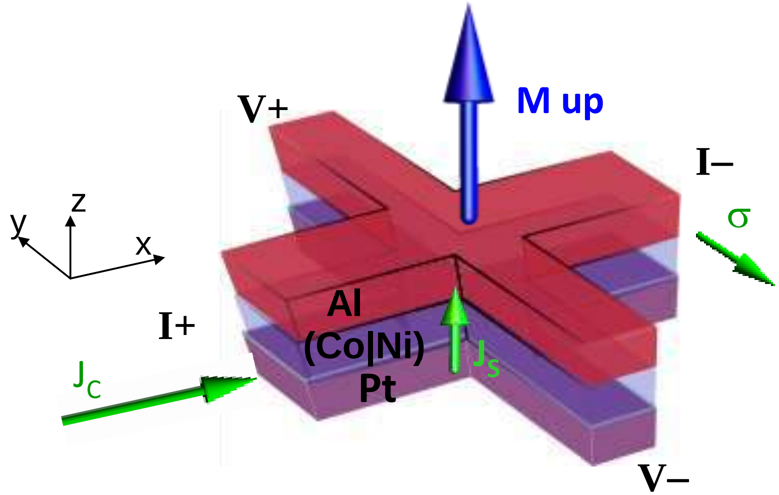

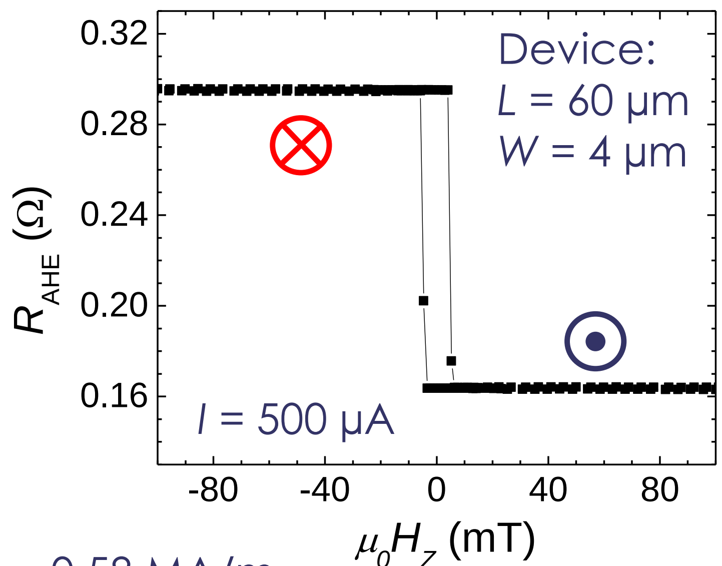

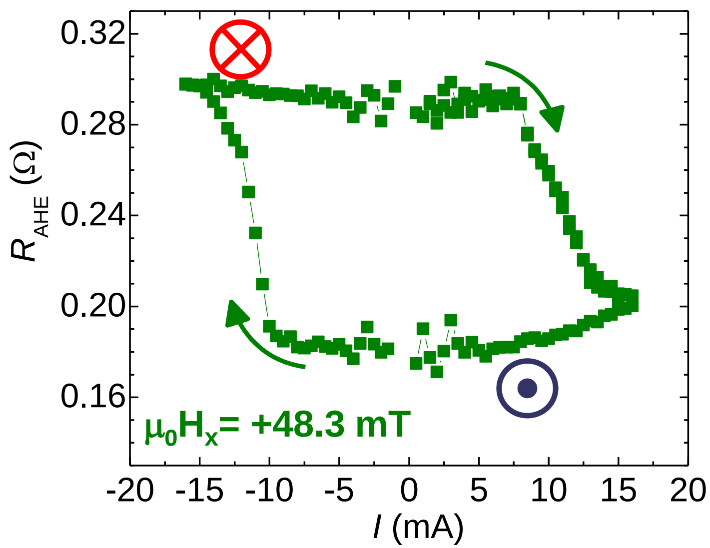

M_s = 0.58 MA/m
K_u = 3.8 MJ/m^3

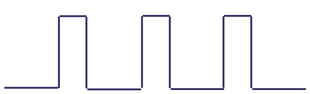

dc pulsed current

Current-induced Magnetization Switching - Device

Hall bar geometry

- ‖ Pt 6nm | { Co 0.2nm | Ni 0.6nm $\}_3$ | Al 5nm
- Using "large" current pulses, magnetization can be switched.

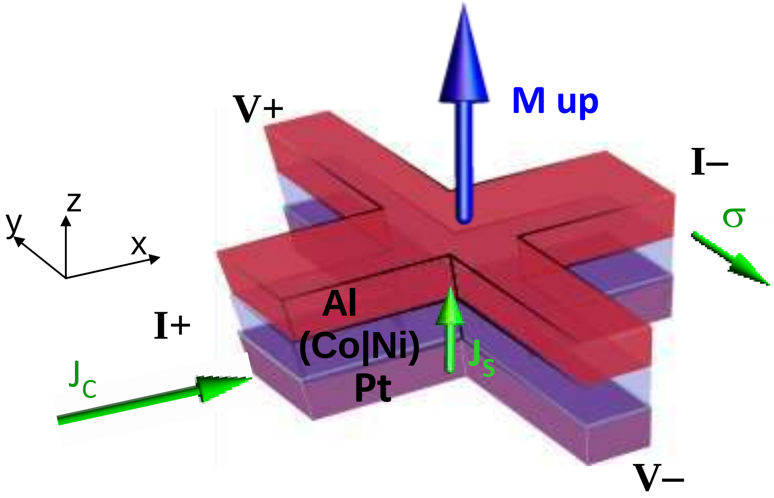

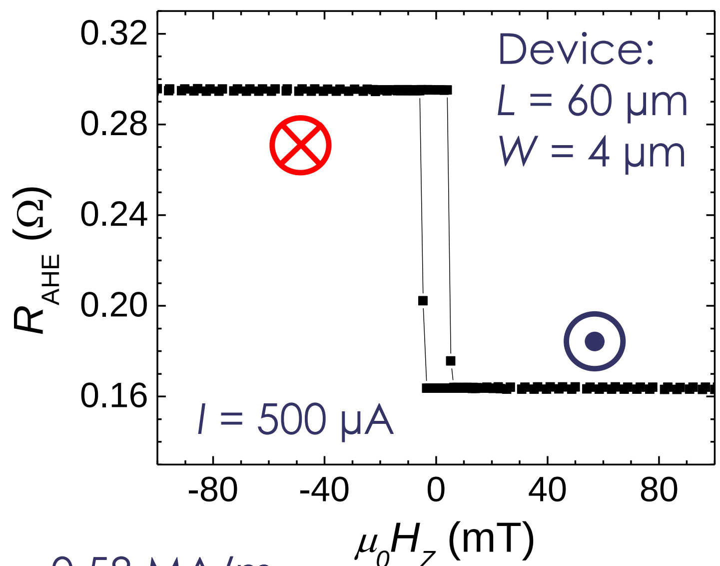

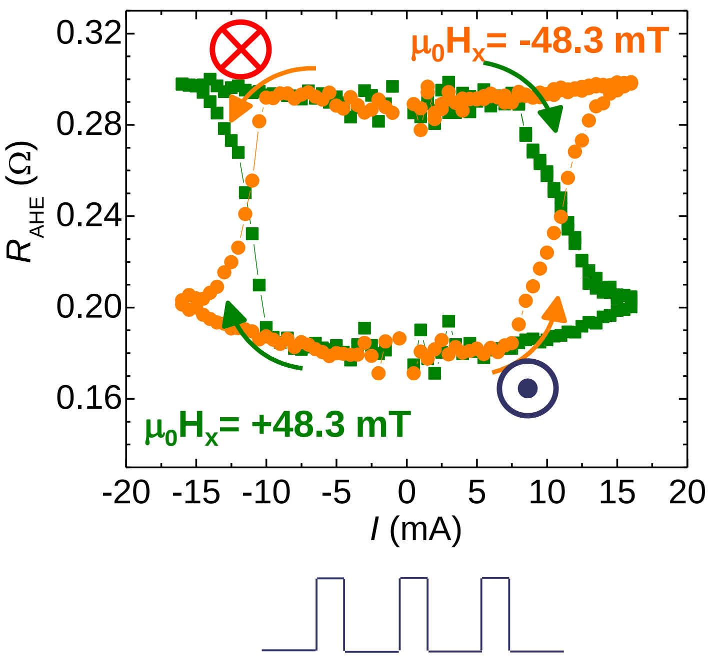

M_s = 0.58 MA/m
K_U = 3.8 MJ/m^3

dc pulsed current

H_x-I "Phase Diagram"

Phase diagram reveals

- Need a minimum in-plane field
- Deterministic switching above a critical current which depends on the applied field

I = 10 mA ~ J(Pt) = 0.13 TA/m^2

(0.08 TA/m^2 in Co|Ni)

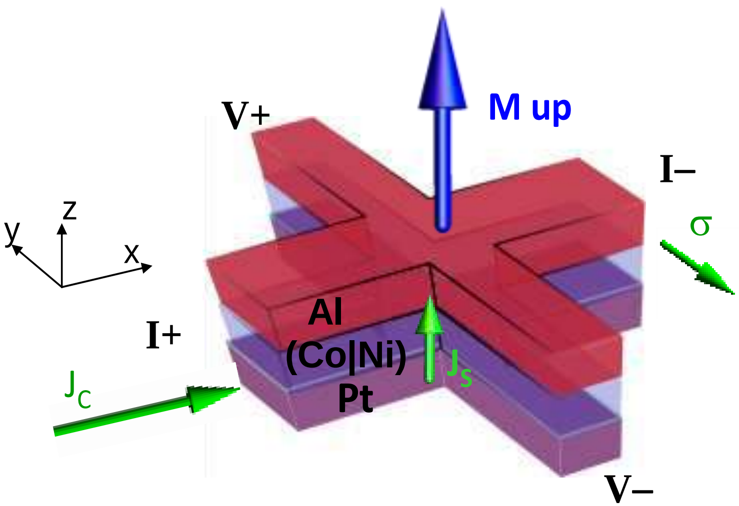

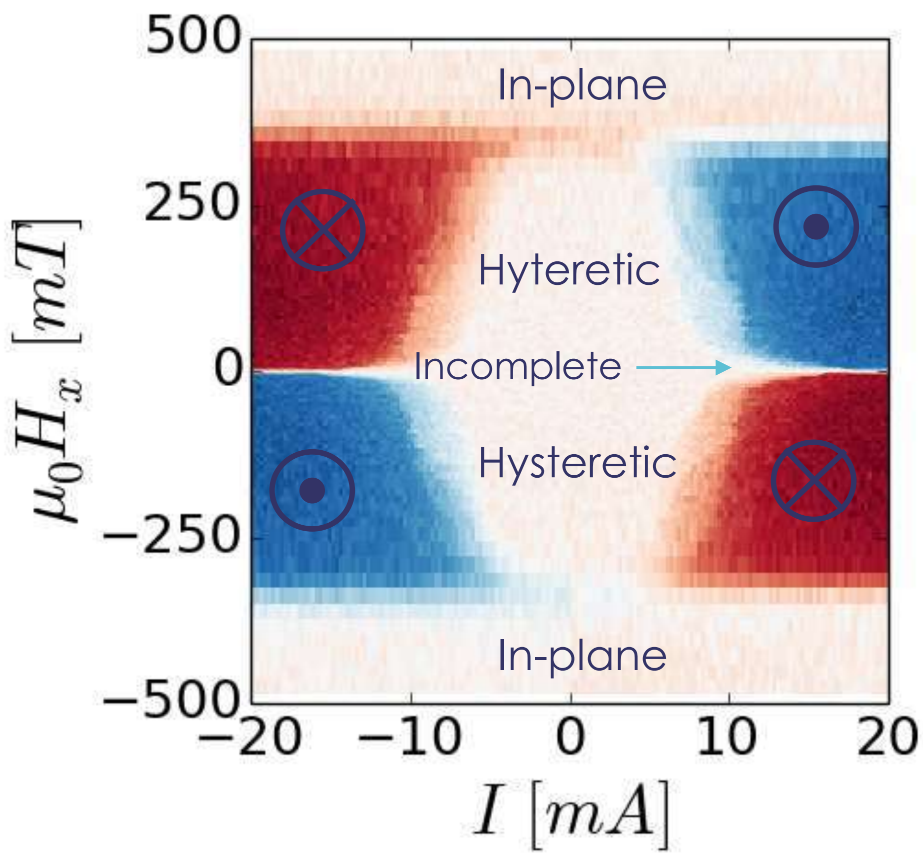

J.-C. Rojas-Sanchez *et al*, *Appl. Phys. Lett.* **108**, 082406 (2016)

Spin-Orbit Torques Efficiencies

Injection geometry	Torque origin	DW type	Result
parallel	SHE and/or IRE	Bloch	no motion
		Néel	==steady motion==
		HTH	no motion
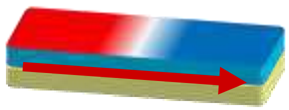	Rashba	Bloch	no motion
		Néel	shift
		HTH	no motion
perpendicular	SHE and/or IRE	Bloch	==steady motion==
		Néel	no motion
		HTH	no motion
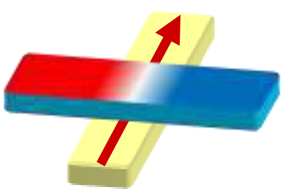	Rashba	Bloch	shift
		Néel	no motion
		HTH	==steady motion==

A.V. Khvalkovskiy *et al*, *Phys. Rev. B* **87**, 020402(R) (2013)

Kerr Microscopy and Explanations

Essential role of the DMI through change of the DW texture

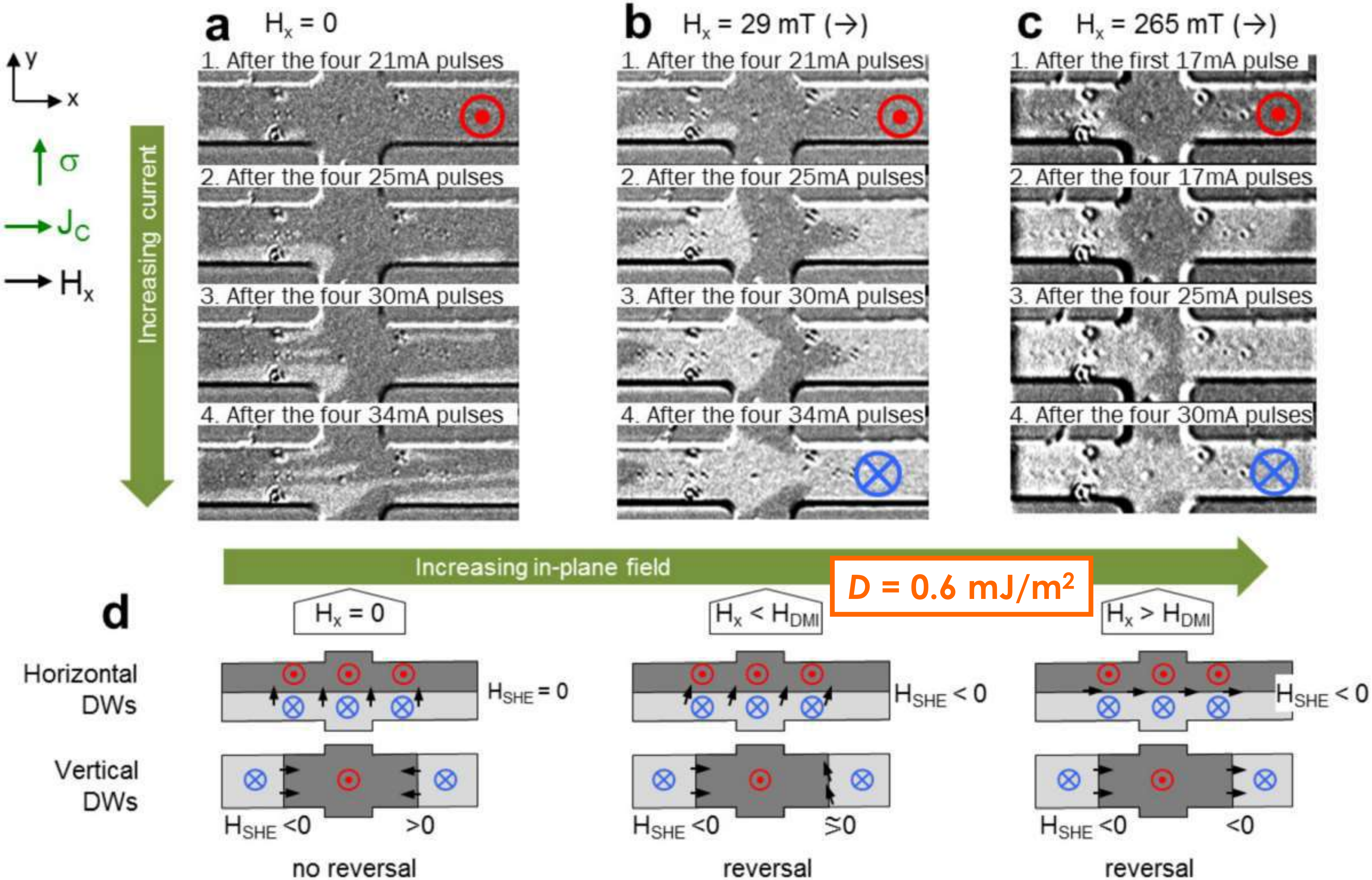

J.-C. Rojas-Sanchez *et al*, *Appl. Phys. Lett.* **108**, 082406 (2016)

Deterministic Switching Mechanism

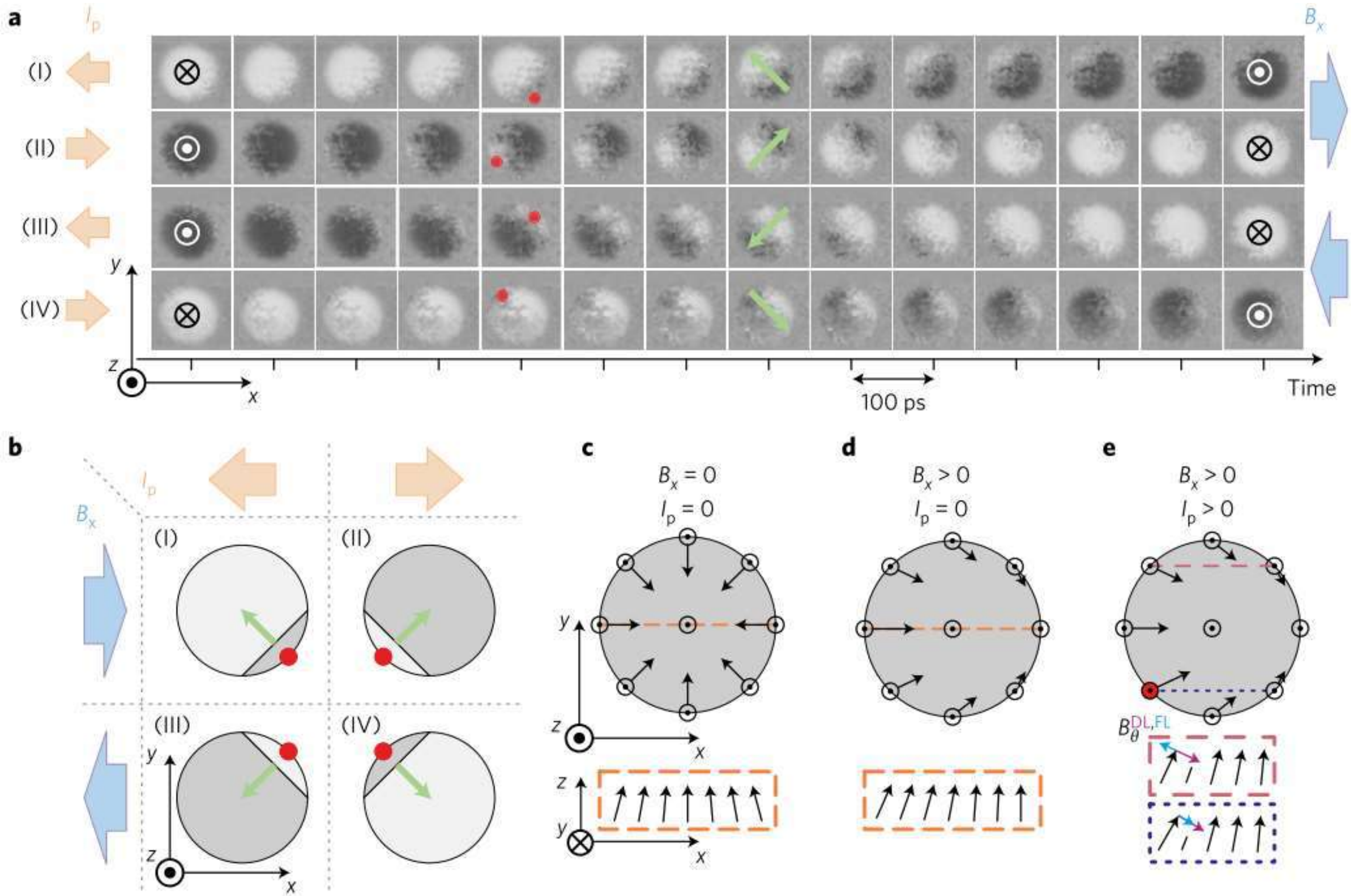

M. Baumgartner *et al*, *Nat. Nanotechnol.* **12**, 980 (2017)

Summary

New ways to generate *pure spin currents* using spin-orbit interaction

- SHE in heavy metals or doped light metals
- EE at Rashba interface / TI surface states

Possibility to detect spin accumulation electrically

- ISHE
- IEE

Stabilization of chiral magnetic textures:

- Deterministic switching using SOT
- Nucleation control
- Sometimes should be avoided…
- …